UNIVERSITÀ
DEGLI STUDI
DI TRIESTE

UNIVERSITÀ DEGLI STUDI DI TRIESTE

XXXVIII CICLO DEL DOTTORATO DI RICERCA IN

NANOTECNOLOGIE

Polymeric Nanoparticles for Oral Delivery of a Chimeric Protein as a Vaccination Approach for the Treatment of Glypican-1-expressing Pancreatic Ductal Adenocarcinoma

Settore scientifico-disciplinare: **BIO/14**

DOTTORANDA
MARTA GAMBIRASI

COORDINATORE
PROF. ALBERTO MORGANTE

SUPERVISORE DI TESI
DOTT. GIUSEPPE TOFFOLI

ANNO ACCADEMICO 2024/2025

UNIVERSITÀ DEGLI STUDI DI TRIESTE

UNIVERSITÀ DEGLI STUDI DI TRIESTE

XXXVIII CICLO DEL DOTTORATO DI RICERCA IN

NANOTECNOLOGIE

Polymeric Nanoparticles for Oral Delivery of a Chimeric Protein as a Vaccination Approach for the Treatment of Glypican-1-expressing Pancreatic Ductal Adenocarcinoma

Settore scientifico-disciplinare: **BIO/14**

DOTTORANDA
MARTA GAMBIRASI

COORDINATORE
PROF. ALBERTO MORGANTE

SUPERVISORE DI TESI
DOTT. GIUSEPPE TOFFOLI

ANNO ACCADEMICO 2024/2025

Abstract

Pancreatic ductal adenocarcinoma (PDAC) is one of the most aggressive and lethal forms of cancer, characterized by strong resistance to conventional therapies and a poor prognosis, with frequent relapse and metastasis even after surgical resection and/or standard chemotherapy. Cancer vaccines are emerging as innovative immunotherapeutic approaches, particularly when proposed as adjuvants to be combined with existing treatments. Although vaccines are traditionally administered via parenteral routes, oral delivery offers several advantages for both patients and healthcare systems.

Therefore, the present thesis focuses on developing an oral (OS) nanotechnology-based vaccine platform as an adjuvant therapy for PDAC. This developing approach was structured into three main phases: (a) selection of a tumor-associated antigen (TAA) and design and production of a protein-based vaccine; (b) preparation of nanoparticles (NPs) to protect the vaccine within the gastrointestinal tract and enhance its intestinal absorption to trigger an effective immune response; and (c) evaluation of the immunogenicity of the vaccine and its effects on tumor growth.

The proteoglycan Glypican-1 (GPC1) was selected as the TAA for the development of the protein-based cancer vaccine, since it is highly expressed in PDAC tissues but absent or present at negligible levels in benign and healthy tissues. Its expression was confirmed in the human PDAC cell line BxPC3 by different techniques. In addition, we selected flagellin (FL) from *Salmonella typhimurium* as an adjuvant component to enhance vaccine immunogenicity. Therefore, we designed the chimeric protein GPC1-FL and expressed and purified it from Chinese Hamster Ovary cells. We evaluated its stability in PBS at 37 °C, and in simulated gastric fluid (SGF) and simulated intestinal fluids (SIF) buffers that, as expected, was very low.

To overcome the limitations of OS delivery, in particular the harsh gastrointestinal environment and the need to target the intestinal immune system, we prepared PLGA/PVA NPs using a microfluidic nanoprecipitation method, and we characterized them by dynamic light scattering (DLS), confirming their stability over time and at physiological temperature in both SGF and SIF. Furthermore, we demonstrated the NP biocompatibility with the *in vitro* models of the intestinal epithelium (Caco-2 cells) and antigen-presenting cells (RAW 264.7). In addition, we performed internalization studies using BSA-FITC as a model protein, showing that PLGA/PVA NPs significantly improved its cellular uptake by Caco-2 compared to the free form.

Given their stability, biocompatibility, and enhanced internalization capacity, we tested the immunogenicity and the effect on tumor growth of the GPC1-FL-loaded NPs *in vivo* using a mouse

model of PDAC expressing the human GPC1. We obtained this model by transfecting the mouse cell line PANC02 with the human GPC1 gene. We demonstrated that the chimeric GPC1-FL protein was immunogenic, eliciting a strong and specific IgG response after subcutaneous administration. This response was further enhanced when the protein was delivered via PLGA/PVA NPs, indicating that NP encapsulation improves antigen presentation and vaccine efficacy.

Following OS administration, the free protein did not elicit any detectable IgG response, whereas GPC1-FL-loaded NPs induced a significant, though lower, antibody response compared to subcutaneous vaccination. Finally, mice receiving SC GPC1-FL-loaded PLGA/PVA NPs showed a significantly longer survival time compared to other experimental groups, whereas the immune response generated by OS administration was insufficient to improve survival outcomes.

In conclusion, this study developed a novel nanoplatform for SC and OS vaccination against PDAC. Through a multidisciplinary approach encompassing antigen selection (GPC1), production of the immunogenic chimeric protein GPC1-FL, preparation of PLGA/PVA NPs, and both *in vitro* and *in vivo* validation, the project demonstrated that PLGA/PVA NPs effectively enhance the anti-GPC1 immune response, particularly following SC administration, leading to a significant increase in survival in a PDAC mouse model. Although the OS route elicited a weaker immune response, insufficient to delay tumor progression, the results highlight the potential of PLGA/PVA NPs as a safe and effective platform for mucosal vaccination. Further optimization of dose, administration scheduling, or formulation must be necessary for the oral administration to achieve an efficacy comparable to that of the subcutaneous one.

TABLE OF CONTENTS

1 ABBREVIATIONS 1

2 INTRODUCTION 2

2.1 Pancreatic ductal adenocarcinoma (PDAC) 2

2.1.1 Epidemiology, molecular features, diagnosis, and treatment 2

2.1.2 Tumor-Associated and Tumor-Specific Antigens in PDAC 3

2.2 Glypican-1 4

2.2.1 The glypican family 4

2.2.2 Glypican-1: structure and functions 4

2.2.3 The role of GPC1 in PDAC 6

2.3 Cancer vaccines 8

2.3.1 The immunological aspects of cancer vaccines 8

2.3.2 Types of cancer vaccines 9

2.3.3 Vaccine administration routes 10

2.4 OS vaccination 12

2.4.1 Intestinal immune system and immunological basis of OS vaccination 12

2.4.2 Challenges of OS vaccination 16

2.4.2.1 Harsh pH gradient 16

2.4.2.2 Enzymatic degradation 17

2.4.2.3 Mucus barrier 18

2.4.2.4 Epithelial barrier 18

2.4.2.5 Gastrointestinal microbiota 19

2.4.2.6 Low immunogenicity 20

2.4.3 Strategies to overcome the limitations of OS vaccination 20

2.4.4 Flagellin from *Salmonella typhi* as an adjuvant for OS immunization 23

2.5 Nanotechnology and Nanomedicine 24

2.5.1 Nanomedicine in cancer therapy 24

2.5.2 Classification of NPs used in nanomedicine 25

2.6 Poly(lactic-co-glycolic acid) (PLGA) NPs 26

2.6.1 Physicochemical and Biological Properties of PLGA NPs 26

2.6.2 Preparation of PLGA NPs 27

2.6.2.1 Emulsion-solvent evaporation method 27

2.6.2.2 Salting out 28

2.6.2.3 Nanoprecipitation 29

2.6.2.4 Microfluidic 30
2.6.3 Application in cancer medicine of PLGA NPs 33
2.6.4 PLGA NPs for cancer immunotherapy 33
2.6.5 PLGA/PVA NPs for OS delivery 34
3 AIM 36
4 MATERIALS AND METHODS 38
4.1 Cell culture: cell lines and culture media 38
4.2 Bacteria and bacterial growth media 38
4.3 Antibodies and proteins 39
4.4 Evaluation of GPC1 expression on PDAC cells 39
4.4.1 Western blot 39
4.4.2 Flow cytometry 40
4.4.3 Immunofluorescence 40
4.5 Production and characterization of the chimeric protein GPC1-FL 41
4.5.1 Production of the GPC1-FL protein 41
4.5.2 Quantification and characterization of the GPC1-FL protein 42
4.5.3 GPC1-FL stability in temperature, Simulated Gastric Fluid (SGF) and Simulated Intestinal Fluid (SIF) buffers 42
4.6 Preparation of polymeric NPs 42
4.6.1 Microfluidic nanoprecipitation method 42
4.7 NP characterization 43
4.7.1 Dynamic light scattering (DLS) 43
4.7.2 NP Tracking Analysis (NTA) 43
4.7.3 Encapsulation efficiency (EE%) 44
4.7.4 NP stability over time, at body temperature, in SGF and SIF buffers 44
4.7.5 Cell viability assay 45
4.7.6 NP internalization by the *in vitro* model of intestinal epithelium 45
4.8 Establishment of a syngeneic murine model of PDAC 45
4.8.1 Characterization of the mouse cell line PANC02 for the murine model of PDAC 45
4.8.2 Transfection of PANC02 cells 46
4.8.2.1 Vector design 46
4.8.2.2 Vector amplification in *E.coli* Dh5alpha 46
4.8.2.3 Vector purification and quantification 47
4.8.2.4 Puromycin selective antibiotic kill curve assay 47
4.8.2.5 PANC02 transfection by electroporation 47
4.8.2.6 *In vitro* and *ex vivo* verification of GPC1 expression 48
4.8.2.7 Doubling time 48

4.9 Animal studies **48**
4.9.1 Immunization protocol 48
4.9.2 Safety observation 49
4.9.3 Blood collection 49
4.9.4 Detection of specific anti-GPC1 IgG antibodies by ELISA 49
4.9.5 Tumor inoculation and mouse survival 49
4.10 Statistical analysis **50**
5 RESULTS **51**
5.1 Evaluation of GPC1 as a Vaccine Target for PDAC **51**
5.2 Production and characterization of the chimeric protein GPC1-FL **53**
5.3 GPC1-FL stability in stomach and intestine **56**
5.4 Preparation and characterization of polymeric NPs **58**
5.4.1 Preparation and physical characterization of NPs 58
5.4.2 NP stability over time 59
5.4.3 NP stability at body temperature 60
5.4.4 NP stability in gastric juice and intestinal fluid 61
5.4.5 *In vitro* biocompatibility of PLGA/PVA and BSA-FITC-loaded PLGA/PVA NPs 64
5.4.6 NP internalization by the *in vitro* model of intestinal epithelium 65
5.4.7 GPC1-FL-loaded PLGA/PVA NP: preparation and characterization 66
5.5 Establishment of a syngeneic murine model of PDAC **68**
5.6 *In vivo* studies of the NP-based Cancer Vaccine **74**
5.6.1 Detection of specific anti-GPC1 IgG antibodies in mouse serum 74
5.6.1.1 *In vivo* vaccination via SC administration 74
5.6.1.2 *In vivo* vaccination via OS administration 77
5.6.2 Mouse survival 79
5.6.2.1 SC administration 79
5.6.2.2 OS administration 82
5.6.3 *In vivo* Safety profile of free GPC1-FL and GPC1-FL-loaded PLGA/PVA NPs 84
6 DISCUSSION **85**
7 CONCLUSIONS **91**
8 BIBLIOGRAPHY **92**

1 ABBREVIATIONS

BSA	Bovine Serum Albumin
CHO	Chinese hamster ovary cells
D (h)	Hydrodynamic diameter
DLS	Dynamic light scattering
FITC	Fluorescein Isothiocyanate
FL	Flagellin
FRR	Flow rate ratio
GPC1	Glypican-1
NP	Nanoparticle
OS	Oral
PDAC	Pancreatic ductal adenocarcinoma
PdI	Polydispersity index
PLGA	Poly Lactic-co-Glycolic Acid
PVA	Poly(vinyl alcohol)
SC	Subcutaneous
SGF	Simulated gastric juice buffer
SIF	Simulated intestinal fluid buffer
TAA	Tumor-associated antigen
TFR	Total flow rate
T-GPC1 PANC02	GPC1-expressing PANC02
WT PANC02	Wild type PANC02
ZP	Zeta potential

2 INTRODUCTION

2.1 Pancreatic ductal adenocarcinoma (PDAC)

2.1.1 Epidemiology, molecular features, diagnosis, and treatment

Pancreatic ductal adenocarcinoma (PDAC) accounts for 85% of all pancreatic cancers. It is very lethal and aggressive, with a generally poor prognosis, a consequence of a late diagnosis and inefficacy of the available therapies. Indeed, the 5-year survival rate of PDAC is about 5% [1]. PDAC occurs mainly in people with associated risk factors, such as age, as it occurs mainly in people aged 60 to 80 years, smoking, alcohol consumption, new-onset diabetes, obesity, chronic pancreatitis and, in some cases, genetic predisposition [2]. At the molecular level, PDAC is characterized by frequent genetic mutations that, in 80% of cases, involve the activation of KRAS gene, as well as inactivating alterations in TP53, CDKN2A and SMAD4 [3–5]. These mutations often result from precancerous lesions such as pancreatic intraepithelial neoplasms (PanINs) or intraductal papillary mucinous neoplasms (IPMNs) [6].

One of the main problems with this tumor is the late diagnosis. Indeed, in 80% of cases PDAC is diagnosed when it is already in advanced stages and metastases are just present in other organs [7].

This happened because the initial symptoms are often vague and include abdominal pain, unexplained weight loss, jaundice (especially if the tumor involves the head of the pancreas) and newly diagnosed diabetes [8]. Therefore, most cases are only discovered in advanced stages when the disease has already spread.

The diagnosis is made by imaging examinations such as CT, MRI, often in combination with measurement of the tumor marker CA19-9 and biopsies to confirm the malignancy of the lesion [9].

Treatment depends on the stage of the disease. In the early stages, surgery is the only way to cure the disease, but this can only be applied in 15-20% of patients. In advanced stages, treatment is based on chemotherapy with regimens such as FOLFIRINOX or gemcitabine with 5-Fluorouracil in combination with nab-paclitaxel and, sometimes, radiotherapy [10]. However, the response to these therapies is often limited and immunotherapy, although a promising alternative, is still under investigation [11].

Currently, research focuses on strategies for early detection of PDAC and the development of targeted therapies to avoid tumor progression and improve patient survival.

2.1.2 Tumor-Associated and Tumor-Specific Antigens in PDAC

Tumor-associated antigens (TAAs) and tumor-specific antigens (TSAs) are proteins or molecules expressed by tumor cells, and absent or weakly expressed in normal tissue. Tumor antigens play a key role in understanding, identifying, diagnosing, treating, and monitoring diseases.

In detail, TSAs are exclusive to tumor cells and result from mutations that lead to the production of abnormal proteins. In PDAC, the main TSAs are neoantigens derived from mutations, such as mutated KRAS, which is present in more than 85% of PDAC cases [12]. The mutation leads to an oncogenic KRAS protein that is not found in normal tissues, making it a potential target for vaccines and targeted therapies. Another antigen involved in PDAC is the mutated TP53, which generate abnormal p53 proteins. It overcomes tumor growth arrest and supports cancer metastasis [13]. Finally, one of the most important neoantigens in PDAC, together with KRAS and p53 mutations, is SMAD4, altered in 60% of cases [14].

Moreover, gene Fusion Derived Proteins are also involved in PDAC. Although rarer in PDAC than in other cancers, some proteins from gene fusions could serve as specific antigens. Usually, they are present in KRAS wild-type PDAC and involve BRAF, FGFR2, RET, NTRK, NRG1, and ALK [15].

TAAs are molecules highly expressed during embryonic development. Then, in adult tissues they are absent or expressed at low levels. However, they might be highly expressed in tumor cells. Major TAAs of PDAC include the carbohydrate antigen 19-9 (CA 19-9), carcinoembryonic antigen (CEA), MUC1 and MUC4, and proteoglycans.

CA 19-9 is the most widely used tumor marker for PDAC [16]. It is a cell surface glycoprotein that can be detected in blood but has limited specificity, as it can be elevated even in benign conditions such as pancreatitis or obstructive jaundice. Although useful for monitoring disease progression and response to treatment, it is not ideal for early detection [17].

CEA is a glycoprotein expressed at high levels in many tumor types, including PDAC. It is less sensitive than CA 19-9 but can be useful as a complementary marker [18].

MUC1 and MUC4 are high molecular weight transmembrane mucins. When they are aberrantly methylated, they play a role in tumor progression and immune evasion, making them promising targets for targeted therapies [19].

Finally, several studies demonstrated that proteoglycan, such as the glypican family, are involved in PDAC [20].

2.2 Glypican-1

2.2.1 The glypican family

Glypicans are a family of cell membrane-associated proteoglycans that play a crucial role in regulating many cellular functions [21,22]. They are characterized by having a protein core linked to heparan sulfate or chondroitin sulfate chains, which allow them to interact with a wide variety of biological molecules [23].

This family includes six main members in humans (GPC1-GPC6), each with specific tissue localizations and distinct functions [23]. In general, glypicans are involved in essential biological processes, such as cell signaling, modulation of the extracellular microenvironment, and cell adhesion. They often act as co-receptors, facilitating the interaction of growth factors, cytokines, and extracellular matrix molecules with membrane receptors [23]. They are particularly important in signaling pathways such as Wnt [24], Hedgehog [24–26] and fibroblast growth factor (FGF) [27–29].

In the pathological setting, glypicans play a significant role. Their disruption can promote tumor progression by facilitating cell proliferation, angiogenesis, and metastasis [23]. In addition, they are involved in rare genetic diseases, such as Simpson-Golabi-Behmel syndrome, caused by mutations in GPC3 genes [30], and in neurodegenerative processes, such as cognitive dysfunction and Parkinson's disease [31].

Clinically, glypicans are the subject of great interest. They could be used as biomarkers to diagnose or monitor diseases, especially in oncology, and they represent promising targets for the development of targeted therapies and immunotherapies due to their crucial role in cell signaling pathways [23].

In summary, glypicans are multifunctional molecules at the center of many physiological and pathological processes, with significant potential for novel therapeutic applications.

2.2.2 Glypican-1: structure and functions

Glypican-1 (GPC1) is a heparan sulfate proteoglycan encoded by the human GPC1 gene located at 2q37.3 chromosome [32]. The GPC1 protein is 558 amino acids long and consists of several structural regions, including a secretory signal peptide (residues 1-23), an N-terminal core protein (residues 24-474), a C-terminal heparan sulfate (HS) chain attachment region (residues 475-530), and a glycosylphosphatidylinositol (GPI) anchor that attaches the protein to the cell membrane (residues 531-558) [32,33] (Figure 1). Post-translational modifications to GPC1 include the addition

of three HS chains at Ser-486, Ser-488, and Ser-490, as well as two N-linked glycans at Asn-79 and Asn-116. These modifications influence the protein expression and the attachment of HS chains [34].

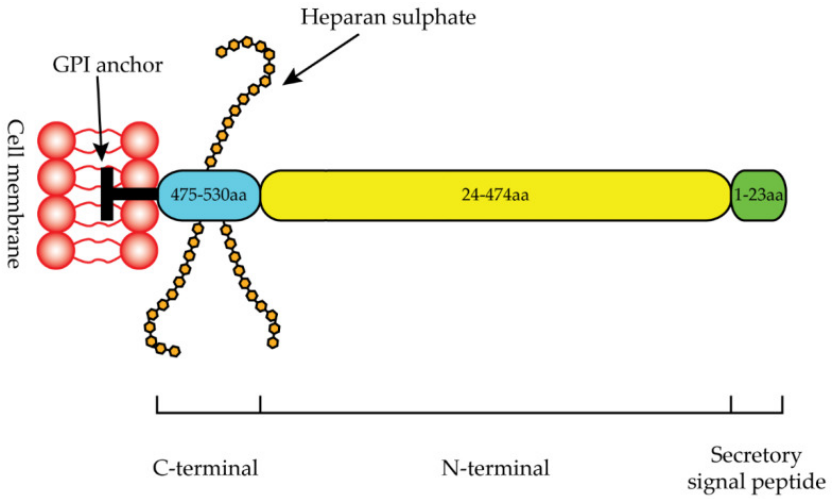

Figure 1. Representation of the glypican-1 (GPC1) protein. The protein GPC1 is organized into distinct functional regions: N-terminal region, which includes a secretory signal peptide that directs the protein into the secretory pathway for processing and trafficking to the cell surface; the C-terminal region; and the glycosylphosphatidylinositol (GPI) anchor at the C-terminus, which tethers GPC1 to the plasma membrane [2].

Studies by Svensson et al. [35] revealed the crystal structure of the core protein of GPC1, devoid of HS chains, at a resolution of 2.6 Å (Figure 2). The structure is elongated and cylindrical, adopting an all α-helical fold (a1-a14) with three significant loops (L1, L2, and L3). The protein can be divided into three main regions: a Cys-rich region near the N-terminal lobe, a central lobe stabilized by two conserved hydrophobic centers, and a C-terminal lobe that contains a protease site. Six disulfide bonds are crucial for the structural stability of GPC1, connecting the different regions of the protein. These disulfide bonds are particularly important in maintaining the proper conformation of the Cys-rich lobe and protease site. Further structural analysis has shown that the C-terminal region of GPC1 displays significant flexibility and extends approximately 35–40 Å from the core protein. This flexibility plays a role in its interactions with the cell membrane. Specifically, the C-terminal domain orients the core protein transversely relative to the membrane, allowing GPC1 to interact with signaling molecules or membrane receptors [35].

Although the full-length GPC1 structure has not been fully elucidated in terms of its interactions with signaling components, it is clear that GPC1 participates in different cellular signaling pathways by modulating interactions with ligands and receptors on the cell surface. These interactions have a

significant impact on cellular functions, which can either activate or inhibit specific signaling pathways depending on the physiological context [2].

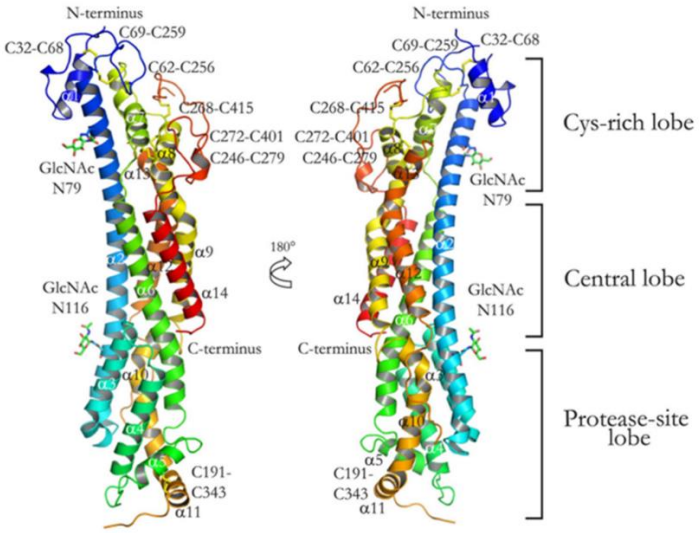

Figure 2. Crystal structure of Glypican-1 (GPC1) protein. Overview of the GPC1 crystal structure, shown schematically with a rainbow color scheme (N terminus in blue and C terminus in red). The main loops (L1–L3) and α-helices (α1–α14) are highlighted. Disulfide bonds are marked in yellow, while the first residues of the N-glycans (GlcNAc) are indicated. The figure also shows the subdivision of the structure into distinct lobes [35].

2.2.3 The role of GPC1 in PDAC

An immunohistochemical analysis revealed that the GPC1 is expressed in PDAC cells in 80% of patients [20]. Consequent studies demonstrated that GPC1 plays a critical role in PDAC by modulating multiple cellular signaling pathways that drive tumor growth, invasion, and metastasis [32] (Figure 3). As a heparan sulfate proteoglycan anchored to the cell membrane, GPC1 works as a co-receptor for key signaling molecules and pathways, including fibroblast growth factors (FGFs), vascular endothelial growth factor (VEGF), transforming growth factor-beta (TGF-β), Wnt, and Hedgehog (Hh) pathways, all involved in cancer progression [36]. Moreover, in PDAC, GPC1 overexpression enhances FGF2 and heparin-binding epidermal growth factor (HB-EGF) signaling, promoting cell proliferation and survival [2]. Studies have shown that GPC1 silencing abrogates the mitogenic effects of FGF2 and HB-EGF, underscoring its importance in tumor cell growth [37]. Moreover, GPC1 facilitates angiogenesis by enhancing VEGF-A interactions with VEGF receptors, which contributes to increased tumor vascularization and metastatic potential [36]. In addition to

promoting tumor cell proliferation, GPC1 influences epithelial-to-mesenchymal transition through its interaction with TGF-β, which is known to regulate cell migration and invasion[38]. Notably, Wnt and TGF-β pathways act synergistically in tumorigenesis, and GPC1 expression is upregulated in response to their combined activation, further reinforcing its role in PDAC progression [39]. GPC1 also modulates the tumor microenvironment by regulating cancer-associated fibroblasts (CAFs) [40], which in turn secrete pro-tumorigenic factors such as hepatocyte growth factor (HGF) and FGF, reinforcing a feedback loop that promotes tumor growth and invasion [41]. Additionally, GPC1 has been implicated in Hedgehog signaling, which is crucial for stromal remodeling and immune evasion in PDAC [36].

Finally, high GPC1 expression levels are associated with poor prognosis in this type of tumor [42,43].

Given its multifaceted role in PDAC, GPC1 is increasingly recognized as a promising therapeutic target, with strategies such as antibody-based immunotherapy and NP-based targeted therapy [2,23].

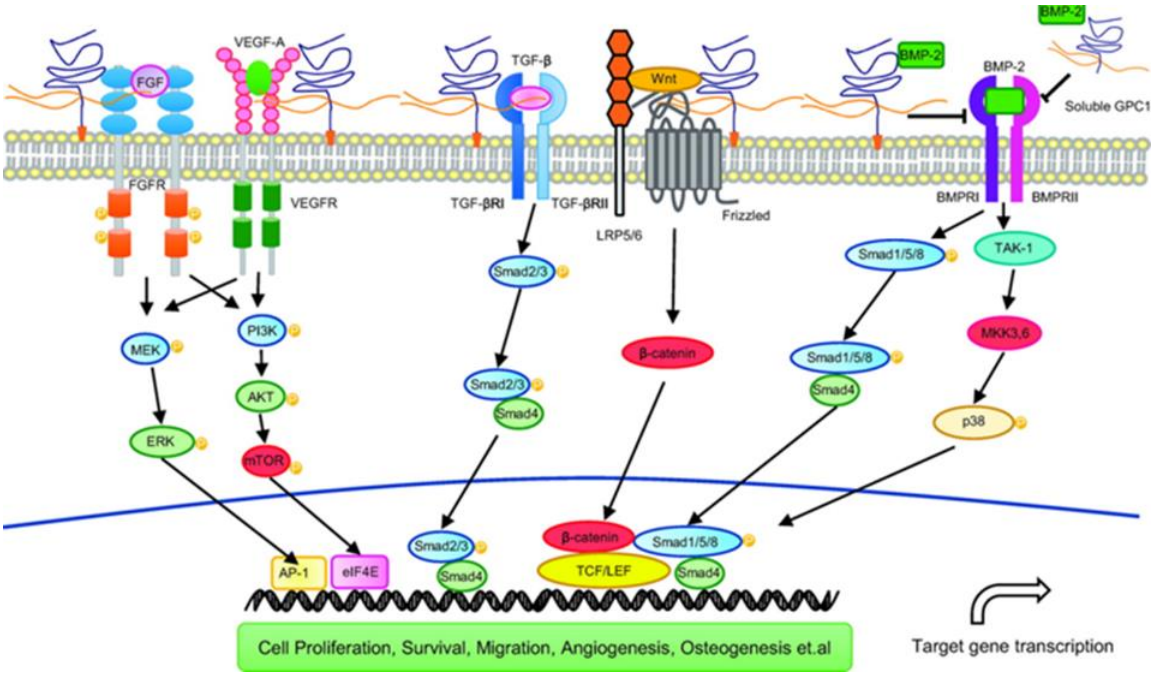

Figure 3. The regulatory roles of glypican-1 (GPC1) in multiple-signaling pathways. GPC1 is involved in different signaling pathways that participate in both cancer progression and physiological functions. GPC1 can interact with both heparin-binding growth factors (FGF and VEGF-A) and their receptors to stabilize their assembly and enhance MARK or PI3K/Akt signaling. Moreover, GPC1 binds TGF-β and its receptors to promote SMAD signaling. However, GPC1 plays a negative role in BMP cascades by competing with BMP receptors to interact with BMPs. GPC1 might acts as coreceptor in the Wnt signaling. Abbreviation: BMP: bone morphogenic protein; FGF: fibroblast growth factor; FGFR: fibroblast growth factors receptor; GPC1: glypican-1; GPI: glycosyl-phosphatidylinositol; HS: heparan sulphate; TGF-β: transforming growth factor-β; VEGF-A: vascular endothelial growth factor-A [32].

2.3 Cancer vaccines

2.3.1 The immunological aspects of cancer vaccines

Unlike traditional vaccines that prevent infection, tumor vaccines are designed primarily to stimulate a response against existing cancers or to prevent recurrence of them [44].

Tumor vaccines represent one of the most promising frontiers of immunotherapy, an approach that takes advantage of the natural ability of the immune system to recognize cancer and kill its cells (Figure 4). In detail, the principle behind these vaccines is to teach the immune system to recognize and attack cancer cells, which often escape immune surveillance because they are perceived as "self" [45].

These vaccines typically rely on immunogenic TAAs or TSAs, which are capable of being recognized as foreign by the immune system, thereby triggering a potent specific immune response [46].

Dendritic cells (DCs) play a central role in this process by capturing these antigens, processing them into fragments, and presenting them on their surface. This presentation activates T cells to mount a targeted response against the tumor [47].

Tumor vaccines have been studied in several types of cancer, including melanoma [48], pancreatic cancer, breast cancer [49], and lung cancer [50]. Although some vaccines have reached clinical practice, such as Sipuleucel-T for prostate cancer [51], many are still being tested. Among the most innovative approaches are personalized vaccines, which use neoantigens unique to a patient's tumor, identified through advanced genetic sequencing technologies [52].

Tumor vaccines offer many advantages, such as specificity, as they directly target tumor cells that express the tumor antigens and not normal cells, reducing the risk of systemic side effects. Furthermore, tumor vaccines are able to trigger both a systemic and humoral immune response [53]. Moreover, they provide a specific immune memory leading to long-term protection against recurrence [54]. In addition, tumor vaccines can work in combination with other therapies, such as immune checkpoint inhibitors, strategies that increase the probability of success [44]. For example, cancer vaccines are showing synergistic potential when used in combination with established immunotherapies, such as checkpoint inhibitors (PD-1/PD-L1) [55]. However, cancer vaccines also have some challenges, such as the individual variability in the body response [54] and immune evasion [56,57].

Research is focusing on increasingly sophisticated vaccines, such as those based on personalized neoantigens or combined with technologies such as nanomaterials to improve their delivery and efficacy, and control their release to have a long-term effect [58–60].

In conclusion, cancer vaccines represent a breakthrough in the fight against cancer, offering more targeted and personalized approaches than traditional treatments.

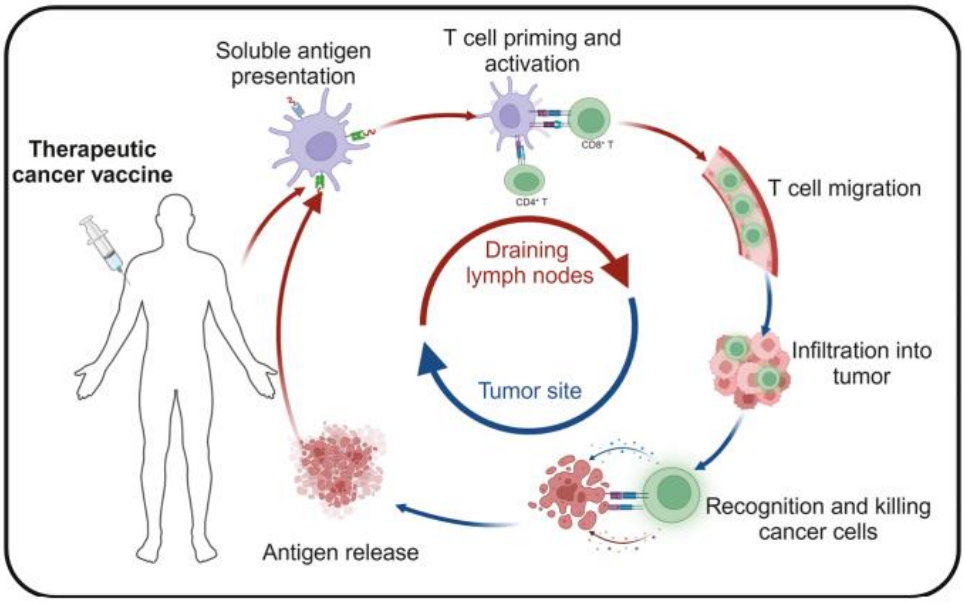

Figure 4. ***In vivo*** **mechanism of cancer vaccines**. Once tumor antigens enter the body, they are recognized and processed by antigen-presenting cells (APCs). APCs fragment the antigens and expose these fragments on their surface through major histocompatibility complex (MHC) molecules. The MHC-antigen complexes interact with T-cell receptors (TCRs) on antigen-specific T cells, triggering their activation and enabling them to selectively target and eliminate tumor cells [44].

2.3.2 Types of cancer vaccines

There are several strategies for developing cancer vaccines, each with specific advantages and disadvantages [44]. A cancer vaccine can be cell-based, employing modified or unmodified whole tumor cells to stimulate a global immune response. They can be autologous (from the patient himself) or allogeneic (from other patients) [61]. Their advantages are the capacity to strongly activate the immune response and the multi-form antigen loading. The disadvantages depend on the high cost of production and the need for patient-specific customization [62,63].

Cancer vaccines can also be based on peptides or proteins. Peptide-based or protein-based cancer vaccines are peptides or proteins engineered to mimic TAA or TSA from the tumor [64]. The advantages of peptide vaccines are the high specificity and safety, the cell-independent production, the low risk of autoimmunity, and the direct presentation on MHC in short peptides [44]. However, their production is very expensive because of the complex manufacturing procedures. Finally, they require strong adjuvants to work [44].

Moreover, dendritic vaccines exist. They are based on DCs, loaded with tumor antigens in the laboratory, and reinfused into the patient [65].

In addition, nucleic acids, such as DNA or RNA, can be used to stimulate a specific immune response [66,67]. DNA-based or RNA-based cancer vaccines are used to deliver to cells a specific genetic information that instructs them to produce tumor antigens, leading to the activation of the desired immune response [68]. DNA vaccines are cheap, they ensure a long-term immune response and can be projected for targeting multiple neoantigens. However, the risk of integration into the host genome is high, as the probability of activating autoimmune reactions [44]. RNA-based vaccines are safer than DNA-based vaccines. They can be rapidly developed and allow easy modifications. They are highly immunogenic and have intrinsic adjuvant effects. On the other hand, they are quickly degraded and might trigger inflammatory reactions [44].

Lastly, viruses and bacteria can be used to immunize against cancer [69,70]. Vector vaccines use genetically modified viruses to carry tumor antigens, stimulating a more potent response, while bacteria-based vaccine use modified or killed bacteria [69–71]. A historical example is the approach of William Coley, who used bacterial toxins to treat cancers, paving the way for the search for bacteria-based cancer vaccines [72,73].

Vaccines based on viruses and bacteria are adjuvants themselves, therefore they are highly immunogenic. Furthermore, they have a long-lasting immune response. However, they are not so safe as they lead to inflammatory reactions [44].

2.3.3 Vaccine administration routes

The decision of the vaccine administration routes is a key aspect in the vaccine design to ensure an efficient immunization. Indeed, each route has specific advantages and disadvantages, and the choice depends on the type of vaccine, the disease to be prevented or treated, and the characteristics of the patients. The main routes of vaccine administration are the intramuscular (IM), the subcutaneous (SC), the intradermal (ID), the transdermal, the nasal, and the oral (OS).

The IM is the most common for many vaccines. In this modality, the vaccine is injected directly into the muscle, usually the deltoid muscle of the arm or the vastus lateralis muscle of the thigh in children [74]. IM administration is ideal for vaccines that require a gradual release in the body and a robust immune response. This route is used for vaccines against diseases such as influenza [75], tetanus [76], diphtheria [77], and hepatitis B [78]. The main advantage is the greater absorption. Moreover, it is effective for most protein-based or inactivated vaccines. However, it may cause pain and swelling at the injection site and it is not suitable for vaccines that require a rapid and immediate response [79].

Regarding the SC route, the vaccine is injected into the most superficial layers of the skin, below the epidermis, but above the muscle tissue. It is suitable for vaccines that need a slower and more constant release, and the advantage is that it is less painful than intramuscular administration, even if is less absorbed. Furthermore, it is more suitable for smaller doses of vaccine [80]. It is used for vaccines such as rubella [81] and smallpox [82].

With the ID the vaccine is directly injected into the most superficial layer of the skin, the dermis. The advantages include the stronger, localized immune response and the small amounts of vaccine that are needed. On the other hand, it requires precise injection techniques, and it may cause greater pain or irritation in the area of administration [83]. It is used for vaccines such as the tuberculosis vaccine (BCG) [84].

Moreover, the transdermal administration exists. It is a relatively new modality that takes advantage of patches or devices that use microneedles to introduce the vaccine through the skin [85]. These devices are designed to be noninvasive and easy to use. It is potentially painless and easy to administer, and it does not require specialized equipment such as syringes. However, this technology is still under development and it may be less effective for vaccines that require rapid action [86].

In addition, some vaccines, such as the intranasal influenza vaccine, are administered through the nose. These vaccines contain live attenuated viruses that stimulate an immune response in the nasal mucous membranes. It is non-invasive as it does not require an injection. Moreover, it stimulates a response in the respiratory tract, where many viral infections enter the body. However, it is suitable only for certain types of vaccines [87].

Furthermore, vaccines may be orally administered. In this case, after deglutition, they travel in the gastrointestinal tract to reach the intestine. Here, they are recognized and processed by intestinal immune system cells [88].

OS administration has a lot of advantages, in particular the easy administration, as it can be self-administered, improving patient compliance and the costs for the hospital and medical personnel. It is pain-free and avoids the anxiety associated with injections. In addition, the danger of an acute reaction is minimal. Furthermore, as it is cheaper than other types of vaccines due to the different manufacturing procedures, it is suitable for large groups of people, even those who live in less developed countries [89].

On the other hand, there are also critical points to be considered, as the gastrointestinal tract has a harsh environment due to the presence of a pH gradient and enzymes able to destroy the vaccine [89]. Examples of vaccines administered in this way are those against polio (oral polio vaccine, OPV) [90] and rotavirus vaccine [91].

2.4 OS vaccination

OS cancer vaccines are gaining attention as a promising immunotherapy strategy aimed at stimulating or enhancing a specific antitumor immune response. The OS administration route offers several advantages over traditional parenteral methods, for both patients and medical personnel, as it improves patient compliance and would not require authorized medical personnel [89], an aspect that can facilitate widespread vaccine distribution, particularly in resource-limited world areas [92,93].

OS vaccination also plays a critical role in engaging the immune system, especially in preventing carcinogenesis, by involving the intestinal mucosa. The gastrointestinal tract (GIT), known as the body's primary immunological site, houses about 70% of total lymphocytes [94,95], making it pivotal in immune responses [96]. Furthermore, the OS administration of the vaccine can trigger a dual immune response: a localized activation of the intestinal mucosa through immunoglobulin A (IgA) production and a systemic response mediated by immunoglobulin G (IgG) [96]. This emerging field of research holds great potential and is an exciting avenue for future advancements in cancer immunotherapy.

Despite their potential, OS administration of cancer vaccines remains largely experimental in current clinical practice, particularly because of its limitations. Indeed, OS administration requires an effective delivery system to protect the vaccine from the harsh gastrointestinal microenvironment [89]. In addition, this approach must break immune tolerance in the gut and activate antigen presentation in antigen-presenting cells (APC), particularly DCs, for the priming and activation of T lymphocytes, thus recognition and elimination of malignant cells [97].

2.4.1 Intestinal immune system and immunological basis of OS vaccination

The intestinal immune system is organized into two main compartments: the inductive compartment and the effector compartment [98]. The inductive sites, including Peyer’s patches, Microfold (M) cells, isolated lymphoid follicles, and mesenteric lymph nodes, are the regions where immune responses are initiated, and naïve T and B cells are activated. Meanwhile, the intestinal epithelium and lamina propria are essential for executing these immune responses, ensuring the system's effectiveness in maintaining gut immunity and overall health [98] (Figure 5).

In particular, M cells, located in the intestinal epithelium, are essential for mucosal immune response, as they transport antigens from the intestinal lumen and present them to the components of the immune system located in the lamina propria, such as DCs [99,100].

M cells are unique among intestinal epithelial cells due to their distinct morphology. They are characterized by short, irregular microvilli, called microfolds, and an invaginated plasma membrane that creates a niche for immunocompetent cells. Unlike their neighboring epithelial cells, M cells are covered by a thinner mucus layer and possess small cytoplasmic vesicles, a reduced glycocalyx, and fewer lysosomes, which contribute to their specialized role in immune surveillance [101]. Several M-cell-specific markers have been identified, including glycoprotein-2 (GP2), the transcription factor Spi-B (Spib), and the chemokine ligand CCL9 [99].

Antigen uptake by M cells is typically mediated by specific receptors such as β1-integrin, glycoprotein-1 (GP2), and others. Transcriptome analyses have revealed that M cells express various intracellular molecules likely involved in vesicular transport during the transcytosis process. However, the precise mechanisms by which intracellular transport regulates antigen transcytosis remain poorly understood and warrant further investigation [99,101,102].

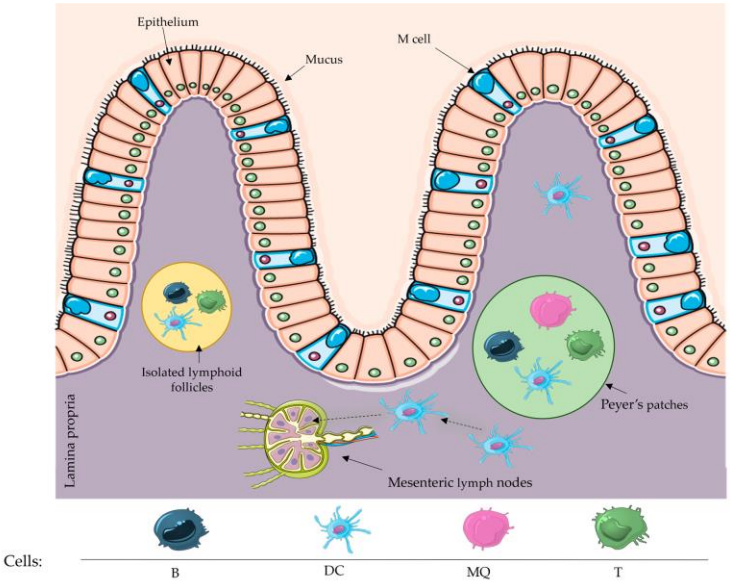

Figure 5. Structure of the intestinal immune system. Abbreviations: LP: lamina propria; cDCs: conventional dendritic cells; ILFs: isolated lymphoid follicles; PPs: Peyer's patches; MQ: macrophages [103].

Once the antigen crosses the epithelial barrier, particularly thanks to M cells, a cascade of cellular events is triggered within the organized lymphoid tissues and the mucosal lamina propria of the gut. DCs, along with naïve T and B lymphocytes, orchestrate the immune response to produce antigen-specific antibodies and cytotoxic T lymphocytes (CTLs) [100].

Antigen-loaded DCs in Peyer's patches and mesenteric lymph nodes (MLNs) secrete cytokines and stimulatory molecules, including TGF-β, IL-10, IL-6, and retinoic acid (a vitamin A derivative). These factors are essential for the development of antigen-specific Th2 lymphocytes and Foxp3+ T

regulatory cells (Tregs) [104,105]. Tregs can further differentiate into T-follicular helper cells (Tfh), a process described by Tsuji [106].

These T-helper subsets play a pivotal role in activating B lymphocytes to undergo IgA class switching. This process is driven by signals from the B-cell receptor, CD40-CD40L interactions, and cytokines such as IL-4, IL-5, IL-6, IL-10, TGF-β, and IL-21. In addition to T cell-dependent mechanisms, specific DC subtypes in PPs, such as TNF/iNOS-producing DCs (Tip-DCs), facilitate T cell-independent IgA class switching. They do so by increasing nitric oxide production, which enhances the expression of TGF-β receptors on naïve follicular B cells, promoting IgA class switching without requiring T cell involvement [107].

It has been observed that Tip-DCs, along with other subsets of DCs in Peyer's patches and mesenteric lymph nodes (MLNs), such as plasmacytoid and follicular DCs, can stimulate IgA antibody production by B cells within the follicles. This process bypasses the need for CD40-CD40L interactions and is instead driven by cytokines like BAFF and APRIL. Additionally, isolated lymphoid follicles (ILFs) and the lamina propria play critical roles in initiating the IgA immune response. Within ILFs, DCs secrete biologically active TGF-β1, while microbial stimulation through Toll-like receptor (TLR) signaling prompts DCs and stromal cells to produce BAFF and APRIL [107]. In the lamina propria, specific DC subsets expressing TLR5 respond to bacterial flagellin (FL) by secreting retinoic acid and IL-6, along with BAFF and APRIL. This activity is further supported by DCs expressing TNF-α and iNOS, which produce these cytokines through TLR signaling [107]. Epithelial cells also contribute to BAFF and APRIL secretion, promoting T-cell-independent IgA class switching, a process highlighted by Fagarasan [108]. However, its functionality in human systems remains under discussion, as noted by Berkowska [109].

IgA-committed B cells, generated through both T-cell-dependent and -independent pathways, differentiate into dimeric IgA-producing plasma cells in the lamina propria. This differentiation is regulated by Th2 cytokines IL-5 and IL-6. The dimeric IgA antibodies are then transported across epithelial cells into mucosal secretions through polymeric Ig-receptor-mediated transcytosis, ultimately releasing secretory IgA (sIgA) into the gut lumen [110].

While IgA is the predominant antibody in mucosal secretions, IgG also plays a significant role in the adaptive immune defenses of the gut. Most IgG in the gut lumen originates from the bloodstream, with a smaller portion produced locally [111]. Notably, IgG can be actively transported across the intestinal epithelium via the neonatal Fc receptor (FcRn), which is expressed in intestinal epithelial cells. This specialized receptor facilitates bidirectional movement of IgG across the epithelium. Although FcRn expression decreases after weaning in rodents, it remains

present in the absorptive intestinal epithelial cells of humans, pigs, and cattle throughout adulthood [112].

Intriguingly, FcRn also transports IgG-antigen complexes from the gut lumen to the underlying connective tissue, where they are delivered to APCs. This critical function, demonstrated by Yoshida, highlights FcRn's dual role in immune defense and antigen presentation within the intestinal mucosa [113].

Cytotoxic T lymphocytes (CTLs) in the mucosa are pivotal to the immune response initiated by OS vaccination. These CTLs play an essential role in defending against invasive pathogens, such as viruses and intracellular bacteria, that breach the mucosal barrier [114]. CTLs are primarily generated in Peyer's patches by CD8+ lymphocytes, which are activated by CD8α+ DCs and/or Th1 cells. Within mucosal tissues, several CD8+ lymphocyte populations exist, with a predominant presence of cells expressing T-cell receptors αβ (TCRαβ) in conjunction with CD8αβ or CD8αα. These subsets are closely associated with potent effector and cytotoxic activities [115].

CD8αβ+ TCRαβ+ CTLs, as demonstrated by Muller et al., exhibit strong cytotoxic activity against cells infected with viral pathogens and intracellular protozoan parasites [116].

Additionally, CD8+ T cells secrete cytokines such as IFN-γ and TNF-α [117], which enhance inflammatory responses in the lamina propria, thereby supporting phagocytic cells in eliminating bacteria that penetrate the mucosal barrier. Given the critical role of CTLs in mucosal immunity, it is essential to evaluate their involvement and effectiveness when designing OS cancer vaccines to ensure robust immune defense [118,119].

Effector B and T lymphocytes activated at intestinal mucosal induction sites possess a unique ability to migrate back to mucosal effector sites in the intestine [120,121].

After activation, these lymphocytes detach from stromal cells in structured lymphoid tissues and travel through the lymphatic system to the mesenteric lymph nodes (MLNs), where they undergo further differentiation. From there, they enter the bloodstream and disseminate throughout the intestinal mucosa [122].

The migration of lymphocytes to the intestine is directed by interactions between homing receptors on the lymphocytes and specific ligands on the vascular endothelium of the intestinal mucosa. Intestinal DCs play a crucial role in this process by secreting retinoic acid, which promotes the upregulation of intestinal homing receptors such as α4β7 integrin and the chemokine receptors CCR9 and CCR10. These receptors bind to molecules like MadCam-1, CCL25, and CCL28, facilitating targeted migration throughout the gastrointestinal tract [120,121,123].

In contrast, lymphocytes activated in peripheral lymphoid organs express molecules such as α4β1 integrin, L-selectin, and CCR4, which limit their movement toward mucosal surfaces [124]. This

distinct molecular expression pattern explains why OS vaccines, unlike injectable vaccines, are particularly effective at inducing mucosal immunity.

2.4.2 Challenges of OS vaccination

OS vaccines have the potential to induce different types of immunogenicity capable of supporting effective cancer therapy, but some key criticisms need to be discussed, as they limit this strategy. The first problem is represented by the GIT, characterized by a harsh pH gradient, enzymes able to degrade the vaccine, mucus layers, epithelial barriers, and microbiota [89] (Figure 6).

In addition, the immunogenicity of the vaccine can be low due to an incorrect choice of the antigen, the activation of tolerance mechanisms, and the immunosuppressive nature of the tumor microenvironment [125]. Overcoming these obstacles is critical for enhancing the efficacy of OS cancer vaccines.

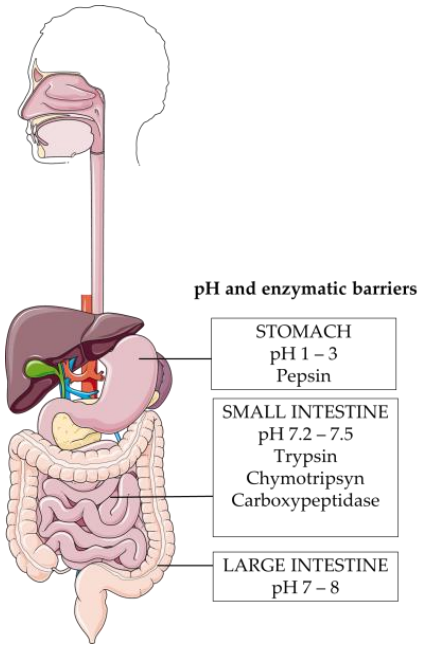

Figure 6. Barriers for antigens in the gastrointestinal tract (GIT). The harsh pH gradient and the presence of digestive enzymes in the GIT are the primary barriers to oral vaccination [103].

2.4.2.1 Harsh pH gradient

The first problem of the OS administration of vaccines regards the pH gradient that characterizes the GIT. Each section of the GIT exhibits a distinct pH, ranging from 1 to 8. In detail, the pH is between 1 and 3 in the stomach, approximately 7 in the small intestine, and between 7 and 8 in the large intestine [126,127].

This pH range can vary over time, depending on age, food intake, and pathological conditions. At birth, the pH of the stomach is higher but decreases rapidly, stabilizing throughout life [128]. Additionally, the stomach pH increases following food consumption, while the pH of the colon varies between individuals based on diet [129]. Pathological conditions, including colon cancer, inflammatory bowel disease (IBD), ulcerative colitis (UC) [130], and Crohn's disease (CD) [131], also significantly affect the pH of the colon.

The pH gradient impacts the stability of DNA, RNA, and proteins, where DNA remains stable across a wider pH range around physiological conditions compared to the RNA, and proteins and peptides are stable within a pH range close to their isoelectric point (pI); however, they can undergo unfolding, oxidation, hydrolyzation, or deamidation, leading to a loss of functionality [132].

As a result, cancer vaccines are vulnerable in different regions of the GIT depending on their pH sensitivity. Therefore, it is essential to provide protective measures to prevent vaccine inactivation and degradation.

2.4.2.2 Enzymatic degradation

The stability of OS cancer vaccines is significantly influenced by the enzymes within the GIT. Enzymes, both endogenous and those synthesized by host bacteria, play a critical role in catalyzing digestive reactions [133].

In the stomach, the most present enzymes are pepsins, peptidases that work in highly acidic conditions. These enzymes catalyze the cleavage of specific sites within proteins and peptides [134], leading to the hydrolysis of peptide bonds and the fragmentation of them, but also to the destruction of nucleic acids and bacterial membranes [129].

Pancreatic enzymes, including trypsin, chymotrypsin, carboxypeptidase A, carboxypeptidase B, and elastase, contribute to the rapid degradation of peptides [129]. For instance, studies have shown that insulin is degraded by pancreatic enzymes within just one hour of administration.

Once peptides and nucleic acids reach the small intestine, they are further processed by enzymes such as aminopeptidases, endopeptidases, and enteropeptidases. These enzymatic actions prepare the products for absorption into the bloodstream via capillaries [135].

In summary, an OS vaccine undergoes significant biochemical alterations in the GIT due to the action of proteolytic enzymes. These alterations can impact its potency and efficacy; therefore, it is essential to account for the enzymatic barrier during vaccine development.

2.4.2.3 Mucus barrier

The mucus forms a protective barrier that lines the entire gastrointestinal tract and plays a crucial role in maintaining homeostasis in the body. It is composed primarily of water (90-95%), along with lipids (1-2%), electrolytes, proteins, and other components. Its high-water content gives mucus its fluid nature, while its viscoelastic properties are attributed to its main structural proteins, the mucins [136].

Mucins are highly O-glycosylated glycoproteins [137,138]. They are classified into two categories: transmembrane mucins and gel-forming mucins. Transmembrane mucins are located on the apical surface of enterocytes and contribute to the formation of the glycocalyx. In contrast, gel-forming mucins, which exhibit gel-like properties, are secreted by goblet cells [139,140]. Among these, MUC2 is the primary component and the most extensively studied [137].

The mucus layer has various functions, all essential for maintaining tissue homeostasis. It acts as the first barrier between the external environment and the body, protecting against bacteria, toxins, digestive enzymes, and antigens in general. Larger antigens are excluded from penetrating the mucus due to their size, while smaller particles–can bypass the barrier by interacting with hydrophobic and charged residues within the mucus [141].

The mucus also protects intestinal epithelial cells from dehydration and mechanical stress caused by peristalsis. This protection is due to the lubricating properties of mucins, which arise from their glycan composition. Furthermore, the relationship between mucus and the immune system has been investigated [141]. Specifically, MUC2 can interact with DCs in the small intestine, regulating immune responses by facilitating antigen sampling and promoting immune tolerance [142].

The physical and chemical properties of mucus, along with its functions, can pose challenges to the diffusion of protein and peptide-based cancer vaccines and hinder the activation of an immune response. To address these challenges, researchers have explored substances with mucoadhesive properties or those that can enhance absorption by overcoming the limitations of the mucus barrier.

2.4.2.4 Epithelial barrier

The intestinal epithelium, along with the mucus layer, works as a physical barrier protecting the body from foreign antigens. This monolayer is composed of various cell types, including enterocytes, Paneth cells, goblet cells, and M cells [143]. While each cell type has distinct functions, they collectively maintain the integrity of the intestinal barrier and ensure tissue homeostasis [144].

Molecules can cross the intestinal epithelium through three primary pathways: the transcellular, carrier-mediated, and paracellular pathways. The transcellular pathway involves passive diffusion across the cell membrane. The carrier-mediated pathway relies on specific carriers and receptors to facilitate transcellular uptake. The paracellular pathway, on the other hand, is characterized by passive diffusion between adjacent cells. Molecule absorption via the paracellular route depends on tight junctions that connect neighboring epithelial cells [145]. These tight junctions are composed of various transmembrane and cytosolic proteins, such as occludins, claudins, zonula occludens, and junctional adhesion molecules. Moreover, these proteins interact with the cytoskeleton to maintain a robust and selective barrier between cells [145].

When the intestinal epithelial barrier works optimally, these pathways enable the absorption of nutrients, water, and essential ions while simultaneously preventing the uptake of foreign antigens, proteins, and lipids [146].

Due to the strong barrier properties of the intestinal epithelium, the absorption of OS protein-based cancer vaccines is highly challenging [103]. However, vaccine structures can be specifically designed to include components that target enterocytes, particularly M cells [147,148].

2.4.2.5 Gastrointestinal microbiota

The intestine homes over 1000 bacterial species, predominantly from the phyla Firmicutes, Bacteroidetes, and Actinobacteria. The collective genome of these microorganisms is called the microbiome [149]. Since the composition of the microbiota varies among individuals, each person possesses a unique microbiome [150]. These interindividual differences have been shown to influence bacterial drug metabolism, leading to variations in drug toxicity and efficacy. While it is well established that gut bacteria can alter the pharmacokinetics and pharmacodynamics of drugs, further research is needed to fully understand the mechanisms underlying these processes [151].

In general, the microbiota can interfere with drugs, including therapeutic proteins and peptides, through several mechanisms, such as producing metabolites that affect drug metabolism, synthesizing enzymes that modify or inactivate drugs, and altering the expression of genes encoding metabolic enzymes [151].

For example, proteins are the primary substrate for the production of short-chain fatty acids (SCFAs) and metabolites, which are generated by the gut microbiota during proteolytic fermentation [152,152,153].

As a result, OS cancer vaccines are vulnerable to inactivation by bacterial enzymes and metabolites in the intestine. To address this challenge, it is essential to develop delivery systems that protect OS vaccines from the microbiota and prevent their degradation

2.4.2.6 Low immunogenicity

Although OS cancer vaccines have the potential to elicit a broader spectrum of immunogenicity compared to parenteral vaccines, their overall immunogenicity is typically low. This necessitates the development of specific strategies to enhance their effectiveness [154].

A critical factor to consider is the choice of the antigen. Cancer vaccines should target highly immunogenic antigens to elicit a robust T-cell response against tumor cells. TSAs are generally more immunogenic than TAAs. TSAs are recognized by T cells with high affinity due to their tumor specificity, whereas TAAs are more prone to tolerance mechanisms [154].

In addition to the antigen, the type of vaccine plays a pivotal role in immunogenicity. For nucleic acid-based cancer vaccines, DNA vaccines face challenges related to efficient transfection, while mRNA vaccines suffer from instability [69]. For protein and peptide-based cancer vaccines, immunogenicity is influenced by their length. Short peptides, typically around nine amino acids, bind directly to MHC molecules without requiring processing but are quickly degraded. In contrast, long peptides, around 30 amino acids, are internalized and processed by APCs before being presented by MHC molecules, resulting in stronger immunogenicity compared to short peptides [155].

Beyond antigen selection, several factors can influence the immune response, including immune cell exhaustion following prior therapies, aging, and the immunosuppressive tumor microenvironment [154].

Strategies to enhance the immunogenicity of vaccines, particularly those targeting TAAs, include modifying amino acid sequences to increase their affinity for HLA molecules and incorporating adjuvants. To address the immunosuppressive tumor microenvironment, polytherapy can be employed to counteract immune escape mechanisms.

2.4.3 Strategies to overcome the limitations of OS vaccination

For improving cancer vaccine protection and immunogenicity, adjuvants, targeting strategies, and specialized delivery systems can be used.

Adjuvants are substances that enhance the immune response, thereby improving vaccine efficacy. Therefore, they are particularly useful in addressing the low immunogenicity of OS cancer vaccines. In recent years, numerous OS adjuvants have been studied, which can be broadly classified into different categories: toxin derivatives, Pathogen Recognition Receptor (PRR) ligands, also known as pathogen-associated molecular patterns (PAMPs), Gut-peptide cell adjuvants, and cytokines [156] (Table 1).

Cholera toxin (CT) and heat-labile enterotoxin (LT) are the most studied toxin derivatives as they can activate APCs and promote an IgA response [157]. Additionally, these adjuvants promote the differentiation of intestinal stem cells into M cells, increasing the internalization of the vaccine by intestinal epithelium and improving immune surveillance in the lamina propria [158,159].

However, both CT and LT exhibit high toxicity in humans. To address this issue, modified versions such as multiple mutant cholera toxin (mmCT) and double mutant heat-labile enterotoxin (dmLT) have been developed. These modifications aim to retain their adjuvant properties while significantly reducing their toxicity [160].

PAMPs, on the other hand, are recognized by their corresponding PRRs, which are essential for host defense against pathogens. PRRs can be categorized into Toll-like receptors (TLRs), NOD-like receptors (NLRs) [161], RIG-I-like receptors (RLRs) [162,163], and C-type lectin receptors (CLRs) [163], the latter of which also play a role in microbial sensing. These receptors are expressed by various cell types, including intestinal epithelial cells and APCs, and are located either in the cytoplasm or on the plasma membrane. Recent studies have demonstrated that incorporating PAMPs into OS vaccine formulations targeting PRRs can enhance vaccine immunogenicity, particularly by increasing the production of IgA and IgG antibodies [164].

Type of Adjuvants	**Subtypes**
Toxin derivatives	Cholera toxin (CT) Labile enterotoxin (LT)
Pattern-Recognition Receptor (PRR) ligands	Toll-like receptor (TLR) ligands NOD-like receptor (NLR) ligands RIG-I-like receptor (RLR) ligands C-type lectin receptor (CLR) ligands
Gut Peptide Cell Adjuvants	M-Cell Peptides/Ligands
Cytokine Adjuvants	IL-1β, IL-2, IL-12

Table 1. Type of adjuvants for oral vaccine. To improve the immunogenicity of oral vaccines, different types of adjuvants can be used, including toxin derivatives, Pattern-Recognition Receptor (PRR) ligands, gut peptide cell adjuvants, and cytokines [103].

In addition to adjuvants, targeting enterocytes, M cells, and APCs offers a solution to bypass the mucus and epithelial barriers that limit the efficacy of OS vaccines. These cells are characterized by distinct marker molecules that can be leveraged to enhance the uptake of OS vaccines and trigger an immune response in the gut-associated lymphoid tissue (GALT). Examples of M-cell markers

include clusterin, Cathepsin E [147], Glycoprotein 2 (GP2) [148], Sialyl Lewis A antigen [165], and the complement 5a receptor (C5aR) [166]. For enterocyte targeting, the neonatal Fc receptor (FcRn) is the most studied marker. This receptor facilitates the internalization of IgG antibodies through transcytosis by interacting with their Fc segment. The effectiveness of this approach was demonstrated by Pridgen, E. M., and colleagues, who used FcRn-targeted NPs to target the intestinal epithelium. They showed that targeted NPs achieved an absorption efficiency of 13.7%, compared to just 1.2% for non-targeted NPs [167].

Targeting of APCs, particularly intestinal DCs, triggers their maturation and activation. For this purpose, OS vaccines can be delivered to DCs by adding PAMPs or other receptor ligands, such as lectins or FcRn, to the vaccine formulation [168,169].

Identifying the most suitable markers for targeting intestinal cells following OS vaccine administration still requires further research. However, the fact that this approach holds promise for enhancing the effectiveness of OS vaccines offers new hope for improving their impact.

Various delivery systems can be employed to protect the vaccine, enhance its absorption by the intestinal epithelium, allow a controlled release of the vaccine [170], and boost the immune response. These systems can be categorized into live and non-live delivery systems. Live delivery systems include recombinant bacterial and viral vectors. Their proteins are recognized by PRRs. Thus, they work both as vaccine vectors and immunopotentiators. Among recombinant bacteria, lactic acid bacteria and Salmonella strains are the most promising, while adenoviruses are the better choice as viral vectors [171,172].

Non-living delivery systems encompass virus-like particles (VLPs), microparticles, and NPs. These platforms have a low immunogenicity but offer high protection to the vaccine during its transit through the gastrointestinal tract [171]. In detail, coated VLPs, which resemble viruses but lack genetic material, can safeguard the vaccine from the harsh gastrointestinal environment, preserve its properties, and promote the breakdown of immune tolerance [173,174].

Additionally, micro- and NPs, especially those made from polymers, such as poly(lactic-co-glycolic acid) (PLGA), protect the internalized material from degradation in the gastrointestinal tract [175]. Furthermore, polymeric materials enhance the internalization of particles by APCs, thereby contributing to immune system stimulation. Moreover, their design allows a controlled release of the vaccine. For these reasons, NPs represent a promising solution to address the challenges associated with the OS administration of cancer vaccines [176,177].

2.4.4 Flagellin from *Salmonella typhi* as an adjuvant for OS immunization

Salmonella typhi flagellin (FL), the main structural protein of the bacterial flagellum, has emerged as a potent immunostimulatory agent with significant potential as an adjuvant for OS vaccines. FL is recognized and interacts with the pathogen-recognition receptor Toll-like receptor 5 (TLR-5) and it binds it through its D1 domain [178].

TLR5 is composed of three domains: an extracellular region with leucine-rich repeats (LRRs), a transmembrane segment, and a Toll/Interleukin-1 receptor (TIR) domain [179].

The ability of this receptor to recognize FL is related to specific conserved amino acid residues located at both the N- and C-terminal ends of the protein. When TLR5 recognizes and binds FL, it undergoes structural rearrangement, leading to the formation of a symmetrical dimer that brings its intracellular TIR domains into proximity. This dimerization process is critically influenced by residues 12 and 13 within the LRR region [178,179].

In detail, TLR-5-FL complex can activate both MyD88-dependent and MyD88-independent pathways. In the MyD88-dependent pathway, downstream adapter molecules are recruited to stimulate the MAP kinase and IκB kinase cascades, ultimately leading to the activation of AP-1 and NF-κB transcription factors, which regulate numerous immune-related genes [179].

On the other hand, the MyD88-independent pathway involves the formation of a TLR5/TLR4 heterodimeric complex. It leads to the activation of the TRIF-mediated pathway, which results in the production of IFN-β via the IRF3 transcription factor. IFN-β, in turn, activates STAT1, which enhances the transcription of inducible nitric oxide synthase (iNOS), thus an increase in the NO production [179].

Finally, this regulation leads to the production of proinflammatory cytokines and a robust immune response that involves both the systemic and mucosal immune system, including the production of antigen-specific IgA and IgG [179,180]. As an example, it has been demonstrated that *Salmonella* FL can trigger the production and release of the chemokine CCL20 in intestinal epithelial cells. The release of CCL20 promotes the chemotaxis of immature DCs. Consequently, DCs transport the pathogen from the intestinal mucosa to deeper tissues, including mesenteric lymph nodes. Thus, the ability of FL to induce chemokine secretion is likely to be a key factor in facilitating the recruitment of DCs to the subepithelial compartments of Peyer's patches and villi [181].

TLR5 is widely expressed across different cell types, such as monocytes, macrophages, neutrophils, lymphocytes, natural killer (NK) cells, DCs, epithelial cells, and lymph node (LN) stromal cells. It is particularly abundant in the gut, especially in the intestinal epithelial cells and intestinal DC [179].

These findings underscore the potential of *S. Typhi* FL as an effective immunomodulator in OS vaccination strategies, paving the way for the development of novel vaccines against mucosal infections.

2.5 Nanotechnology and Nanomedicine

Nanotechnology is an interdisciplinary scientific field centered on the manipulation of matter at the atomic and molecular scale, typically within the 1 to 100 nanometer range. Its foundations trace back to Richard Feynman's groundbreaking 1959 lecture *"There's plenty of room at the bottom,"* in which he envisioned the possibilities of manipulating matter atom by atom, but it gained significant traction in the late 20th century with the discovery of advanced nanomaterials like fullerenes and carbon nanotubes, revolutionizing multiple industries [182,183].

Nanotechnology has been developed rapidly and will be increasingly involved in science and technology applications, such as the computer industry, bioprocessing industry, agricultural industry, food industry, packaging industry, construction industry and civil engineering, textiles industry, transport and automobile industry, healthcare and medical field [184].

2.5.1 Nanomedicine in cancer therapy

Nanomedicine has emerged as an innovative approach in cancer treatment to overcome the challenges associated with therapies, such as chemotherapy and immunotherapy (Figure 7). NPs might offer enhanced drug targeting to the tumor site, and controlled drug release, significantly optimizing treatment efficacy while reducing systemic toxicity [185]. For example, nanocarriers are able to improve the solubility, bioavailability, and targeting of chemotherapeutic agents, mitigating adverse effects associated with non-specific drug distribution [186]. Therapies based on the immune system, such as immune checkpoint blockade and cancer vaccines, can be improved by nanotechnology, as it facilitates the delivery, the antigen presentation, and sustained immune activation. Nanomedicine is a promising strategy for the future of precision oncology thanks to its capacity to enhance drug stability, targeting efficiency, and reducing off-target effects [185,186].

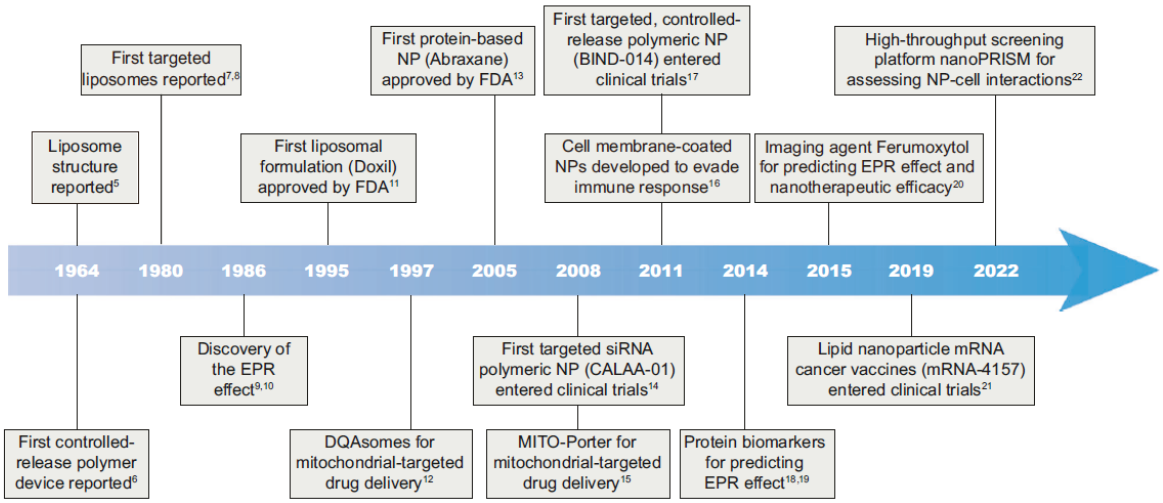

Figure 7. Key events in the history of cancer nanomedicine. Abbreviation: DQAsomes: dequalinium-based liposome-like vesicles; EPR: enhanced permeability and retention; FDA: US Food and Drug Administration; MITO-Porter: octaarginine (R8)-modified liposomes composed of 1,2-dioleoyl-sn-glycero-3-phosphoethanolamine and sphingomyelin; mRNA: messenger RNA; PRISM: Profiling relative inhibition simultaneously in mixtures; siRNA: small interfering RNA [185].

2.5.2 Classification of NPs used in nanomedicine

NPs used in nanomedicine can be classified based on their composition, size, shape, and surface properties. The main classification refers to the composition, as the NPs can be organic, derived from natural materials or synthetic polymers [187], and inorganic, generally based on metals or carbon [188]. Organic NPs include liposomes, polymeric NPs, and dendrimers, while inorganic NPs include gold NPs, quantum dots, and silica-based NPs [189]. Organic NPs are widely used for drug delivery due to their biocompatibility and biodegradability, while inorganic NPs offer unique optical, magnetic, and electrical properties that enhance imaging and therapeutic applications [187,190]. Moreover, size and shape significantly influence the biological interactions and biodistribution of NPs. The range of the size is about 1-100 nm, while about the shape, NPs can be spherical, cylindrical, conical, tubular, hollow core, spiral, or irregular. Spherical NPs are the most common [189]. In addition, NP can be distinguished depending on their surface properties, including charge and hydrophilicity, characteristics that play a crucial role in determining circulation time and immune system recognition [189]. Considering the different frameworks that a NP can have, is essential for optimizing NP design in personalized nanomedicine and precision therapy.

2.6 Poly(lactic-co-glycolic acid) (PLGA) NPs

2.6.1 Physicochemical and Biological Properties of PLGA NPs

PLGA (poly(lactic-co-glycolic acid)) is a copolymer extensively used for the preparation of NP with medical aims, as it has received approval from both the FDA and the European Medicines Agency thanks to its biocompatibility and biodegradability [191].

PLGA is composed of two monomers, lactic acid (LA) and glycolic acid (GA) [192] (Figure 8). This copolymer is typically synthesized via a catalyst-mediated ring-opening copolymerization process, forming ester linkages between its monomeric units. PLGA is degraded by hydrolysis in the body, ultimately metabolizing into its respective endogenous components. Once hydrolyzed, both LA and GA enter the metabolic pathways. This composition and type of degradation ensure minimal toxicity and make PLGA highly biocompatible [192].

The PLA and PGA ratio strongly influences the physicochemical properties of PLGA, such as the degradation rate. Indeed, a higher PLA/PGA ratio results in increased hydrophobicity, leading to slower degradation and extended drug release, as PLA (poly(lactic acid)) is more hydrophobic than PGA (poly(glycolic acid)). Conversely, an increase in PGA content accelerates degradation of PLGA [191]. Additionally, molecular weight significantly impacts both polymer degradation and NP size, influencing drug release kinetics. PLGA with low molecular weight degrades more rapidly, produces smaller NPs, and exhibits a good ability to bypass biological barriers and reach target tissues, even if the drug-loading capacity tends to be low [191].

The shape and surface properties of PLGA NPs play a crucial role in their biological behavior. For example, needle-shaped NPs may exhibit higher cellular uptake compared to spherical ones, therefore facilitating more efficient intracellular drug delivery. However, the problems of the NPs with this needle-shape are the cytotoxic effects. Indeed, they tend to damage lysosomal membranes and trigger apoptosis [193].

Furthermore, the cellular uptake can be improved by modifying the surface charge of the NPs, which is negative for PLGA. Still, this aspect can be modified through the functionalization with polyethylene glycol (PEG) [194] or chitosan [195,196], which neutralize or render the surface cationic, improving the interaction between NPs and cell membranes. In addition, PEGylation extends the blood circulation time of NPs by preventing opsonization and phagocytosis, enhancing their pharmacokinetic profile. However, this effect may also reduce cellular uptake, potentially affecting therapeutic efficacy [197].

Moreover, the versatility of PLGA allows for its combination with other polymers, beyond PEG and chitosan. For example, polyvinyl alcohol (PVA) is used to stabilize the structure of NPs [198],

and D-α-tocopheryl PEG 1000 succinate (TPGS) to fine-tune its degradation rate, hydrophobicity, and drug release properties [199].

Additionally, various copolymer architectures, including block and grafted structures, can be synthesized using PLGA in combination with other polymers like poly(caprolactone) (PCL) and polyethylenimine (PEI) [200].

By adjusting polymer composition, molecular weight, and surface modifications, PLGA-based NPs can be tailored to achieve optimized therapeutic outcomes in diverse biomedical applications.

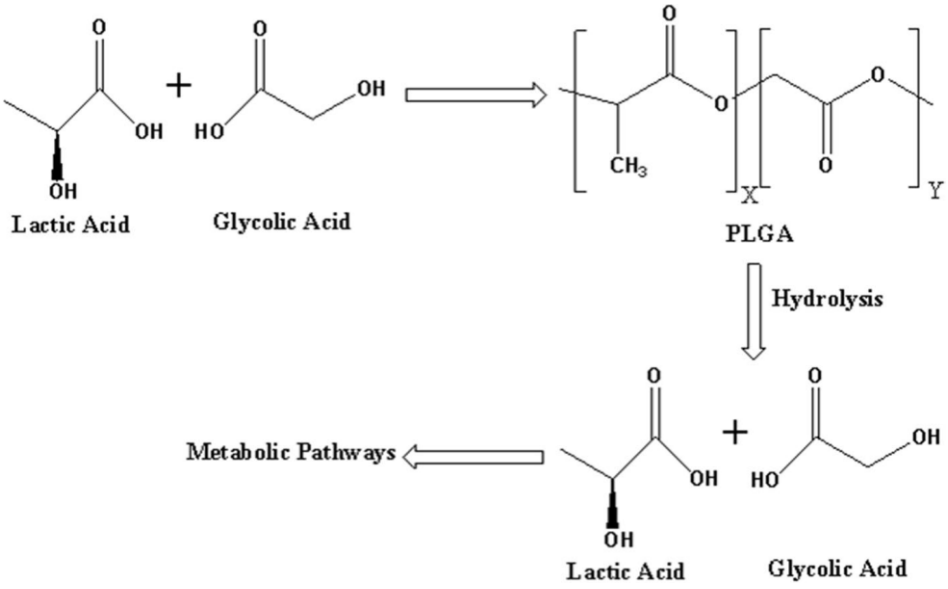

Figure 8. The copolymer PLGA (poly(lactic-co-glycolic acid)). Description of PLGA preparation and metabolism, with X and Y indicating the quantities of lactic acid and glycolic acid units, respectively [201].

2.6.2 Preparation of PLGA NPs

2.6.2.1 Emulsion-solvent evaporation method

The most employed method used for the preparation of PLGA NPs is the emulsion-evaporation method (Figure 9). This approach can be categorized based on the type of emulsion formed (single, such as oil-in-water [O/W], or double/multiple, such as water-in-oil-in-water [W/O/W]) [202]. In this process, PLGA polymers and hydrophobic drugs are dissolved in water-immiscible organic solvents like chloroform or dichloromethane [203]. This solution is then introduced into an aqueous phase containing a surfactant, such as poly(vinyl alcohol) (PVA), to create an O/W emulsion. Then,

a nanodroplet dispersion is generated in the emulsion using high-speed homogenization or ultrasonication. Following this, a suspension of NPs is obtained after the evaporation of the organic solvent by continuous magnetic stirring at room temperature or in a slow process of reduced pressure. The resulting NPs are washed and collected by a different number of centrifugation steps [203].

The emulsion method is versatile, allowing the encapsulation of both hydrophobic and hydrophilic drugs. However, this technique presents some challenges, such as the need for heat or vacuum for solvent removal and the incomplete elimination of stabilizers.

The dimensions of NPs obtained with this method are 200-300 nm [204].

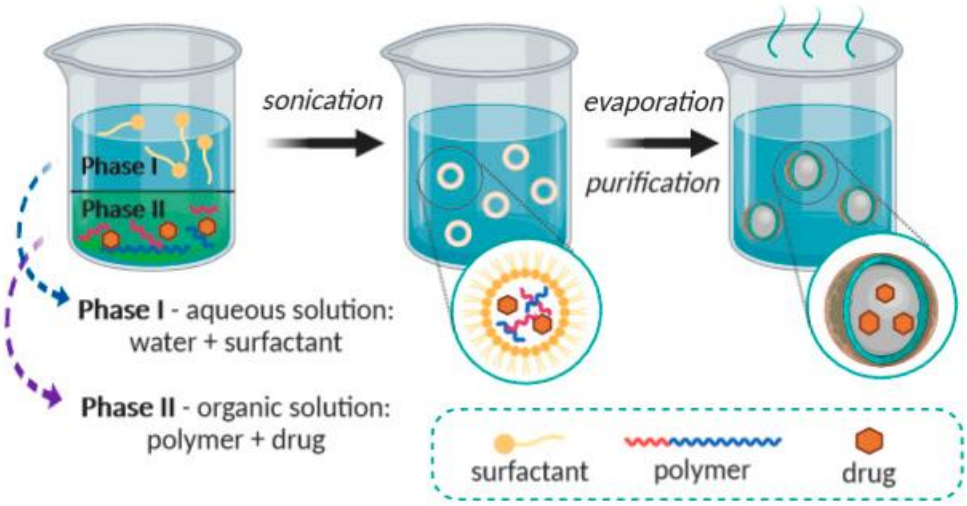

Figure 9. The Emulsion-solvent evaporation method. Schematic representation of the emulsion solvent evaporation method for the preparation of PLGA nanoparticles (NPs) [203].

2.6.2.2 Salting out

Another method for the production of PLGA NPs is called salting out (Figure 10). The salting-out method relies on the separation of a water-miscible solvent from an aqueous solution, driven by a salting-out effect that can lead to the formation of nanospheres. In detail, the drug and polymer are first dissolved in a water-soluble polar solvent. This solution is then introduced into an aqueous phase containing a salt, such as magnesium chloride ($MgCl_2$) or calcium chloride ($CaCl_2$), along with a stabilizing agent. The mixture is vigorously stirred to achieve a uniform emulsion [205].

To reduce the ionic strength of the electrolyte, distilled water is gradually introduced into the prepared oil-in-water (O/W) emulsion under magnetic stirring. During this process, hydrophilic organic solvents diffuse from the oil phase into the aqueous phase, promoting the formation of NPs.

In the final step, the salting-out agent is removed through centrifugation, and the resulting samples are purified [205].

The nanospheres produced using this method range in size from 170 to 900 nm. By adjusting the polymer concentration in the internal phase and the volume of the external phase, the average diameter can be tuned between 200 and 500 nm [204].

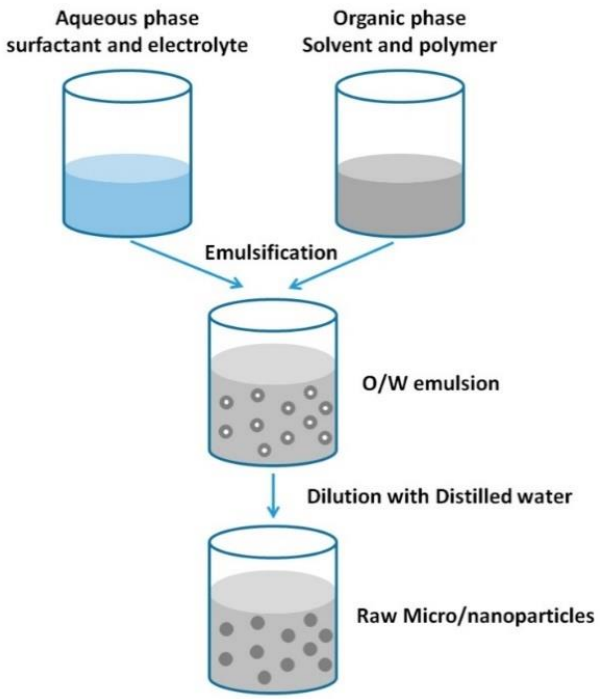

Figure 10. The salting out method. Schematic representation of the salting out method for the production of PLGA nanoparticles (NPs) [205].

2.6.2.3 Nanoprecipitation

The nanoprecipitation technique, also known as the solvent displacement method, involves the use of two miscible solvents (Figure 11). The internal phase typically consists of a polymer dissolved in a water-miscible organic solvent such as acetone or acetonitrile. These solvents, being immiscible with water, can be easily removed through evaporation [203]. The core principle of this method lies in the interfacial deposition of the polymer, which occurs when the organic solvent diffuses from a lipophilic phase into an aqueous environment [206]. In practice, the polymer is dissolved in a solvent of intermediate polarity that mixes well with water, and this solution is then gradually introduced into an aqueous phase under stirring or by controlled addition rate. As a consequence, the rapid diffusion of the solvent into the water leads to the immediate formation of NPs, driven by

the polymer's tendency to avoid contact with water. As the solvent leaves the nanodroplets, the polymer precipitates, resulting in either nanospheres or nanocapsules [203].

The NPs produced via this method usually have a uniform size and a narrow distribution, often surpassing those formed by emulsion-solvent evaporation techniques. Nanoprecipitation is widely employed for creating polymer-based NPs around 120- 170 nm in size [204].

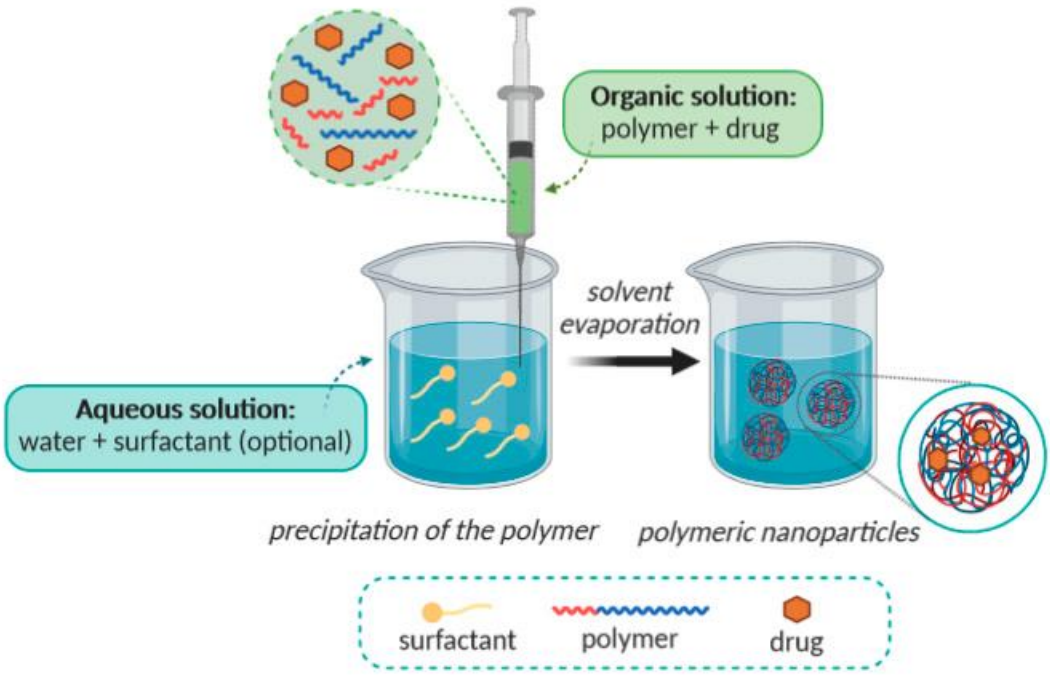

Figure 11. The nanoprecipitation method. Schematic representation of nanoprecipitation method for the preparation of PLGA nanoparticles (NPs) [203].

2.6.2.4 Microfluidic

The microfluidic technique is a sophisticated method that allows for the creation of NPs with precise size control and consistent reproducibility. It operates by processing small liquid volumes, typically in the micro- or nanoliter scale, within a microchannel. Microfluidic systems can be categorized based on the type of reagent flow into two types: (a) continuous-phase flow and (b) droplet-phase flow [207,208] (Figure 12).

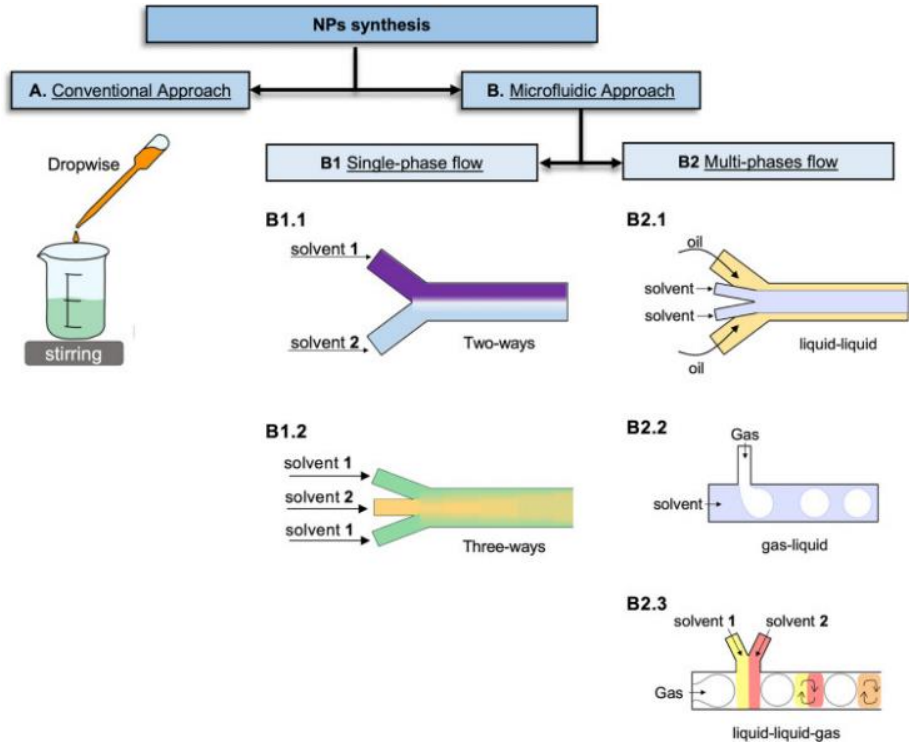

Figure 12. Microfluidic. Schematic representation of the two types of microfluidic systems: single-phase flow (also called continuous-phase flow) and multiphase flow (also called droplet-phase flow). The image shows (A) the dropwise technique; (B) different design of microfluidics chips that can be employed for the nanoparticles (NPs) production depending on the flow used. They can be categorized into (B1) single-phase flow featuring either (B1.1) two-way channels or (B1.2) three-way channels, and (B2) multiphase flow systems, that can be (B2.1) liquid-liquid, (B2.2) gas-liquid, and (B2.3) liquid liquid-gas [208].

In the context of NP production using microfluidic devices, the continuous flow systems, also called single-phase flow systems, are among the most widely employed approaches. Their popularity stems from their straightforward design, consistent reaction environment, and high adaptability in controlling key process parameters such as flow rate, reagent concentration, reaction time, and temperature [209,210].

Typically, single-phase preparation is carried out under laminar flow conditions, characterized by a Reynolds number below 10. In this regime, turbulence is absent, and mixing primarily occurs through molecular interdiffusion. As a result, continuous flow microfluidics offers a reliable platform for nanoprecipitation, enhancing the precision, reproducibility, and uniformity of NP characteristics. The controlled and homogeneous environment provided by single-phase systems is especially suitable for producing small NPs with narrow size distributions, an essential requirement in pharmaceutical applications [210].

However, molecular interdiffusion is inherently slow, which can limit the overall reaction rate [211]. Additionally, single-phase flow reactors exhibit a parabolic velocity profile, leading to a

nonuniform residence time distribution [212]. This becomes particularly problematic in NP preparation, where the early-stage crystallization kinetics are sensitive to residence time. Consequently, particles traveling near the channel walls may grow larger than those in the center. These limitations, however, can be addressed by introducing turbulence through geometric modifications such as channel bending, folding, or stretching, thereby improving mixing efficiency [210].

In contrast to single-phase microfluidics, droplet-phase flow systems, also called multiphase or segmented flow systems, involve the use of two or more immiscible fluids. These heterogeneous flow regimes promote passive mixing by improving mass transfer, reducing residence time variability, and limiting reagent or product accumulation along the channel walls [213].

As the name suggests, droplet-based microfluidics centers on the generation and manipulation of individual droplets within microchannels. The formation of these droplets is governed by factors such as channel geometry, dimensions, and the flow rates of the participating fluids, which allows for precise control over material preparation processes [214].

Multiphase systems are typically divided into two categories: gas-liquid (bubble-based) and liquid-liquid segmented flows. Gas-liquid flows are especially attractive due to the ease of separating gas from liquid, making them suitable for NP production [210]. In these systems, reactions occur within segmented liquid slugs, with gas segments inducing internal circulation and enhancing mixing efficiency. Bubbles can be generated through active means, such as high-voltage pulses, acoustic microstreaming, or liquid metal actuators, or passively, by simply introducing gas into the liquid stream [208]. These techniques often take advantage of the microchannel surface roughness to accelerate mixing and homogenization. Depending on the relative velocities of gas and liquid, annular flow patterns may also arise, characterized by a gas core flowing through the center of the channel, surrounded by a liquid film [210].

In liquid-liquid segmented flow systems, droplet formation results from interfacial tension between the immiscible liquid phases. Commonly observed configurations include water-in-oil and oil-in-water dispersions, which often require surfactants to prevent droplet coalescence [215].

Due to their fast processing and analytical capabilities, droplet-based systems are ideal for producing particles with tailored sizes, shapes, and morphologies-features that are otherwise difficult to control. Furthermore, droplet microreactors offer enhanced mass and heat transfer, precise fluid manipulation, efficient automation, and high production throughput. Consequently, multiphase flow platforms have become vital tools in a wide range of scientific fields. They are widely used for creating emulsions, microdroplets, microparticles, and NPs with customized structures, and can even function as miniature reaction chambers for cell culture applications [210].

Nonetheless, certain limitations must be addressed when working with multiphase systems. One common issue is the instability of droplets, which can sometimes be mitigated with surfactants, though this is not always appropriate, depending on the application. Additionally, complete isolation between droplets is rarely achieved, as some degree of material exchange typically occurs. Whether these drawbacks impact the outcome largely depends on the specific goals of the microfluidic application [210].

2.6.3 Application in cancer medicine of PLGA NPs

PLGA NPs have emerged as a promising tool in cancer therapy and broader biomedical applications due to their tunable physicochemical properties, targeted drug delivery capabilities, biocompatibility, and biodegradability [216]. The principal physicochemical characteristics, such as molecular weight, LA/GA ratio, morphology, surface charge, and hydrophobicity, influence the performance of PLGA NPs [216]. Moreover, these NPs can be engineered for various targeting strategies, including passive targeting through the enhanced permeability and retention (EPR) effect and active targeting via surface modifications to interact with cancer cells and their receptors [217]. Thanks to their versatility, PLGA NPs can be applied in multiple therapeutic approaches, including chemotherapy, gene delivery, immunotherapy, photothermal therapy, and hyperthermia [216,218]. Additionally, PLGA NPs can incorporate stimuli-responsive drug release mechanisms and magnetic targeting, further enhancing their potential in precision medicine. Their versatility makes them a powerful platform for cancer treatment and broader medical applications, ensuring controlled drug release and reduced systemic toxicity [216].

2.6.4 PLGA NPs for cancer immunotherapy

PLGA has emerged as a key component in cancer immunotherapy due to its ability to engage and modulate the immune system [219]. One of its primary actions involves stimulating APCs, such as DCs and macrophages, to internalize antigens [220,221]. This process enhances both humoral and cellular immunity by facilitating antigen presentation through MHC class I and II. The antigen processing cascade typically includes endosomal escape, proteasomal degradation, and subsequent antigen loading either in the endoplasmic reticulum or within endosomal compartments [222].
Beyond its role in antigen delivery, PLGA has been shown to influence immune signaling more broadly. It can modulate inflammatory responses, reduce neuroinflammation after central nervous

system injury, and shift microglia from a pro-inflammatory to an anti-inflammatory state, especially in response to stimuli like lipopolysaccharide. Furthermore, PLGA can suppress immune cell activation within the CNS and promote their redistribution to peripheral immune organs such as the spleen [219,223].

These various immunomodulatory effects stem from PLGA ability to enhance antigen presentation, fine-tune inflammatory pathways, amplify the immune effects of therapeutic antigens, and interact with various immune cell populations. Short-term immune activation includes rapid stimulation of DCs and T lymphocytes, particularly when PLGA NPs are used to deliver potent immunoadjuvants such as CpG oligonucleotides, which can also activate natural killer cells [224]. In the long term, PLGA systems contribute to the establishment of memory T cells, offering durable immune surveillance against tumor recurrence. Crucially, appropriately engineered PLGA formulations can prevent immune tolerance toward therapeutic antigens, thereby sustaining immune activity over time [224]. These insights highlight the importance of understanding how PLGA is involved in the immune system interactions for the rational design of advanced, long-acting immunotherapeutic strategies based on targeted delivery, synergistic combinations, and controlled release mechanisms [219].

2.6.5 PLGA/PVA NPs for OS delivery

OS administration route remains the most patient-friendly and convenient method for drug delivery, but it is often limited by poor drug stability in the harsh gastrointestinal microenvironment, and low bioavailability, particularly for biologics such as peptides, proteins, and nucleic acids [89].

PLGA NPs have shown significant potential as OS delivery systems for therapeutic agents such as drugs and vaccines. Their biocompatibility, and the ability to protect labile compounds from harsh conditions, and to control their release, make them particularly attractive for overcoming the limitations of OS administration [89].

Upon OS intake, PLGA NPs can protect encapsulated molecules from pH and enzymatic degradation in the stomach and intestine, improving bioavailability and therapeutic efficacy [89]. Moreover, their nanoscale size and the mucoadhesive properties facilitate the uptake by M cells in Peyer's patches of the intestinal epithelium, which are specialized for antigen sampling and immune activation [225]. This characteristic is particularly advantageous for OS vaccination strategies, as it enables efficient delivery of antigens to GALT stimulating both mucosal and systemic immune responses. Additionally, surface modification of PLGA NPs with targeting ligands (e.g., lectins,

folic acid, or antibodies) or PEG or PVA can enhance their stability in intestinal fluids and improve their transport across the epithelial barrier via transcytosis or paracellular pathways [226].

Moreover, PLGA NPs enable controlled and sustained release of their cargo, allowing for prolonged therapeutic effects and reduced dosing frequency. Their GRAS (Generally Recognized As Safe) status by the FDA, along with the possibility of large-scale production, further supports their clinical translation.

Preclinical research has shown that PLGA-based delivery systems can effectively administer a wide range of therapeutic compounds orally, such as insulin [227] or heparin [228], and nucleic acid vaccines. An example is the OS formulations of Glucagon-like peptide-1 (GLP-1) receptor agonists for the treatment of type 2 diabetes [229].

However, there are still different challenges that need to be overcome, such as the batch-to-batch reproducibility, scalability, and the complexity of bypassing the mucus barrier.

3 AIM

PDAC is one of the most aggressive and lethal forms of cancer, characterized by strong resistance to conventional treatments and poor prognosis, with high rates of relapse and metastasis even after surgery and/or conventional chemotherapy regimens. Cancer vaccines with therapeutic purposes are innovative immunotherapeutic strategies, that are emerging as potential tools to stimulate an immune response capable of controlling disease progression and reducing recurrence in cancer treatment, including PDAC. However, the development of an effective vaccine for PDAC faces several challenges, such as the choice of a target tumor antigen with immunogenic features and the need for efficient and targeted antigen delivery.

A target in PDAC could be the TAA GPC1, which is highly expressed in PDAC but absent or only weakly expressed in benign tumors and normal tissues. Nonetheless, TAAs are generally less immunogenic than TSAs, making the inclusion of adjuvants essential to boost vaccine efficacy. In this regard, FL from *Salmonella typhi* has been investigated as a potent adjuvant, since it activates the immune system through Toll-like receptor 5 (TLR5).

While vaccines are usually administered parenterally, the OS administration route offers several advantages for both patients and healthcare systems: it can be self-administered, and it is non-invasive, cost-effective, and associated with minimal risk of acute adverse reactions. Moreover, it stimulates both mucosal and systemic (humoral and cellular) immune responses. However, OS vaccination is also characterized by various critical points that can limit its effectiveness, such as the harsh gastrointestinal environment (pH gradient, digestive enzymes, microbiota), the intestinal epithelium barrier, and the need to overcome mucosal immune tolerance.

In recent years, nanotechnology has opened new opportunities to improve the efficacy and safety of cancer therapies. Among the various nanosystems, polymeric NPs, including those based on the use of PLGA/PVA polymers, stand out due to their advantageous properties: tunable physicochemical characteristics, the ability to encapsulate a wide range of drugs or biomolecules and protect them against degradation, leading to prolonged circulation time, and the possibility to functionalize their surface with targeting ligands that allow selective delivery to tumor cells, thereby minimizing off-target effects and shielding healthy tissues from toxicity. These features make PLGA/PVA NPs especially suitable for OS vaccine delivery.

Therefore, the aim of this project is to develop an OS NP-based cancer vaccine in which a chimeric protein constituted by the GPC1 protein associated with FL from *Salmonella typhi* is included in PLGA/PVA NPs to be administered as a potential adjuvant therapy for PDAC prevention after surgical resection and conventional chemotherapeutic treatments.

In detail, the specific aims are:

- Design and production of the immunogenic chimeric protein GPC1-FL.
- Design and preparation of PLGA/PVA NPs for the OS delivery of the GPC1-FL protein.
- *In vitro* characterization of the physical and biological properties of the chimeric protein GPC1-FL
- *In vitro* characterization of the physical and biological properties of the PLGA/PVA NPs.
- *In vivo* evaluation of the immunogenicity of the GPC1-FL-loaded PLGA/PVA NP vaccine platform, and its effect in reducing PDAC tumor growth and increasing survival of treated mice in a PDAC mouse model.

4 MATERIALS AND METHODS

4.1 Cell culture: cell lines and culture media

BxPC-3 (human PDAC), Jurkat (human acute T cell leukemia), Caco-2 (human colorectal carcinoma), and RAW 264.7 (Mus musculus macrophage) cell lines were provided by American Type Culture Collection (ATCC). Panc02 (mouse PDAC) cell line was provided by Cytion. All cell lines were grown at 37°C, 5% CO_2 and in the proper medium. BxPC-3 and RAW 264.7 were cultured in DMEM (1X) + GlutaMAX^{TM}-I (Gibco, Thermo Fisher Scientific) supplemented with 10% of fetal bovine serum low endotoxin (FBS) (Gibco, Thermo Fisher Scientific), 1% of MEM non-essential aminoacids 100X (Euroclone S.p.A.), and 1% of penicillin-streptomycin solution 100X (Euroclone S.p.A.). Caco-2 were cultured in MEM (1X) + GlutaMAX^{TM}-I (Gibco, Thermo Fisher Scientific) supplemented with 20% of fetal bovine serum low endotoxin (FBS) (Gibco, Thermo Fisher Scientific), 1% of MEM non-essential aminoacids 100X (Euroclone S.p.A.), and 1% of penicillin-streptomycin solution 100X (Euroclone S.p.A.). Jurkat and Panc02 were cultured in RPMI Medium 1640 (1X) + GlutaMAX^{TM}-I (Gibco, Thermo Fisher Scientific) supplemented with 10% of fetal bovine serum low endotoxin (FBS) (Gibco, Thermo Fisher Scientific), 1% of MEM non-essential aminoacids 100X (Euroclone S.p.A.), 1% of penicillin-streptomycin solution 100X (Euroclone S.p.A.). In the case of Panc02, 1% of sodium pyruvate 100 mM (Euroclone S.p.A) was added.

4.2 Bacteria and bacterial growth media

NEB® 5-alpha Competent *E. coli* (High Efficiency) (New England Biolabs) was used for vector amplification. They were grown in a medium containing Tryptone (Millipore), yeast extract (Millipore), Sodium chloride (Sigma-Aldrich), with the addition of 2% agar (Millipore) in case of solid medium. The components were dissolved in distilled water and then sterilized in an autoclave set to 120 °C for 20 minutes, using a PBI Sistematic III unit (Gemini, Apeldoorn, The Netherlands). To support the growth of the bacteria, the medium was supplemented with ampicillin at a concentration of 100 µg/mL. Liquid cultures were incubated at 37 °C under constant shaking at 250 rpm in a 222DS Benchtop Shaking Incubator (Labnet International, Edison, NJ, USA). Solid cultures were incubated at 37°C using a Heraeus incubator (Gemini, Apeldoorn, The Netherlands).

4.3 Antibodies and proteins

The primary antibodies used were the commercial Glypican 1 polyclonal antibody (PA5-28055) (Thermo Fisher Scientific) for evaluating GPC1 expression. This antibody was produced in rabbit and it is reactive with human, mouse, and rat samples; the anti-GAPDH polyclonal antibody, E-AB-20059 (Elabscience Biotechnology Inc.) for verifying GAPDH expression. It was produced in rabbit and reacts with both human and mouse samples.

The secondary antibodies used were: F(ab')2 Goat anti-Rabbit IgG-F(ab')2 Fragment cross-adsorbed Antibody Dy Light® 488 Conjugated A120-212D2 (Bethyl laboratories Inc.); F(ab')2 Goat anti-MOUSE IgG-F(ab')2 Fragment cross-adsorbed Antibody Dy Light® 488 Conjugated A90-241D2 (Bethyl laboratories Inc.); Rabbit Anti-Mouse IgG H&L (HRP) (Abcam, ab6728); Goat Anti-Rabbit IgG H&L (HRP) (Abcam, ab6721).

The proteins used were: Glypican1 protein (Bio-Techne) was used for ELISA coating. Albumin, Fluorescein isothiocyanate Conjugate from bovine (BSA-FITC) A 9771 (Sigma-Aldrich, Inc.).

4.4 Evaluation of GPC1 expression on PDAC cells

4.4.1 Western blot

Cell pellets (from $1x10^6$ cells) were lysated and proteins were extracted using RIPA buffer (Sigma-Aldrich, Merck KGaA) supplemented the proteinase inhibitors NaF 5 mM, Na_3VO_4 2 mM, EDTA 1 mM and Complete™ EDTA-free Protease Inhibitor Cocktail (Roche). Proteins were quantified using the Protein Assay kit (Bradford assay) (Bio-Rad Laboratories) and NanoDrop 2000 spectrophotometer (Thermo Fisher Scientific). 30 µg of total extract, plus 5 µL of 4X Laemmli Sample Buffer (Bio-Rad Laboratories) up to volume of 20 µL with RIPA buffer were denatured at 95°C for 5 minutes, then loaded and separated in 8-16% Mini-PROTEAN TGX precast denaturing polyacrylamide gel (Bio-Rad Laboratories) which is immersed in 1X Tris/glycine/SDS running buffer (Bio-Rad Laboratories). After 1 hour of electrophoretic run, performed at 100 V, proteins were transferred to the nitrocellulose membrane Amersham™ Protran™ 0.2 µm NC (GE Healthcare Life science) following by a blocking phase for 1 hour with Tris-Buffered Saline solution (TBS-T) with 1% of Tween 20 (Sigma, LifeScience) and 5% of nonfat dried milk (Euroclone S.p.A.).Then, after 3 washes with TBS-T, the incubation with the primary antibody, diluted in TBS-T, was performed overnight, under slowly shaking, at 4°C. The day after, 3 washes with TBS-T were performed, following the incubation for 1 hour with the secondary antibody,

diluted in TBS-T, under gently shaking at room temperature. Finally, 3 washes with TBS-T were done. The secondary antibody was linked to the horseradish peroxidase (HPR) to allow the signal production and detection after the addition of ECL Star solution (Euroclone S.p.A.). Signal was detected by ChemiDoc™ Touch Imaging System instrument (Bio-Rad Laboratories Inc.).

4.4.2 Flow cytometry

Before performing the flow cytometry, cells were detached using a solution of Trypsin-EDTA (Sigma, Life Sciences) diluted 1:5 with Versylene® Fresenius NaCl 0.9 % (Fresenius Kabi). Then, they were washed with Phosphate Buffered Saline (PBS) buffer w/o Calcium w/o Magnesium (Euroclone) and counted. 300.000 cells were collected for the flow cytometry analysis. They were subjected to a blocking step with DPBS plus 2% Bovine Serum Albumin (BSA) (Sigma-Aldrich), to incubation with the primary antibody for 1 hour at room temperature (RT), under shacking, 2 washes with PBS and to incubation with the secondary antibody (Alexa Fluor 488) for 1 hour, at RT, under shacking, followed by 2 washes with PBS. Finally, cells were resuspended in 350 µl of PBS plus 2% BSA. Analysis was performed with BD FACSCanto™II Cell Analyzer (Becton, Dickinson and Company) acquiring 10000 events. Obtained data were analyzed with BD FACSDiva software (BD Biosciences).

4.4.3 Immunofluorescence

30000 cells were seeded in high precision microscope cover glasses (Superior Marienfeld Laboratories Glassware, Paul Marienfeld GmbH & Co. KG) previously treated with poly-D-Lysine (Millipore, Merck KGaA) in order to improve cell adhesion. Cells were grown for 24 hours at 37°C, 5% CO_2. Then, cells were washed three times with PBS and were fixed with 4% Paraformaldehyde (PFA) solution in PBS (Sigma-Aldrich) for 11 minutes at room temperature. After the fixation step, cells were washed twice with PBS and treated with 0.1 M of glycine (Sigma, Life Science) in Dulbecco's Phosphate Buffer Saline (DPBS) with calcium and magnesium (Euroclone S.p.A.) to reduce autofluorescence. After two washes with PBS, cells were blocked with DPBS Bovine Serum Albumine (BSA) 5% (Sigma, Life Science) for 1 hour at RT. Then, cells were incubated with the primary antibody for 1 hour, at RT, washed twice with DPBS and incubated with the secondary antibody for 1 hour, at RT. Both primary and secondary antibodies were diluted in DPBS plus BSA 1%. After the antibody incubation, cells underwent to a rapid wash of 5 minutes. Then they were exposed to DAPI (Sigma-Aldrich) for 10 minutes for nuclear staining. Finally, cells were washed

with distilled water and mounted through the FluorSave™ mounting medium (Calbiochem, Merck KGaA) to Superfrost® Microscope Slides (Thermo Scientific, Thermo Fisher Scientific). Nikon Eclipse Ti-U microscope (Nikon Europe B.V.) was used to acquired images.

Tumors of murine models of human GPC1-expressing PDAC were embedded into Killik O.C.T. (OCT) (Bio-Optica Milano S.p.A.) medium and maintained at -80 °C. A cryostat (Thermo Electron Corporation) was utilized to cut tumor masses into slices of 7 μm, which were subsequently mounted into SuperFrost® Plus (Thermo Scientific, Thermo Fisher Scientific) glass slides and stored at -80 °C. For immunofluorescent analysis, samples were fixed for 10 minutes with cold PBS-PFA 4%, washed with DPBS and blocked using a solution of 2% BSA, 0.25% casein from bovine milk (Sigma-Aldrich, Merck KGaA), and 0.1% gelatine from cold water fish skin (Sigma-Aldrich, Merck KGaA) in DPBS for 1 h at RT. Slices were then incubated with primary antibodies diluted into blocking solution for 1 h at RT, then washed with blocking solution and incubated with secondary antibodies in blocking solution for 1 h at RT. Samples were further washed in DPBS and incubated with DAPI 5 min at RT. Samples were washed twice with DPBS and then with distilled water. Samples were mounted using FluorSave™ on high precision microscope cover glasses (Superior Marienfeld Laboratories Glassware, Paul Marienfeld GmbH & Co. KG). Images were acquired using the Nikon Eclipse Ti-U microscope.

4.5 Production and characterization of the chimeric protein GPC1-FL

4.5.1 Production of the GPC1-FL protein

The sequence of the human GPC1 and of the FL from *Salmonella typhi* were chosen from NIH (National Library of Medicine, National Center for Biotechnology Information). The two proteins were linked together by a Serine and Glycine linker. In addition, a signal peptide for the secretion of the recombinant protein and a histidine-tag of 6 histidines to allow its purification were added.
After the study of the sequence, that was optimized for the expression by Chinese hamster ovary (CHO) cells, the protein was produce in collaboration with GenScript company. CHO was transfected by electroporation to lead to the internalization of the vector containing the GPC1-FL sequence and favor its expression by CHO and its secretion.
The recombinant protein was stored at -80°C in PBS, pH 7.2.

4.5.2 Quantification and characterization of the GPC1-FL protein

After the transfection, the chimeric protein was purified by the HisTrap™ FF crude Kit (Sigma-Aldrich). After purification, the purity of the GPC1-FL was evaluated by SDS-PAGE in both reducing and non-reducing conditions and by Size Exclusion Chromatography (SEC HPLC) performed with the 1260 Infinity II (Agilent) instrument. In detail, the column used was the Superdex® 200 Increase 10/300 GL (Sigma-Aldrich) and the mobile phase was characterized by 0,1M L-Arg in 2x PBS, pH 10.55.
Moreover, the presence of endotoxin was evaluated, and the concentration and the total amount of GPC1-FL were quantified.

4.5.3 GPC1-FL stability in temperature, Simulated Gastric Fluid (SGF) and Simulated Intestinal Fluid (SIF) buffers

The stability of the recombinant protein GPC1-FL in the gastrointestinal tract was evaluated by SDS-PAGE after 1 hour of incubation in simulated gastric juice (SGF) and simulated intestinal fluid (SIF) buffers. The composition of SGF is: NaCl 300 mM, pepsin (ThermoFisher Scientific) 0.9 mM, HCl 840 mM, pH 1.2, while the composition of SIF is: KH2PO4 49.96 mM, NaOH 0.0154 M, pancreatin 1 g/L (ThermoFisher Scientific), pH 6.

4.6 Preparation of polymeric NPs

4.6.1 Microfluidic nanoprecipitation method

For the preparation of empty PLGA and PLGA/PVA NPs, BSA-FITC-loaded and GPC1-FL-loaded PLGA/PVA NPs, the microfluidic method with nanoprecipitation was used (Automated NP, Particle Works), in collaboration with Alfatest company.
Firstly, the organic solution and the aqueous solution were prepared. The organic solution consists in 0,5% PLGA lactide:glycolide (50:50), mol wt 30000-60000 (Sigma, Aldrich) in acetone, while the aqueous solution consists in MilliQ water or 0,25% PVA 87-90% hydrolyzed, mol wt 30000 – 70000 (Sigma, Aldrich) in MilliQ water. For the production of BSA-FITC-loaded the aqueous solution was made of 0,25% PVA and 1 mg/mL of Albumin, Fluorescein isothiocyanate Conjugate from bovine (BSA-FITC) (Sigma-Aldrich) .
For the preparation of GPC1-FL-loaded PLGA/PVA NPs, the organic solution was prepared as described above, while the aqueous solution was made of 0,25% PVA and 0,406 mg/mL of GPC1-FL. All the solutions were filtered through a 0,22 μm filter.

Finally, the organic and the aqueous solutions were mixed. The chip used for this step was a 275 μm Junction Chip.

At the first junction of the microfluidic chip, PLGA in acetone and aqueous solution are brought together laminarly to generate a hydrodynamic flow of reagents. The reactants diffuse into each other gradually reducing the solubility of PLGA and driving the process of nanoprecipitation. This mixing mode provides highly controlled conditions and promotes the formation of more monodisperse and reproducible NPs.

In detail, for empty PLGA and PLGA/PVA and for BSA-FITC PLGA/PVA NPs, the total flow rate (TFR) was 3 mL/min, the flow rate ratio (FRR) was 1:1. For the production of GPC1-FL-loaded PLGA/PVA NPs we made different sample of NP according to different TFR and FRR, as reported in the Table 2.

GPC1-FL-loaded NPs	TFR	FRR (Protein:PLGA)
Sample 1	3 mL/min	1:1
Sample 2	3 mL/min	2:1
Sample 3	3 mL/min	3:1
Sample 4	6 mL/min	1:1

Table 2. The different conditions used to produce the GPC1-FL-loaded PLGA/PVA NPs.

4.7 NP characterization

4.7.1 Dynamic light scattering (DLS)

Hydrodynamic diameter (D(h)), polydispersity index (PdI) and surface charge (zeta potential) analysis were performed by DLS technique using Zetasizer Nano ZSP (Malvern Panalytical). All measurements were done at a back scattering angle of 173° and at a temperature of 25 °C or 37 °C (when indicated). NP samples were diluted in milliQ water 1:200 (v/v) for all PLGA and PLGA/PVA NPs.

4.7.2 NP Tracking Analysis (NTA)

NTA was performed using NanoSight Pro (Malvern Panalytical) to quantify the NP concentration. For the analysis, NP was diluted 1:2000 (v/v) in MilliQ water immediately before the

measurements. The instrument was equipped with 488 nm blue laser. For the measurement, 10 videos were taken, each 60 seconds long.

4.7.3 Encapsulation efficiency (EE%)

The EE% of BSA-FITC-loaded and GPC1-FL-loaded PLGA/PVA NPs was calculated following the indirect methods. After preparation of PLGA/PVA NPs, the amount of unloaded protein was measured in supernatant of preparation medium by Protein Assay kit (Bradford assay) (Bio-Rad Laboratories) and NanoDrop 2000 spectrophotometer (Thermo Fisher Scientific), after the preparation of a calibration curve. To eliminate potential background signals arising from residual solvents or excipients (e.g., PVA), a blank control was prepared by processing NPs without protein under identical conditions. The supernatant from this blank was measured and subtracted from the corresponding sample readings during protein quantification.
Then, the EE% was calculated following the formula [230]:

$$EE\% = \frac{total\ amount\ of\ protein - amount\ of\ protein\ in\ the\ SN}{total\ amount\ of\ protein}\ x\ 100$$

4.7.4 NP stability over time, at body temperature, in SGF and SIF buffers

The stability of NPs under storage conditions of 4°C was followed for 1 year and was evaluated measuring the D(h), PdI, and zeta potential (ZP) every month by DLS. DLS was also used to check the thermal stability at room temperature (25°C) and body temperature (37°C) after different time points.
Stability of the D(h), PdI and ZP in the gastrointestinal tract was test by DLS after incubation of NPs in SGF buffer (pH 1.2; NaCl 300 mM, pepsin 0.9 mM, HCl 840 mM) and (SIF buffer (pH 6; KH2PO4 49.96 mM, NaOH 0.0154 M, pancreatin 1 g/L). In detail, NPs were diluted 1:200 in the buffers for 1, 2, 4, 6 and 24 hours at body temperature (37°C). Then, they were centrifuged at 10500 rpm for 20 minutes, at 10°C, the supernatant was discharged, and NPs was resuspended in MilliQ water and analyzed immediately.

4.7.5 Cell viability assay

Caco-2 cells, representing intestinal epithelium, and RAW 264.7, representing APCs, were seeded in a 96-well plate at a density of $5x10^3$ cells/well and they were grown for 24 hours at 37°C, 5% CO_2. The day after, cells were exposed to different concentration of protein GPC1-FL (from 10 µg/mL to 90 µg/mL) and NPs (from $1x10^6$ to $1x10^{11}$ NPs/mL) in the culture medium. After 24 or 48 hours, the cell viability was determined using the CellTiter-Glo® Luminescent Cell Viability Assay (Promega). The resulted luminescent signal was analyzed with Infinite M200PRO instrument (TECAN).

4.7.6 NP internalization by the *in vitro* model of intestinal epithelium

Caco-2 cells were seeded in a 6-well plate at a density of $2x10^5$ cells/well and they were grown for 48 hours at 37°C, 5% CO_2. Then, free BSA-FITC (Sigma-Aldrich) and BSA-FITC-loaded PLGA/PVA NPs were added in the respective well at a concentration of 50 µg/mL. After each incubation time (1, 2, 4, 6, 24 hours), cells were washed three times with DPBS, detached with trypsin-EDTA solution (Gibco, Thermo Fisher Scientific), centrifuged, and counted. 300000 cells were washed other two times with DPBS 2% BSA to remove NPs bound to the cell membrane. Finally, they were resuspended in 350 µl of DPBS 2% BSA for the analysis. 10000 events were acquired with BD FACSCanto™II Cell Analyzer (Becton, Dickinson and Company). FITC fluorescence data were analyzed with BD FACSDiva software (BD Biosciences).

4.8 Establishment of a syngeneic murine model of PDAC

The immunocompetent mice C57BL/6 were provided by Envigo RMS S.r.l. Both male and female mice, 6 weeks old, were used in the same percentage.

4.8.1 Characterization of the mouse cell line PANC02 for the murine model of PDAC

PANC02 cell line was tested as mouse PDAC model for the expression of the mouse GPC1, that has a high homology with the human GPC1. Its expression was checked by western blot and flow cytometry analysis.

4.8.2 Transfection of PANC02 cells

4.8.2.1 Vector design

For the transfection of PANC02 to express the human GPC1 on their surface two vectors were designed and their efficiency was compared. The maps of the vectors are reported in the Figure 13. Both the vectors contain the sequence encoding for the human GPC1 (hGPC1[NM_002081.3]); the Kozak translation initiation sequence (Kozak) to facilitate translation initiation of ATG start codon downstream of the Kozak sequence; the human cytomegalovirus immediate early enhancer/promoter (CMV promoter), the puromycin resistance gene (Puro) that allows the selection of positively transfected cells; the Simian virus 40 late polyadenylation signal (SV40 late pA) and the bovine growth hormone polyadenylation signal (BGH pA) that allows transcription termination and polyadenylation of mRNA transcribed bt Pol II RNA polymerase; the pUC origin of replication (pUC ori) that facilitates plasmid replication in *E.coli* and regulates high-copy plasmid number (500-700); Ampicillin resistance gene (Ampicillin) that allows *E.coli* to be resistant to ampicillin, thus allows the selection of bacteria positive to the vector. The two vectors are different for the promoter. In the vector VB230223-1213mcj it is the human eukaryotic translation elongation factor 1 α1 promoter (EF1A), in the VB231006-1170ktm is the CMV early enhancer fused to modified chicken β-actin promoter (CBh).

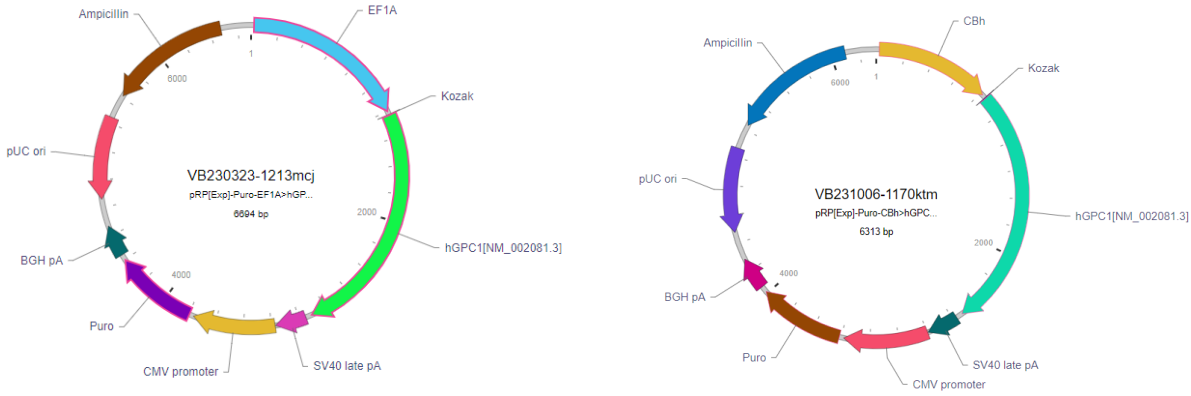

Figure 13. Vectors used to transfect PANC02 cells for the expression of the human GPC1.

4.8.2.2 Vector amplification in *E.coli* Dh5alpha

The vectors were amplified in NEB® 5-alpha Competent *E. coli* (High Efficiency) (New England Biolabs). Bacteria were transformed by heat shock method. A volume of bacteria at least 5 times the

volume of DNA to be added was thawed on ice. Then, the vector is added to the bacteria and allowed to incubate on ice for 30 minutes. Then heat shock is performed, heating the sample for 45 seconds at 42°C. Subsequently, 4 volumes of SOC were added (200 ul of SOC per 50 ul of bacteria) and the reaction was incubated at 37°C for 45 minutes under constant stirring. The bacteria were then plated in a P10 petri dish with LB-agar containing the antibiotic ampicillin for selection of transformed bacteria only. The plate was then incubated at 37°C to allow the bacterial colonies to grow. Then a bacterial colony was taken and grown in 5 mL of LB medium. Once growth had occurred, 100 ul of it was taken and grown in a 50 mL volume of LB.

4.8.2.3 Vector purification and quantification

The vector amplified in NEB® 5-alpha Competent *E. coli* (High Efficiency) was purified by the QIAGEN Plasmid Midi Kit (25) (QIAGEN) and quantified by NanoDrop 2000 spectrophotometer (Thermo Fisher Scientific).

4.8.2.4 Puromycin selective antibiotic kill curve assay

The selection of the most appropriate concentration of Puromycin Dihydrochloride (Gibco, Thermo Fisher Scientific) for the selection of transfected PANC02 was performed through the construction of a concentration-response curve: 5000 PANC02 were seeded in a 96-well plate were exposed to different concentration of puromycin: 1, 3, 6, 9, 12, 15 ug/ml.
The percentage of live cells were measured with the CellTiter-Glo® Luminescent Cell Viability Assay (Promega) after 24 hours of exposition to the antibiotic.
The lowest concentration at which non-transfected PANC02 cells do not survive was chosen to positively select transfected cells.

4.8.2.5 PANC02 transfection by electroporation

After detaching by Trypsin-EDTA (Sigma, Life Sciences), 1,5 million of PANC02 cells were counted for the transfection. Firstly, PANC02 were resuspended in 100 µl of the transfection buffer Ingenio® Electroporation Solution (Mirus) and 3µg of the vector were added. The mix was move in a cuvette and cells were transfected by The Amaxa™ Cell Line Nucleofector™ Kit L (Lonza). Electroporated PANC02 were seeded in a well of a 6-well plate in a medium containing 20% of FBS and incubated at 37°C, 5% CO_2.
The day after, 3 ug/mL of puromycin were added to allow the selection of positively transfected PANC02 (T-GPC1 PANC02).

4.8.2.6 *In vitro* and *ex vivo* verification of GPC1 expression

The GPC1 expression on PANC02 cells were observed by Western blot and Flow cytometry.
The GPC1 expression was also checked *ex-vivo*: C57BL/6 mice were injected with 1,5 million of T-GPC1 PANC02 and after a month the mice were sacrificed, and the tumor masses were collected. They were embedded into Killik O.C.T. (OCT) (Bio-Optica Milano S.p.A.) medium and maintained at -80 °C. Then, in collaboration with Professor Paolo Macor (Department of life sciences, University of Trieste) the tumor masses were cut by cryostat and an immunofluorescence on tissue was performed.

4.8.2.7 Doubling time

To verify whether the GPC1 expression may alter the growth capacity of PANC02, the *in vitro* doubling time of WT and T-GPC1 was observed and compared.
For the *in vitro* doubling time, at each cell splitting cells were counted and the following formula were applied:

$$Doubling\ time = \frac{Duration\ \times In(2)}{In\ (final\ concentration\ \div initial\ concentration)}$$

Were duration referring to the time spent in culture, the final concentration to the number of cells counted after detaching them, and the initial concentration to the number of seeded cells.

4.9 Animal studies

4.9.1 Immunization protocol

Both male and female C57BL/6 mice were vaccinated in the same percentage for the immunization studies. Mice were divided into eight groups, with 6 mice per group. The groups are the following: SC injection with negative control (PBS), SC injection with empty PLGA/PVA NPs, SC injection with free GPC1-FL protein, SC injection with GPC1-FL-loaded PLGA/PVA NPs, OS administration with negative control (PBS), OS administration with empty PLGA/PVA NPs, OS administration with free GPC1-FL protein, OS administration with GPC1-FL-loaded PLGA/PVA NPs. Mice were allowed free access to food and water with 12 h light/dark cycle. They were vaccinated with 50 μg of free GPC1-FL protein or 50 μg of GPC1-FL incapsulated in PLGA/PVA

NPs ($1{,}27\times10^{11}$ NPs) for both SC and OS administration, followed by booster dose after 2nd weeks primary immunization .

4.9.2 Safety observation

All mice were weighed before vaccination and their weight was followed over time until sacrifice. Moreover, physical, and mental stress were monitored.

4.9.3 Blood collection

Blood was collected from mouse cheek at day 0 (before starting the vaccination), at day 14, day 21, day 28, and day 35. Serum was obtained after maintaining blood at room temperature for 30 minutes and after two centrifugation of 1000 xg, 10 minutes. Sera were stored at -80°C.

4.9.4 Detection of specific anti-GPC1 IgG antibodies by ELISA

For the detection of specific anti-GPC1 antibodies, the ELISA test was performed. The recombinant human Glypican 1 (Bio-Techne) was diluted in a bicarbonate buffer in a concentration of 2,5 µg/mL and then was coated in a 96-well plate over night at 4°C. The day after, the blocking was performed using DPBS 2% milk for 1 hour. After three washes with DPBS 0,1% tween and three washes with PBS, the mouse sera, diluted 1:100, were added in the wells for 1 hour at room temperature. Then, three washes with DPBS with 0,1% tween and three with DPBS were performed. Subsequently, the secondary antibody anti-mouse HRP (Rb pAb to Ms IgG, Abcam) used at 1:1000 dilution was incubated for 1 hour at room temperature. Then, the six washes were repeated as describe above. Finally, 100 µl per well of Stabilized Chromogen (Invitrogen, Thermo Fisher Scientific) was added, followed by 100 µl of the Stop Solution (Thermo Fisher Scientific). The absorbance was read at 450 nm.

4.9.5 Tumor inoculation and mouse survival

39 days after the start of the vaccination, 3×10^5 T-GPC1 PANC02 cells were inoculated subcutaneously in the right flank of the mice. The tumor mass growth was observed and measured over time. When the tumor mass reached 12 mm in width and length or became ulcerated, the mice were euthanized. Immediately after euthanasia, the tumor mass, intestines, spleen, and kidneys were collected for future experiments.

4.10 Statistical analysis

The data were statistically analyzed using GraphPad Prism. Specifically, the statistical difference between the means of two data sets was evaluated using the unpaired Student's t-test, while differences among multiple groups were assessed with ordinary one-way ANOVA. The Kaplan-Meier estimator was used to study the survival function of different treatment groups, and p-values for differences in survival were calculated using the log-rank test. Differences with a p-value or adjusted p-value of less than 0.05 were considered statistically significant.

5 RESULTS

5.1 Evaluation of GPC1 as a Vaccine Target for PDAC

Several studies have shown that the proteoglycan GPC1 is highly and specifically expressed in PDAC, and for this reason could be a targetable TAA [2]. Therefore, its protein expression was investigated in the PDAC-like tumor cell line model BxPC-3 by Western blot analysis using a commercial polyclonal anti-GPC1 antibody. The BxPC-3 cell line was used as a human PDAC model, the Jurkat cell line as a negative control, and Glyceraldehyde-3-phosphate dehydrogenase (GAPDH) as a housekeeping protein (Figure 14). As previously reported [231], GPC1 protein was detected in BxPC-3 cells but not in Jurkat cells. In detail, GPC1 has a molecular weight of 62 kDa and in the Western blot, two bands corresponding to this molecular weight were observed. They represent different glycosylation states of the protein, as variations in glycosylation can affect the molecular weight and, consequently, the migration of GPC1 protein in SDS-PAGE.

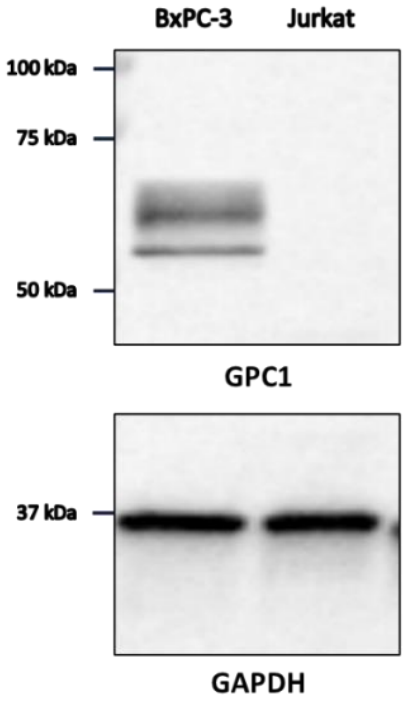

Figure 14. Western blot analysis of GPC1 protein in GPC1-positive human PDAC cell lines (BxPC-3) and in GPC1-negative cancer cell line (Jurkat). Commercial polyclonal anti-GPC1 was employed at a concentration of 0.33 µg/ml. GAPDH protein was analyzed as housekeeping gene at a concentration of 0.11 µg/ml.

To better characterize the presence of GPC1 in human PDAC, its expression was quantified by flow cytometry (Figure 15). The flow cytometry confirmed the overexpression of this TAA on BxPC-3, as the percentage of GPC1-positive cells was 86.95%. On the other hand, the percentage of GPC1-positive Jurkat was 3,05%.

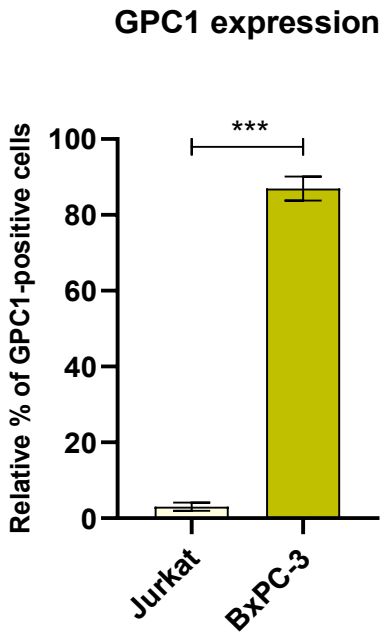

Figure 15. Flow cytometry analysis of GPC1 protein expression in GPC1-positive cancer cell line (BxPC-3) and in GPC1-negative cancer cell line (Jurkat). Data are reported as mean % of positive cells ± Standard Deviation (SD) of three independent replicates. The statistical analysis was performed using unpaired t-test: ***p-value = 0,0008.

To validate these results, an immunofluorescence analysis was performed to observe the GPC1 expression in BxPC-3 and Jurkat cells (Figure 16). As the western blot and flow cytometry analysis, the immunofluorescence highlights in green the GPC1 expression in BxPC-3 cells but not in Jurkat cells, confirming this TAA as a suitable target for the vaccination approach for the treatment of GPC1-expressing PDAC. AB2 indicates the secondary antibody used alone as a control, to verify that no non-specific signal originates from the secondary antibody.

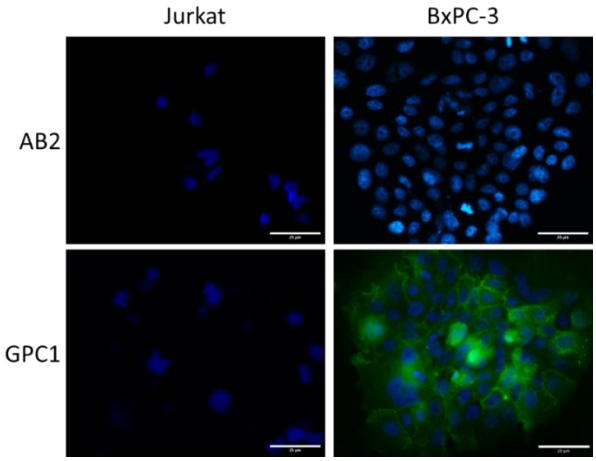

Figure 16. Representative immunofluorescence analysis of GPC1 protein expression in GPC1-positive cancer cell lines (BxPC-3) and in GPC1- negative cancer cell lines (Jurkat). AB2 represents the secondary antibody alone as a control, blue signal represents nuclei and green signal represents GPC1. Commercial polyclonal anti-GPC1 was employed at a concentration of 3.3 µg/ml. Scale bar = 25 µm.

The expression of the TAA GPC1 in the context of PDAC was confirmed using three different techniques: western blot, flow cytometry, and immunofluorescence. The results support the role of GPC1 as a promising target for the development of a vaccine aimed at targeting GPC1-expressing PDAC cells to enable the immune system to recognize and eliminate them.

5.2 Production and characterization of the chimeric protein GPC1-FL

The high expression of GPC1 in PDAC has prompted the development of a vaccine based on this tumor antigen. To enhance the immunogenicity of the vaccine, an additional protein was associated for adjuvant purposes. Specifically, we engineered a protein, called GPC1-FL, consisting of human GPC1 associated with FL from *Salmonella typhi*, through a Glycine-Serine (GS) linker. Moreover, the fused GPC1-FL protein also contains a signal peptide, which is cleaved after expression by the cells, a stop codon, and a His-tag to facilitate purification (Figure 17). The engineered protein was purified from Chinese Hamster Ovary (CHO) cells after the transfection of a vector containing the amino acid sequence of GPC1-FL optimized for production in eukaryotic cells. GPC1 was expressed in CHO cells despite potential differences in glycosylation compared to human cells. CHO cells were chosen due to their high protein yield, well-established culture protocols, and

stability in producing recombinant glycoproteins, which allowed the production of sufficient quantities of GPC1 for immunization experiments.

The final protein consists of 1038 amino acids, with a molecular weight of 110,977.62 kDa (Table 3). Its isoelectric point (pI) is 5.61, and its stability index is 33.58, indicating a stable protein.

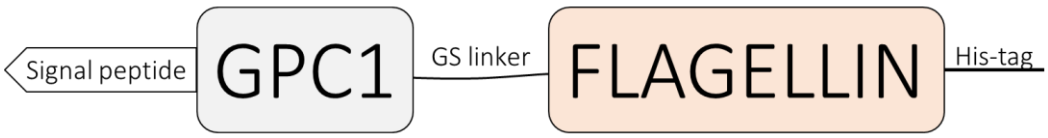

Figure 17. Schematic representation of the engineered chimeric protein GLYPICAN-1-FLAGELLIN (GPC1-FL). The engineered chimeric GPC1-FL protein consists of the tumor-associated antigen (TAA) GPC1, *Salmonella typhi* FL as an adjuvant, a GS linker connecting GPC1 and FL, a signal peptide enabling its expression on the cell membrane surface, and a His-Tag to allow protein purification.

	Number of amino acids	**Molecular weight (Da)**
Signal peptide	18	1875,20
GPC1	505	55889,63
Glycine-Serine (GS) linker	15	963,90
FL	494	51480,07
His-tag	6	840,88
***Mass adjustment**	/	-72
Total	1038	110,977 kDa

Table 3. Summary of the domains of the engineered chimeric protein GPC1-FL, with corresponding amino acid count and molecular weight (Da). * *"Mass adjustment" accounts for the loss of one water molecule (~18 Da) per peptide bond between the parts of the engineered protein; here 4 bonds → 4 × 18 ≈ 72 Da.*

After production, the GPC1-FL protein was purified using an HisTrap FF crude column, and its total amount and concentration were determined. The average protein yield per production was 12,29 mg ± 0,74, with a concentration of 1.22 mg/ml (measured by A280). The purity of the protein was then assessed by SDS-PAGE (Figure 18), in both reducing and non-reducing conditions, and size-exclusion high-performance liquid chromatography (SEC-HPLC) (Figure 19), showing purity levels of ≥80%. In detail, in the SDS-PAGE analysis of the recombinant GPC1 protein, additional

bands are visible at higher and lower molecular weights compared to the expected, corresponding to protein aggregates and degraded fragments. These forms were not removed during nanoparticle preparation. While aggregates and fragments may be less immunogenic than the protein GPC1-FL, they can still contribute to the overall immunogenicity of the vaccine. Additionally, endotoxin levels were assessed, showing ≤0.1 EU/mg.

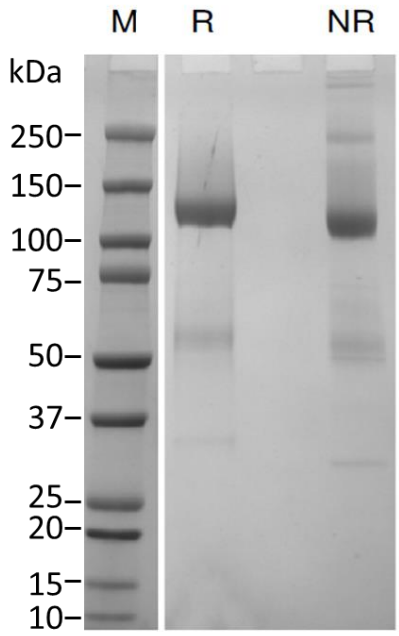

Figure 18. **SDS-PAGE of the chimeric GPC1-FL.** The SDS-PAGE confirms the production of the engineered GPC1-FL under both reducing (R) and non-reducing (NR) conditions. The observed band corresponds to the expected molecular weight of GPC1-FL (110,977 kDa). Abbreviations: M, protein marker; R, reducing condition; NR, non-reducing condition.

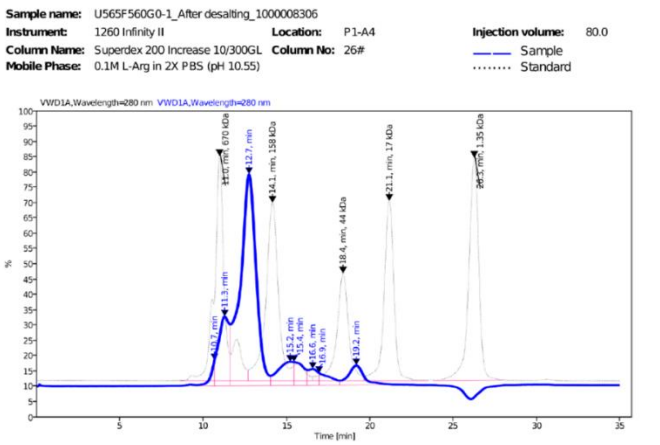

Signal: VWD1A,Wavelength=280 nm

RT [min]	Height	Width [min]	Area	Area%
10.7	1.3	1.8	20.6	2
11.3	3.7	1.0	166.4	14
12.7	11.2	2.4	743.1	62
15.2	1.2	1.4	81.2	7
15.4	1.2	0.8	49.8	4
16.6	0.9	0.7	35.2	3
16.9	0.6	1.2	32.0	3
19.2	1.0	3.5	70.0	6
		Sum	1198.33	

Figure 19. **Size-Exclusion Chromatography (SEC-HPLC) profile of purified chimeric GPC1-FL protein.** Representative chromatogram obtained by SEC-HPLC analysis of the engineered GPC1-FL protein following the final purification step. The elution profile shows a single predominant peak corresponding to the expected. Protein detection was performed at 280 nm.

5.3 GPC1-FL stability in stomach and intestine

As the GPC1-FL protein, after OS administration, is exposed to the stomach and intestinal environment before being absorbed by the intestinal epithelium, particularly by M cells [99,232], its stability in SGF and SIF buffers was evaluated [232]. After 1 hour of incubation of the protein in PBS, SGF, and SIF at 37°C (to simulate body temperature), its integrity was assessed by SDS-PAGE analysis. As shown in the SDS-PAGE (Figure 20), the protein remained stable after 1 hour of incubation at 37°C compared to the control. However, it was degraded when exposed to SGF and SIF, because of the pH and the enzyme component.

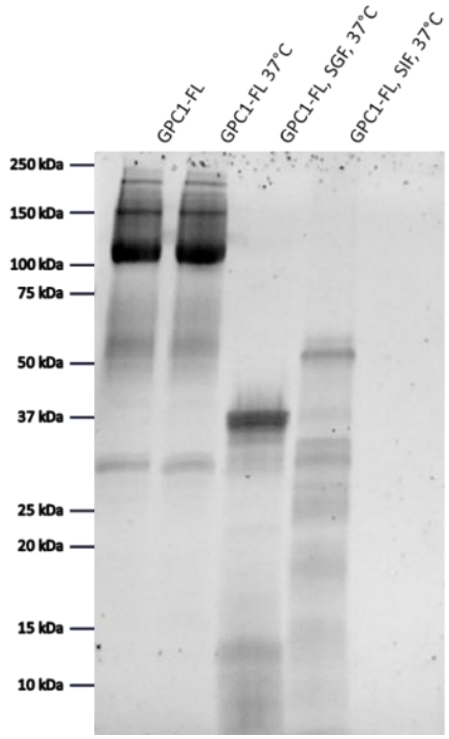

Figure 20. SDS-PAGE of GPC1-FL protein after incubation in SGF and SIF. The SDS-PAGE shows that the GPC1-FL protein is stable at body temperature (37°C) compared to the control; however, it is not stable in SGF and SIF buffers.

Moreover, the safety of the GPC1-FL protein on the intestinal epithelium and APCs was evaluated, respectively using Caco-2 and RAW 264.7 cells as specific cell models. These cells were exposed to different concentrations of the protein, ranging from 10 to 90 µg/mL, for 24 and 48 hours. Cell viability was then assessed using the CellTiter-Glo® Luminescent Cell Viability Assay, and the relative percentage of viable cells was calculated (Figure 21). The results highlighted the biocompatibility of the engineered protein within the tested concentration range, as cell viability

remained comparable to that of unexposed cells after both 24 and 48 hours. These findings indicate that the protein is suitable for use in our study involving OS administration.

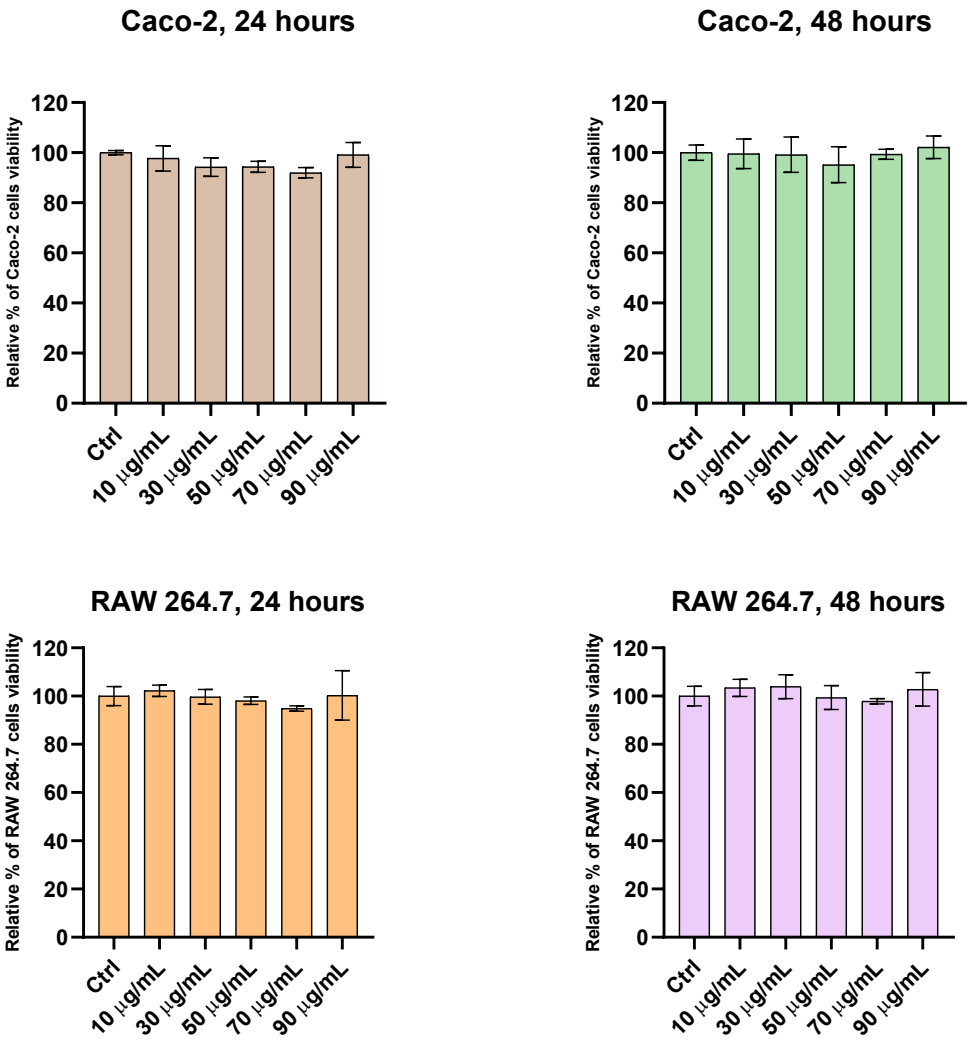

Figure 21. Cell viability assay of the engineered GPC1-FL protein. CellTiter-Glo assay on Caco-2 and RAW 264.7 cells to test *in vitro* GPC1-FL biocompatibility with the intestinal epithelium and antigen-presenting cells (APCs). Data are presented as mean ± standard deviation (SD) of three independent replicates. Statistical analysis was performed using ordinary one-way ANOVA: p-value >0,05.

5.4 Preparation and characterization of polymeric NPs

5.4.1 Preparation and physical characterization of NPs

By using the microfluidic nanoprecipitation method, different types of NPs were produced: empty PLGA and PLGA/PVA, BSA-FITC-loaded PLGA/PVA, and GPC1-FL-loaded PLGA/PVA NPs (Table 4). After preparation, NPs were characterized by DLS to determine D(h), PdI, and zeta potential. At the same time, NP concentration was quantified by NTA, and EE% was also calculated (Table 4). NPs were stored at +4 °C until further use.

The stability of PLGA and PLGA/PVA NP formulation was assessed both under storage conditions and under physiologically relevant conditions (37 °C, SGF, and SIF). Empty PLGA-only NPs were produced to perform comparison experiments with the PLGA/PVA NP formulation, in order to evaluate the role of PVA as stabilizer. Long-term and physiological condition stability experiments were conducted on empty PLGA and PLGA/PVA nanoparticles, as these tests were designed to first validate the stability of the polymeric matrix. After confirming PLGA/PVA as a stable formulation, protein-loaded nanoparticles were produced for functional studies. BSA-FITC-loaded PLGA/PVA NPs were produced to investigate whether encapsulation improves protein uptake by an *in vitro* model of intestinal epithelium. Finally, GPC1-FL-loaded PLGA/PVA NPs were produced as a comprehensive vaccination platform.

	PLGA NPs	PLGA/PVA NPs	BSA-FITC-loaded PLGA/PVA NPs	GPC1-FL-loaded PLGA/PVA NPs
D(h) (nm)	192.400 ± 1.040	191.470 ± 2.20	225.200 ± 1.8	231.1 ± 0.8
PdI	0.038 ± 0.030	0.060 ± 0.003	0.15 ± 0.03	0.10 ± 0.02
Zeta Potential (mV)	-32.830 ± 0.400	-25.670 ± 0.750	-21.5 ± 0.46	-28.83 ± 0.86
Concentration (NPs/mL)	7.50×10^{11}	8.91×10^{11}	1.3×10^{12}	1.1×10^{12}
EE%	/	/	50%	47.38%
Purpose	PLGA stability	PLGA/PVA stability and biocompatibility	Internalization by the *in vitro* model of intestinal epithelium	Final NP platform for mouse vaccination

Table 4. Characterization of nanoparticles (NPs). The table reports the hydrodynamic diameter (D(h)), the polydispersity index (PdI), the zeta potential, the concentration, the encapsulation efficiency (EE%) and the intended purpose of the produced NPs. Data are presented as mean ± standard deviation.

5.4.2 NP stability over time

To test the long-term stability of the NP, D(h), PdI, and zeta potential were measured monthly over the course of one year (Figure 22). The results showed that PLGA/PVA NPs remained stable for at least one year after preparation, as no statistically significant changes were observed in any of the three parameters. In contrast, PLGA NPs maintained a stable D(h) and PdI only for the first four months post-production, then both the D(h) and the PdI increased significantly. On the other hand, after one month, the PLGA NPs started losing their strongly negative surface charge, which became more neutral. This shift led to NP aggregation, resulting in progressively larger size and higher PdI values as measured by DLS.

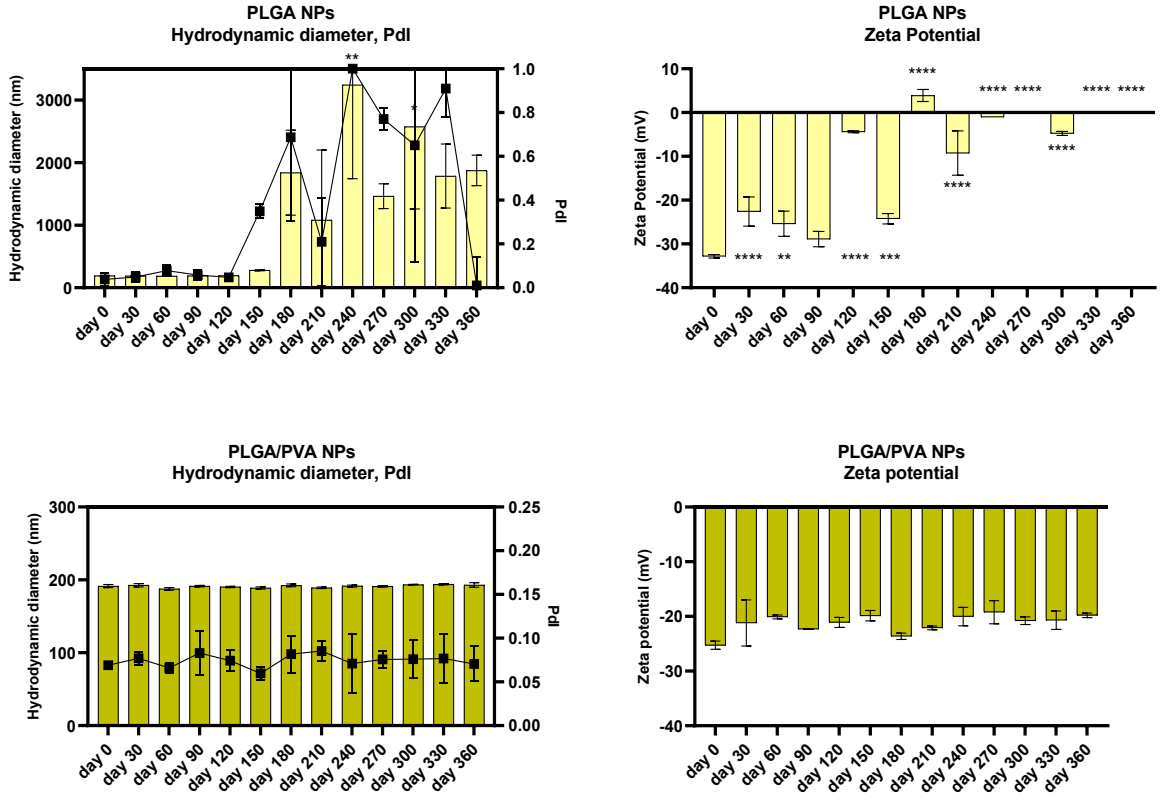

Figure 22. Stability over time of PLGA and PLGA/PVA NPs. DLS analysis to determine the hydrodynamic diameter (D(h)), polydispersity index (PdI) and surface charge over time of PLGA and PLGA/PVA NPs produced by microfluidics. Data are presented as mean ± standard deviation (SD) of three replicates. The statistical analysis was performed using ordinary one-way ANOVA (Dunnett's multiple comparisons test) comparing the parameters measured each month with the control, i.e., the parameters measured immediately after the preparation of the NPs.: ns: ≥ 0.05; *: 0.05 < p ≤ 0.01; **: 0.01 < p ≤ 0.001; ***: 0.001 < p ≤ 0.0001; ****: p<0,0001.

5.4.3 NP stability at body temperature

The stability of PLGA and PLGA/PVA NPs was observed at body temperature (37°C) by monitoring their D(h), PdI, and zeta potential after incubation for 0, 1, 2, 4, 6, and 24 hours (Figure 23). Both NP formulations remained stable over the incubation period, as no statistically significant differences were detected in the measured parameters. Nevertheless, subtle differences between the two systems could be observed. Indeed, PLGA NPs exhibited a loss of their stability, as indicated by the increase in D(h) after 24 hours at 37°C, a higher PdI reflecting a more polydisperse distribution, and a decrease in surface charge, with the zeta potential shifting from -30 mV toward -25 mV. This data suggests a tendency for NPs without the surfactant PVA to aggregate at physiological temperatures, possibly due to reduced electrostatic repulsion between particles. Conversely, the presence of PVA in PLGA/PVA NPs appeared to confer greater stability, maintaining a consistent size distribution and surface charge over time. These findings highlight the stabilizing role of PVA as a surface modifier, supporting its utility in improving the stability of polymeric NPs under physiological conditions.

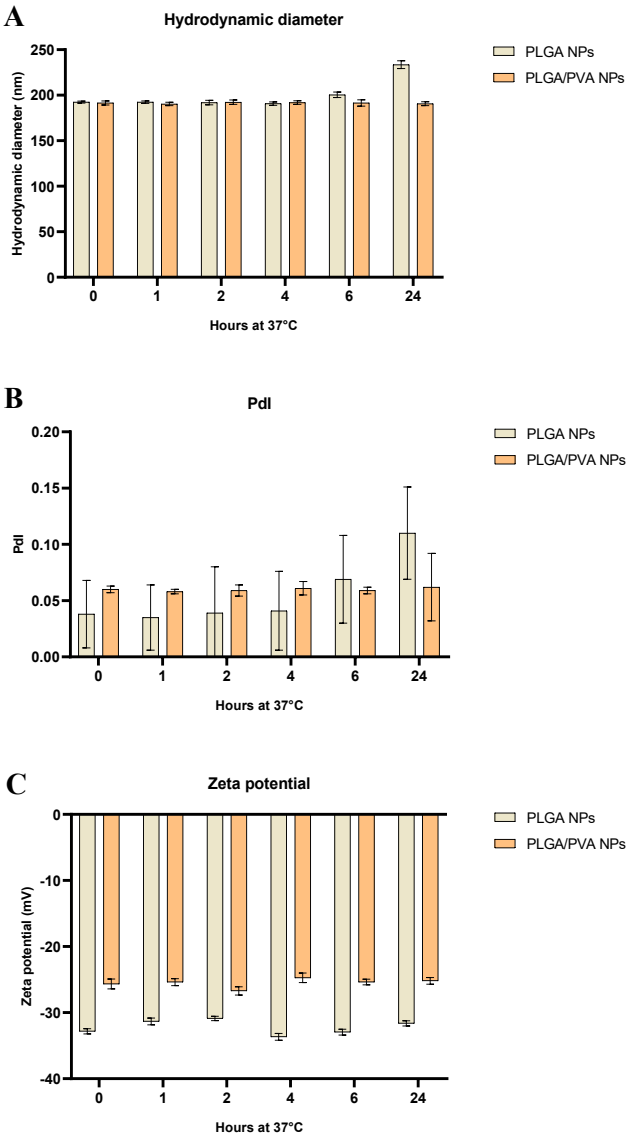

Figure 23. Stability at 37°C of PLGA and PLGA/PVA NPs. DLS analysis to determine the (A) hydrodynamic diameter (D(h)), (B) polydispersity index (PdI) and (C) zeta potential after NP incubation at body temperature (37°C) for different time points. Data are presented as mean ± standard deviation (SD) of three independent replicates. Statistical analysis was performed using t test: p-value > 0,05

5.4.4 NP stability in gastric juice and intestinal fluid

To better mimic physiological conditions and evaluate NP stability in the body, PLGA and PLGA/PVA NPs were incubated at 37 °C in SGF and SIF buffers for 24 hours [232]. The D(h), PdI, and zeta potential were measured after 0, 1, 2, 4, 6, and 24 hours of incubation.

As shown in the graphs (Figure 24), PLGA/PVA NPs remained stable in SGF in terms of D(h), PdI, and zeta potential throughout the incubation period. In contrast, PLGA NPs exhibited significant instability after just 1 hour, with marked changes in these parameters.

In SIF (Figure 25), PLGA/PVA NPs also showed good stability, with only a slight increase in D(h) observed at 24 hours, a PdI suggesting a moderately polydisperse population, and a stable zeta potential. Conversely, PLGA NPs lost stability rapidly: D(h) increased markedly after 1 hour, PdI indicated a highly polydisperse population, while the zeta potential remained relatively stable.

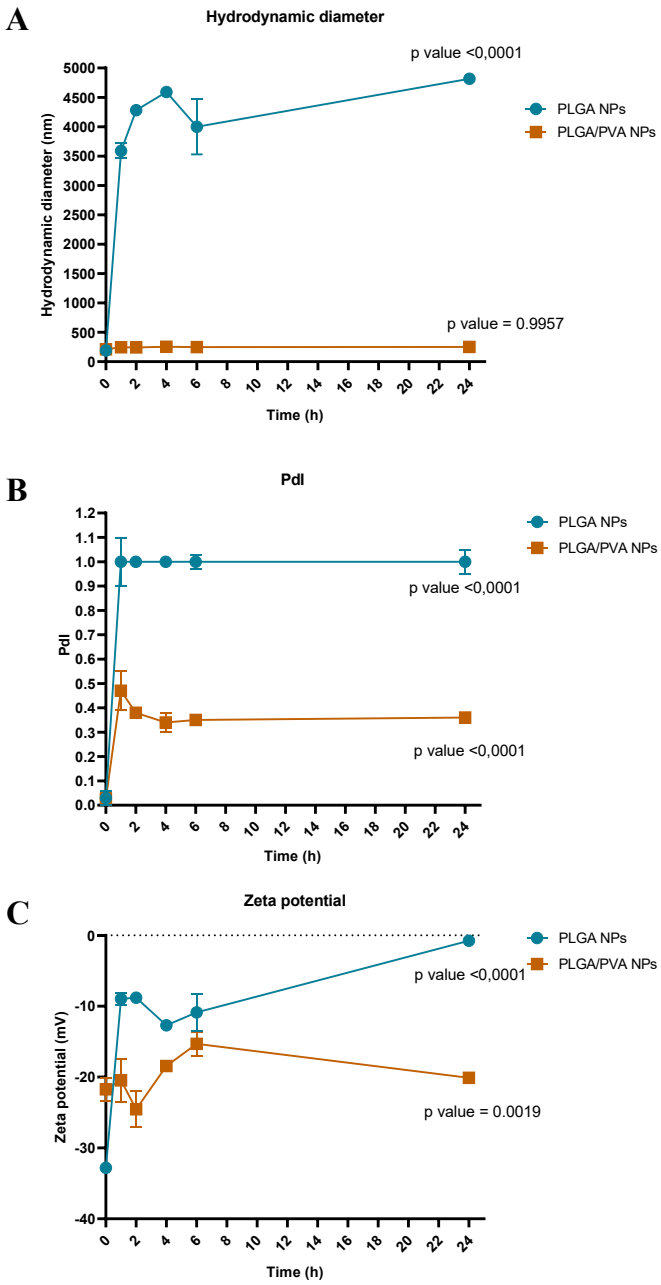

Figure 24. Stability of PLGA and PLGA/PVA NPs in simulated gastric juice (SGF). DLS analysis to determine the (A) hydrodynamic diameter (D(h)), (B) polydispersity index (PdI) and (C) zeta potential after NP incubation at 37°C in SGF for different time points. Data are presented as mean ± standard deviation (SD) of three independent replicates. Statistical analysis was performed using one-way ANOVA.

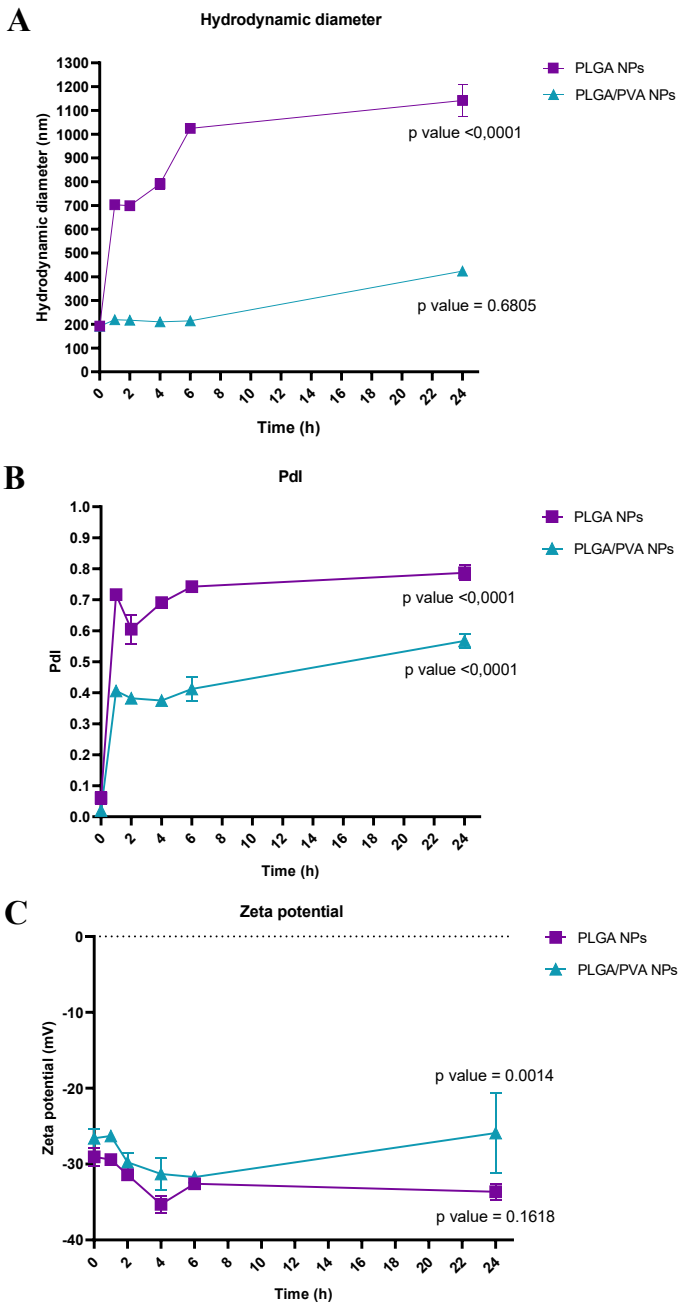

Figure 25. Stability of PLGA and PLGA/PVA NPs in simulated intestinal fluid (SIF). DLS analysis to determine the (A) hydrodynamic diameter (D(h)), (B) polydispersity index (PdI) and (C) zeta potential after NP incubation at 37°C in SIF for different time points. Data are presented as mean ± standard deviation (SD) of three independent replicates. Statistical analysis was performed using one-way ANOVA.

Considering the poor stability exhibited by PLGA NPs, we focused on the use of PLGA/PVA NPs.

5.4.5 *In vitro* biocompatibility of PLGA/PVA and BSA-FITC-loaded PLGA/PVA NPs

To evaluate the role of the NP formulation in the uptake of a given protein in an *in vitro* model of intestinal epithelium, Bovine Serum Albumin conjugated with fluorescein isothiocyanate (BSA-FITC)-loaded PLGA/PVA NPs were produced. In particular, the use of a fluorescent marker, such as FITC can be useful to follow the internalization of NPs. It was therefore selected as a model protein. Consequently, BSA-FITC-loaded PLGA/PVA NPs were prepared via microfluidic nanoprecipitation (Table 4). However, before assessing whether PLGA/PVA NPs enhance protein uptake compared to the free protein, it was essential to evaluate the biocompatibility of the individual components PLGA, PVA and the BSA-FITC with the *in vitro* model of intestinal epithelium, represented by the Caco-2 cell line, and APCs, represented by RAW 264.7. To this end, cells were incubated for 24 and 48 hours at different concentrations of both empty and BSA-FITC-loaded PLGA/PVA NPs, in the range 1 x 10^7 - 1 x 10^{11}, as illustrated in the (Figure 26, 27). Statistical analysis revealed no significant differences in cell viability compared to untreated controls, indicating that neither the polymers nor the BSA-FITC exert cytotoxic effects. Although no significant cytotoxicity was observed, a slight trend of higher apparent toxicity at lower nanoparticle concentrations was noted. This could be due to normal variability in cell metabolism or to minor metabolic contributions from PLGA degradation products (lactic and glycolic acid) entering cellular energy pathways. These findings confirmed the safety of the NP systems for the *in vitro* models of intestinal epithelium and APCs, thus supporting their suitability also for subsequent *in vitro* uptake experiments and *in vivo* studies.

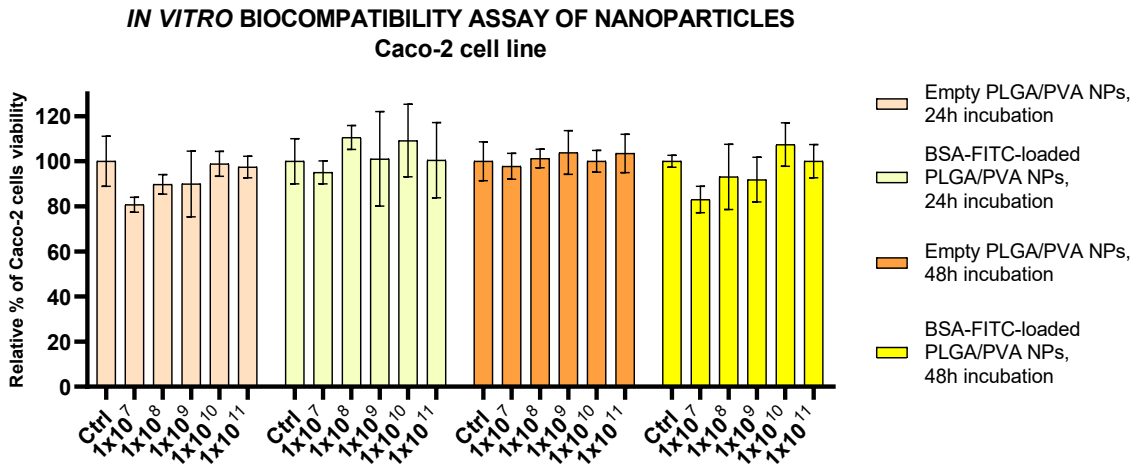

Figure 26. Cell viability assay of the PLGA/PVA NPs. CellTiter-Glo assay on Caco-2 cells to test *in vitro* BSA-FITC and PLGA/PVA NPs biocompatibility with the intestinal epithelium. Data are presented as mean ± standard deviation (SD) of three independent replicates. Statistical analysis was performed using Ordinary one-way ANOVA: ns: ≥ 0.05.

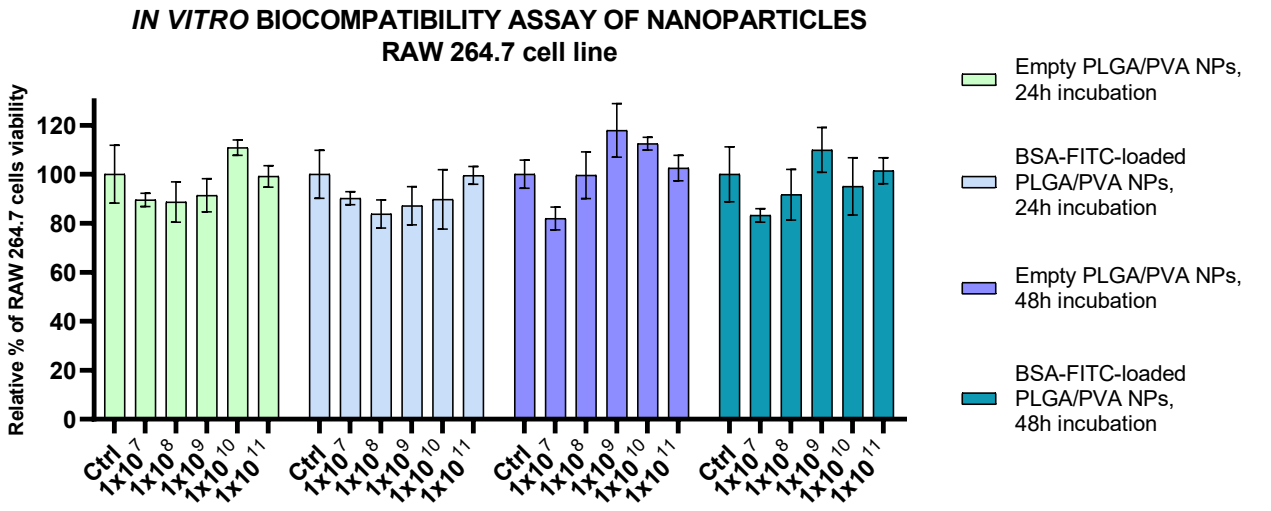

Figure 27. Cell viability assay of the PLGA/PVA NPs. CellTiter-Glo assay on RAW 264.7 cells to test *in vitro* BSA-FITC and PLGA/PVA NPs biocompatibility with the antigen-presenting cells (APCs). Data are presented as mean ± standard deviation (SD) of three independent replicates. Statistical analysis was performed using Ordinary one-way ANOVA: ns: ≥ 0.05.

5.4.6 NP internalization by the *in vitro* model of intestinal epithelium

In addition to finding a system that protects the GPC1-FL protein in the gastrointestinal tract, one of the primary goals of the NP system is to enhance the intestinal uptake of the chimeric protein, with the aim of eliciting a stronger and more specific immune response. To investigate whether PLGA/PVA NPs could improve protein internalization compared to the free form, BSA-FITC-loaded PLGA/PVA NPs were employed as a model system because the fluorescent FITC tag enabled the tracking of protein uptake. Caco-2, used as an *in vitro* model of intestinal M cells, were incubated with 50 µg/mL of either free BSA-FITC or BSA-FITC-loaded PLGA/PVA NPs for 1, 2, 4, 6, and 24 hours. At each time point, the percentage of FITC-positive cells was quantified by flow cytometry. The experiment was performed in triplicate to ensure reproducibility. As illustrated in the (Figure 28), PLGA/PVA NPs significantly enhanced protein internalization over time compared to the free protein.

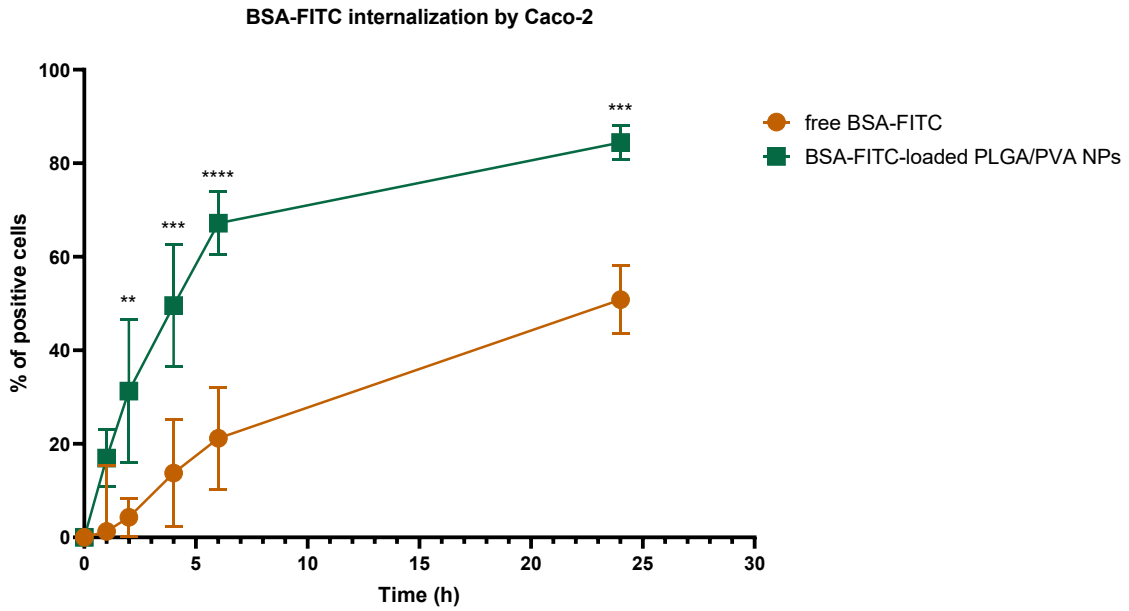

Figure 28. Flow cytometry analysis of the internalization of BSA-FITC and BSA-FITC-loaded PLGA/PVA NP by the *in vitro* model of intestinal epithelium cells (Caco-2). Data are presented as mean ± standard deviation (SD) of three independent replicates. Statistical analysis was performed using two-way ANOVA: ns: ≥ 0.05; **: 0.01 < p ≤ 0.001; ***: 0.001 < p ≤ 0.0001; ****: p <0,0001.

5.4.7 GPC1-FL-loaded PLGA/PVA NP: preparation and characterization

Once it was observed that the PLGA/PVA NPs and the GPC1-FL protein are safe for intestinal epithelial cells and APCs, and that the NPs improve the internalization of the protein by intestinal epithelium compared to its free form, the final NP platform was developed. It consists of PLGA/PVA NPs encapsulating the GPC1-FL protein (GPC1-FL-loaded PLGA/PVA NPs). These NPs were produced using a microfluidic nanoprecipitation method, employing different settings to achieve the desired parameters D(h) of approximately 200 nm, low PdI and highly negative surface charge, as well as to improve the EE%. Following their production, the D(h), PdI, and surface charge were measured using DLS. Additionally, the EE% was calculated. The Table 5 reports the results obtained for each microfluidic condition tested.

Sample	Experimental Conditions GPC1-FL : PLGA	D(h) (nm)	PdI	Zeta Potential (mV)	EE%
1	FRR 1:1 TFR 3 mL/min	261.2 ± 1.0	0.13 ± 0.04	-27.76 ± 0.55	2.83%
2	FRR 2:1 TFR 3 mL/min	252.2 ± 0.7	0.18 ± 0.04	-28.40 ± 1.30	50.14%
3	FRR 3:1 TFR 3 mL/min	231.1 ± 0.8	0.10 ± 0.02	-28.83 ± 0.86	47.38%
4	FRR 1:1 TFR 6 mL/min	210.2 ± 0.9	0.01 ± 0.05	-27.30 ± 0.81	32.58%

Table 5. Preparation of GPC1-FL-loaded PLGA/PVA nanoparticles (NPs). The table summarizes the characterization of four samples produced under different flow rate ratios and total flow rates using the microfluidic nanoprecipitation method.

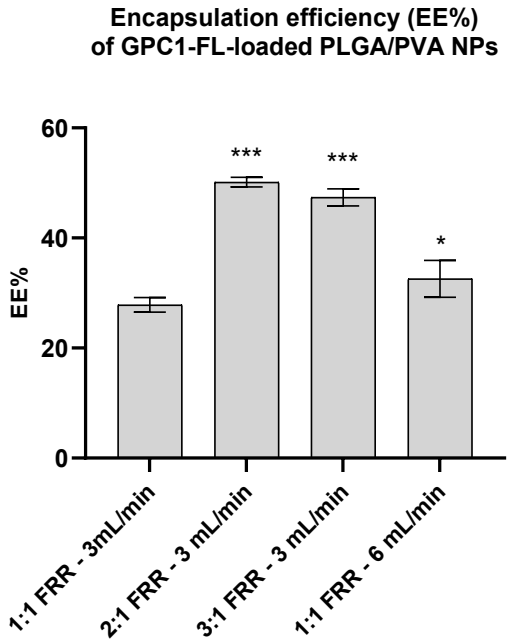

Figure 29. Encapsulation efficiency (EE%) of GPC1-FL-loaded PLGA/PVA NPs. Data are presented as mean ± standard deviation (SD) of three independent replicates. Statistical analysis was performed using ordinary one-way ANOVA: ns: ≥ 0.05; *: 0.05 < p ≤ 0.01; ***: 0.001 < p ≤ 0.0001.

Sample number 3, obtained with an FRR of 3:1 and a TFR of 3 mL/min, was selected as the most suitable formulation for mouse vaccination, as it, together with sample number 2, exhibited the highest EE%. However, compared to sample 2, it had a D(h) close to 200 nm, which favors NP internalization by intestinal epithelial cells, and a lower PdI, indicating a more monodisperse and thus more homogeneous population. Furthermore, the highly negative surface charge is associated with particle stability.
Therefore, sample number 2, despite showing a negative surface charge and the highest EE%, was not considered suitable due to its excessively large D(h) and higher PdI.

5.5 Establishment of a syngeneic murine model of PDAC

To investigate the possible employment of the GPC1-FL-loaded PLGA/PVA NPs as a cancer vaccine, we established a syngeneic mouse model using the murine "PDAC-like" cell line PANC02 that we previously modified to induce human GPC1 expression on the cell surface. In detail, as the first step, we verified the absence of a signal for GPC1 when an antibody cross-reactive for the human and the murine forms of GPC1 was employed. Western blot analysis confirmed the absence of bands corresponding to the GPC1 protein in the PANC02 cells, whereas human PDAC-like BxPC-3 cells showed a band at the expected molecular weight for GPC1 (Figure 30).

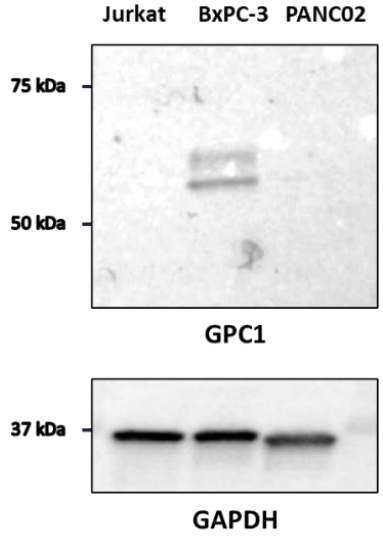

Figure 30. Western blot analysis of Glypican-1 (GPC1) protein in GPC1-positive cancer cell lines (BxPC-3), GPC1-negative cancer cell lines (Jurkat) and mouse cell PANC02. Commercial polyclonal anti-GPC1 was employed at a concentration of 0.33 µg/ml. GAPDH protein was analyzed as housekeeping gene at a concentration of 0.11 µg/ml.

Consequently, to obtain PANC02 cells expressing the human GPC1 on their surface, it was necessary to transfect them with a vector containing the gene sequence of the desired antigen, along with a signal for cell surface expression. Two different plasmid vectors were designed and named VB2hGPC1a and VB2hGPC1b. Both vectors contained the human GPC1 coding sequence, an ampicillin resistance gene for bacterial selection, and a puromycin resistance gene for selecting successfully transfected cells. The main difference between the two vectors is in the promoter used to drive gene expression. VB2hGPC1a carries the EF1α promoter (human eukaryotic translation elongation factor 1 alpha 1), while VB2hGPC1b carries the CBh promoter (a hybrid promoter consisting of the CMV early enhancer fused to a modified chicken β-actin promoter).

After design, the vectors were amplified in *E. coli* DH5α via bacterial transformation. Plasmids were then purified using a MidiPrep kit and quantified using a Nanodrop spectrophotometer.

Before transfecting the PANC02 cells, a puromycin kill curve assay was performed to determine the minimum concentration of antibiotic required to kill non-transfected cells. PANC02 cells were seeded and treated with increasing concentrations of puromycin (1, 3, 6, 9, 12, and 15 µg/mL). The percentage of viable cells was assessed 24 hours after exposure, and 3 µg/mL was selected as the optimal concentration, as it was the lowest dose at which non-transfected PANC02 cells did not survive (Figure 31).

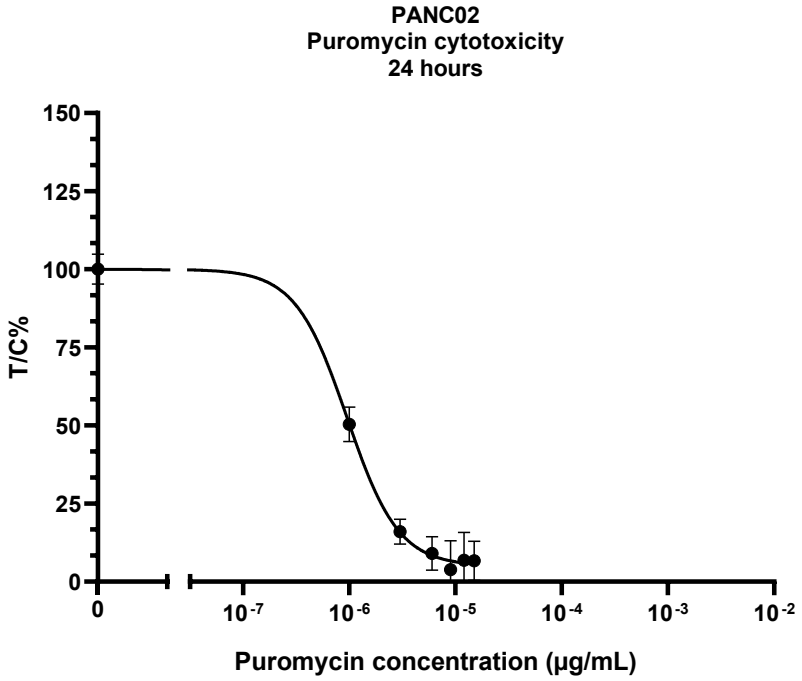

Figure 31. Cytotoxicity curve of puromycin on PANC02 cells. Cell viability was assessed after 24 hours using CellTiter-Glo. Data are presented as mean ± standard deviation (SD) of three independent replicates.

After electroporation-based transfection, flow cytometry was performed to assess the percentage of successfully transfected PANC02 (T-GPC1 PANC02) cells. The percentage of PANC02 cells transfected with the VB2hGPC1a vector was 12.2%, whereas transfection with the VB2hGPC1b vector resulted in 48.3% positivity (Figure 32). Given its higher transfection efficiency, the vector VB2hGPC1b was selected for subsequent experiments.

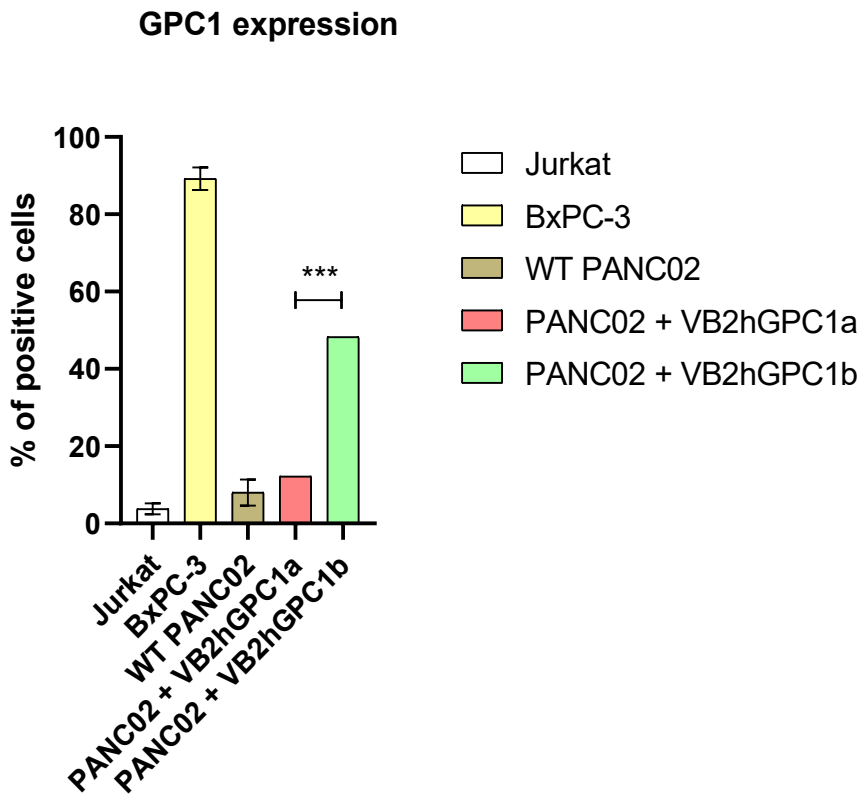

Figure 32. Glypican-1 (GPC1) expression on transfected PANC02 (T-GPC1 PANC02). The percentage of positive PANC02 to GPC1 obtained after transfection with the vectors VB2hGPC1a and VB2hGPC1b was analyzed by flow cytometry. Jurkat and WT PANC02 were used as negative controls, and BxPC-3 as a positive control. Statistical analysis was performed using one-way ANOVA: ***: $0.001 < p \leq 0.0001$.

PANC02 cells transfected with the VB2hGPC1b vector were maintained in culture under selection with 3 µg/ml puromycin. GPC1 expression was monitored by flow cytometry over time (Figure 33). After 28 days of selection, the percentage of GPC1-positive cells reached a plateau, and a western blot was performed to evaluate GPC1 expression in order to validate the flow cytometry results (Figure 34). The specific bands corresponding to GPC1 were observed in the positive control (BxPC-3 cells) and T-GPC1 PANC02 cells at the expected molecular weight of 55-60 kDa.

Additional bands above 75 kDa were detected in all samples, likely reflecting non-specific antibody binding or minor protein modifications. Importantly, these additional bands did not interfere with the interpretation of the specific GPC1 signal.

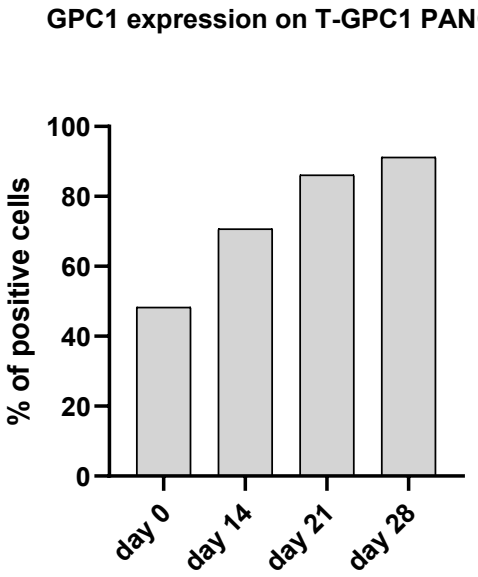

Figure 33. Increase in Glypican-1 (GPC1) expression under puromycin selection. PANC02 transfected with the vector VB2hGPC1b were maintained under constant selection with puromycin, and GPC1 expression was analyzed by flow cytometry over time.

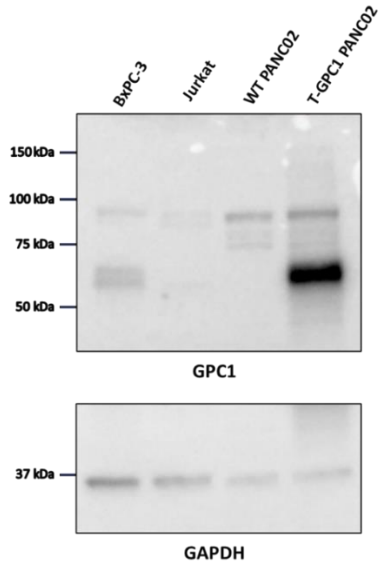

Figure 34. Western blot analysis of Glypican-1 (GPC1) protein in GPC1-positive cancer cell lines (BxPC-3, T-GPC1 PANC02), GPC1- negative cancer cell lines (Jurkat, WT PANC02). Commercial polyclonal anti-GPC1 was employed at a concentration of 0.33 µg/ml. GAPDH protein was analyzed as housekeeping gene at a concentration of 0.11 µg/ml.

To assess whether the vector had stably integrated into the genome, flow cytometry analysis was also performed after removing puromycin selection for one month. The results indicated that stable integration likely occurred, as the percentage of GPC1-positive PANC02 cells remained comparable to that of cells continuously maintained under puromycin selection. Given the possibility of stable integration, we next investigated whether this could affect cellular morphology or growth capacity. Microscopic analysis revealed no significant morphological differences between WT PANC02 and T-GPC1 PANC02 cells (Figure 35). Furthermore, cell proliferation was monitored at each passage, and then the doubling time was calculated (Figure 36). No significant differences were observed between the WT PANC02 and T-GPC1 PANC02 cells in terms of growth capacity. These findings suggested that stable integration of the vector does not alter cell morphology or proliferation capacity, indicating that the T-GPC1 PANC02 could be employed to develop a syngeneic mouse model of GPC1-expressing PDAC.

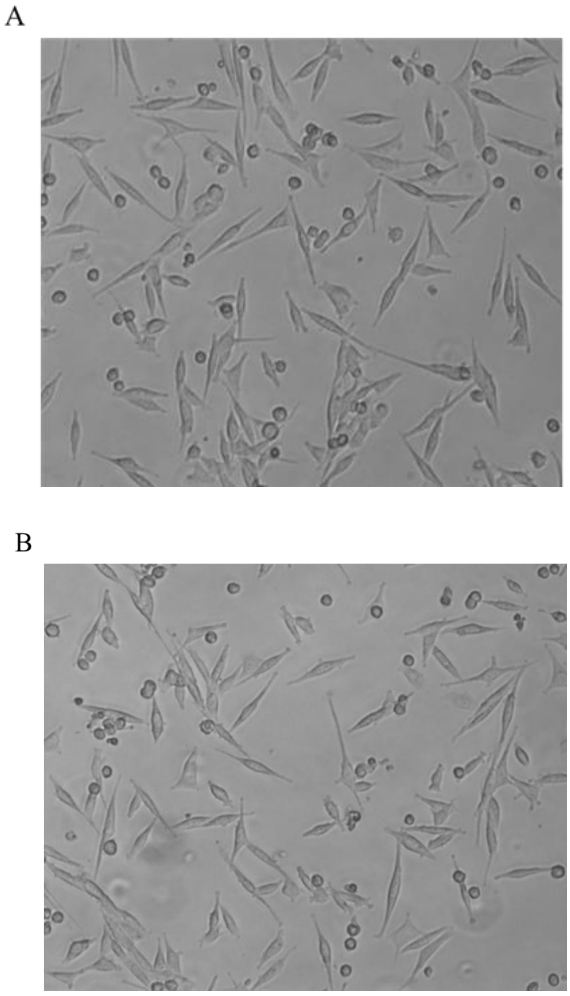

Figure 35. Morphology of (A) WT PANC02 and (B) T-GPC1 PANC02. The cell images were captured using a light microscope at 15X magnification.

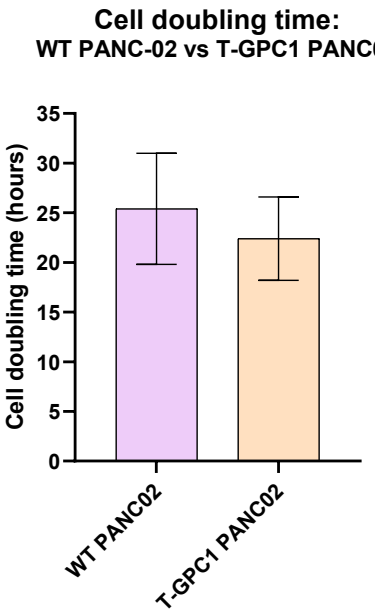

DOUBLING TIME	WT PANC02	T-GPC1 PANC02
Mean (hours)	25.4	22.4
Standard Deviation	5.6	4.2

Figure 36. Cell doubling time. The table and the graph represent the doubling time of WT and T-GPC1 PANC02. Statistical analysis was performed using t test: p value >0,05.

After the *in vitro* validation of the T-GPC1 PANC02 model, the T-GPC1 PANC02 syngeneic mouse model was set up. Specifically, one million of these cells were inoculated into the right flank of C57BL/6 mice, and their growth was assessed *in vivo*. One month after tumor mass development, the mice were sacrificed, and the tumors were excised for immunofluorescence analysis to determine whether GPC1 expression was maintained in T-GPC1 PANC02 tumor mass cells. These *ex vivo* experiments confirmed that GPC1 remained expressed *in vivo* for at least one month, while it was not detected in mice inoculated with WT PANC02 cells (Figure 37).

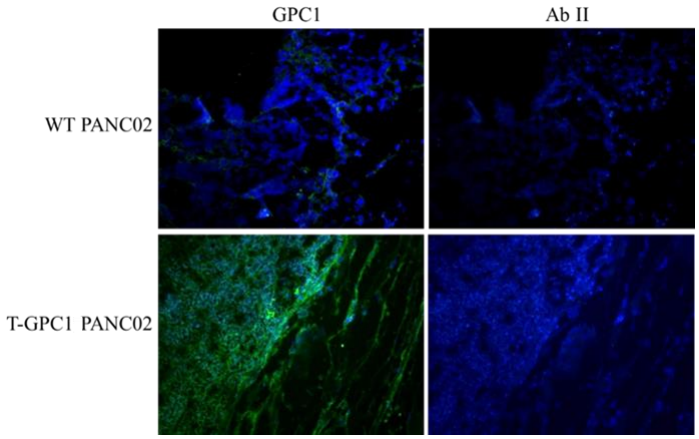

Figure 37. Immunofluorescence staining of *ex vivo* tumor tissues derived from Wild type (WT) and transfected (T-GPC1) PANC02 cells, showing GPC1 expression. GPC1 protein is visualized in green, while cell nuclei are counterstained in blue (DAPI). WT PANC02 cells were used as a negative control, confirming the specificity of GPC1 detection.

5.6 *In vivo* studies of the NP-based Cancer Vaccine

5.6.1 Detection of specific anti-GPC1 IgG antibodies in mouse serum

5.6.1.1 *In vivo* vaccination via SC administration

To investigate the immunogenicity of the chimeric protein and the capability of the PLGA/PVA NPs of further enhancing its immunogenicity, a vaccination protocol with SC administration of the protein was set up *in vivo* in C57BL/6 mice. Four groups of mice, of 6 mice each, were vaccinated subcutaneously with 50 μg per dose of GPC1-FL, either in free form or encapsulated in PLGA/PVA NPs (GPC1-FL-loaded PLGA/PVA NPs), as well as with empty PLGA/PVA NPs or PBS as controls. In detail, treatment with free GPC1-FL was performed to understand if the chimeric protein can be immunogenic; treatment with GPC1-FL-loaded PLGA/PVA NPs was performed to investigate the possible improvement due to the NPs delivery. A first control was represented by treatment with empty PLGA/PVA NPs to evaluate a possible nonspecific effect due to polymers or NP formulation, and PBS treatment was the negative control. According to the protocol, at day 0, the mice were alternatively vaccinated subcutaneously with GPC1-FL-loaded PLGA/PVA NPs, free GPC1-FL, empty PLGA/PVA NPs or PBS. Then they received a booster dose at day 14. Moreover, blood was collected at day 0 (before starting the immunization), 14, 21, 28, and 35 for serum preparation and antibody quantification by ELISA test (Figure 38). The first blood collections after day 0 were performed on day 14, prior to the booster dose, since IgG antibodies typically become detectable starting from the second week post-immunization.

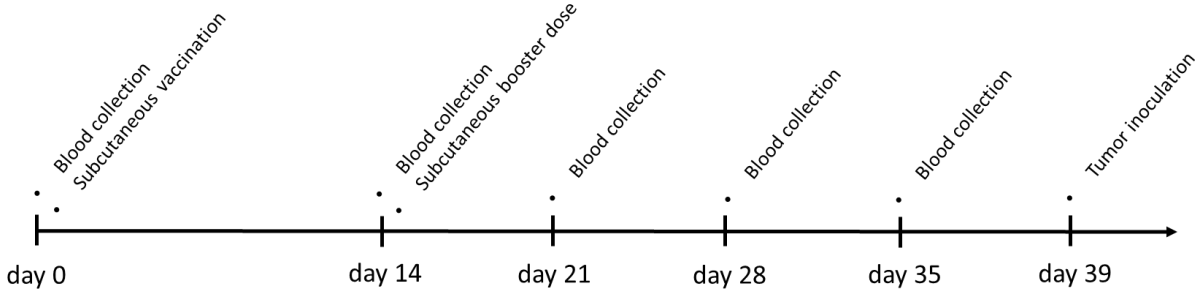

Figure 38. Schedule of the subcutaneous (SC) vaccination. Timeline of the experimental protocol illustrating the schedule of SC vaccinations, blood collection time points, and tumor cell inoculation in mice.

After the obtainment of serum preparation from blood samples for each time-point, the ELISA test was performed in which the four treatment groups GPC1-FL-loaded PLGA/PVA NPs, free GPC1-FL, empty PLGA/PVA NPs, and PBS were compared to evaluate the absorbance at 450 nm corresponding to the anti-GPC1 IgG concentrations. Both the GPC1-FL-loaded PLGA/PVA NPs group and the free GPC1-FL group showed a significant increase in absorbance at 450 nm starting from day 14 to day 28, compared to day 0 in which all groups showed negligible antibody titers. Of note, from day 28 to day 35 there was a decrease in the absorbance values for both GPC1-FL-loaded PLGA/PVA NPs and free GPC1-FL groups. On the other hand, consistently with the absence of the vaccine, both empty PLGA/PVA NPs, and PBS did not show significant increases in absorbance values during the time of the vaccination protocol. Consistently, both GPC1-FL-loaded PLGA/PVA NPs and free GPC1-FL groups significantly showed higher absorbance values compared to empty PLGA/PVA NPs and PBS groups starting from day 14. Notably, the increase in absorbance signal was significantly higher at day 14 for the free GPC1-FL group compared to the GPC1-FL-loaded PLGA/PVA NPs, whereas the absorbance signal for the GPC1-FL-loaded PLGA/PVA NPs became significantly higher at day 21, then continuing to be higher until day 35 (Figure 39).

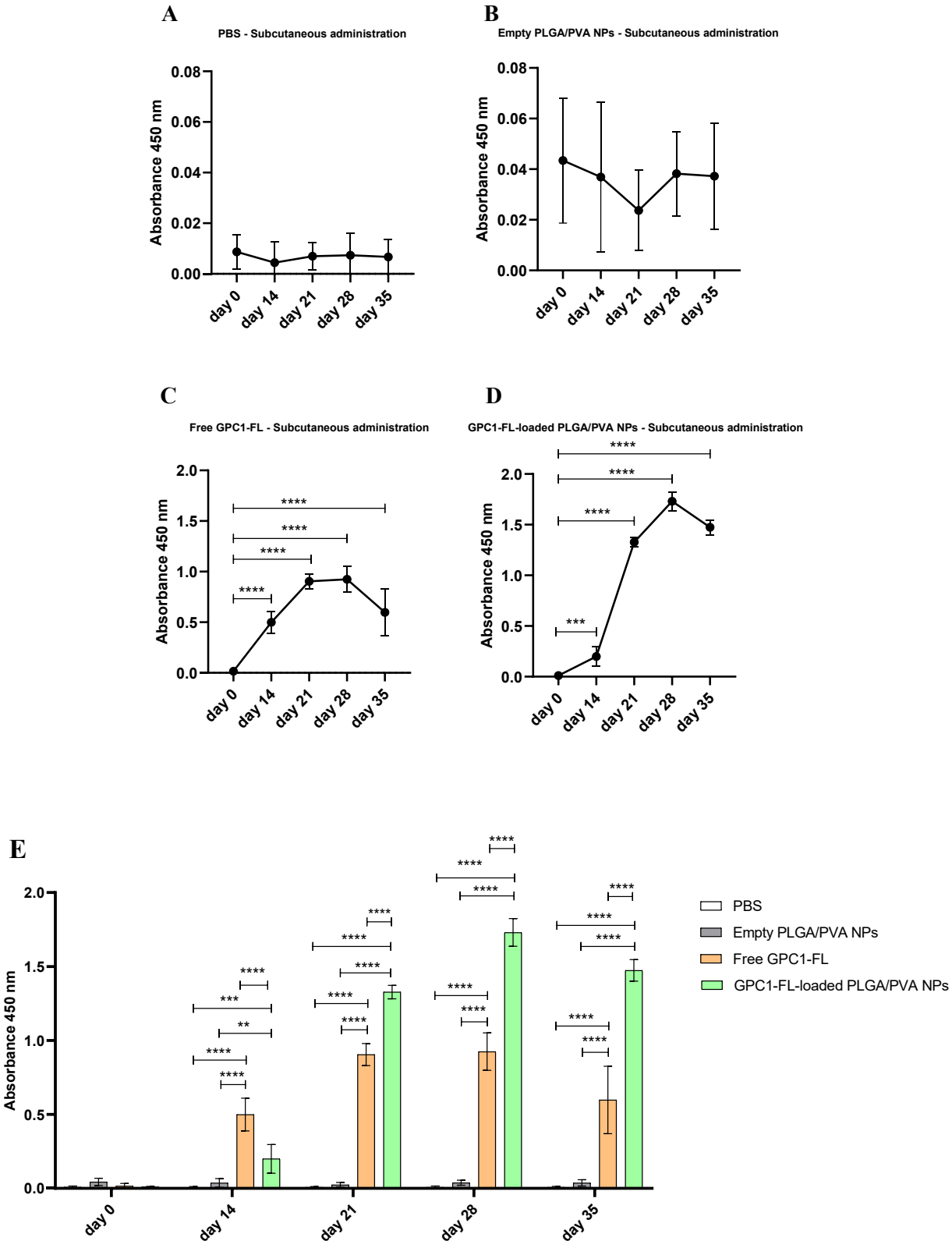

Figure 39. Anti-Glypican-1 (GPC1) IgG titer following Subcutaneous (SC) Immunization. ELISA results showing the detection over time of anti-GPC1 IgG antibodies in mouse serum following SC administration of (A) PBS, (B) empty PLGA/PVA NPs, (C) free GPC1-FL protein, and (D) GPC1-FL-loaded PLGA/PVA NPs (D). Graph (E) summarizes and compares the antibody responses elicited by the four different treatments. Statistical analysis was performed using one-way and two-way ANOVA: ns: ≥ 0.05; **: $0.01 < p \leq 0.001$; ***: $0.001 < p \leq 0.0001$; ****: $p < 0{,}0001$.

5.6.1.2 *In vivo* vaccination via OS administration

Since the GPC1-FL protein proved to be immunogenic, as defined by the increase in absorbance 450 nm signal by ELISA, and PLGA/PVA NPs were able to further enhance this signal, the next step was to evaluate whether PLGA/PVA NPs could successfully deliver the chimeric protein GPC1-FL to the intestine and induce a specific anti-GPC1 IgG response.

In vivo experiments to investigate the possible employment of GPC1-FL-loaded PLGA/PVA NPs for OS vaccination were performed using 4 groups of mice, composed of 6 mice each, in which the same preparation of NPs used previously was administered via OS gavage. Therefore, mice received 50 µg per dose of GPC1-FL, in its free form or encapsulated in PLGA/PVA NPs, and empty PLGA/PVA NPs or PBS as negative controls. The vaccination and the blood collection were carried out using the same conditions and scheduling as in the SC protocol (Figure 40), in order to allow direct comparison between the SC and the OS administration.

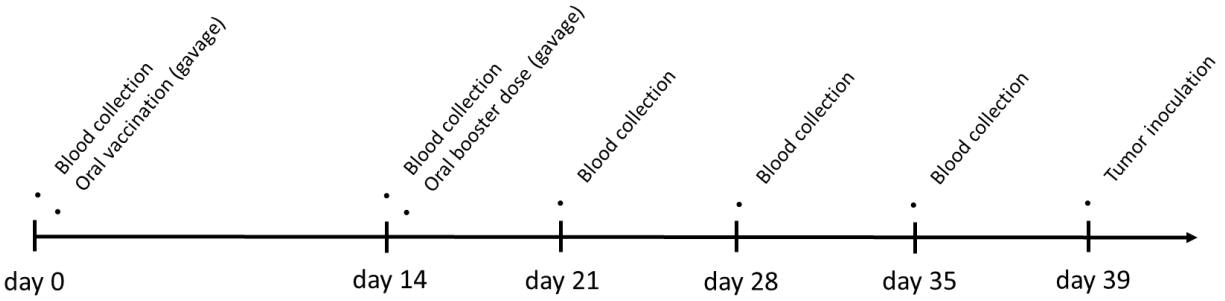

Figure 40. Schedule of the oral (OS) vaccination. Timeline of the experimental protocol illustrating the schedule of OS vaccinations, blood collection time points, and tumor cell inoculation in mice.

ELISA showed that the administration of the free GPC1-FL protein did not induce a significant increase in absorbance at 450 nm, with values comparable to those of the empty PLGA/PVA NPs and PBS negative controls (Figure 41). In contrast, a significant increase in the absorbance was detected for the group of mice treated with GPC1-FL-loaded PLGA/PVA NPs as early as day 14, remaining stable at day 21 before rising further at days 28 and 35 (Figure 41). However, when mice undergoing SC and OS administration were compared, serum samples of mice in which GPC1-FL-loaded PLGA/PVA NPs were orally administered showed significantly lower absorbance signals compared to mice that received the SC treatment (Figure 42).

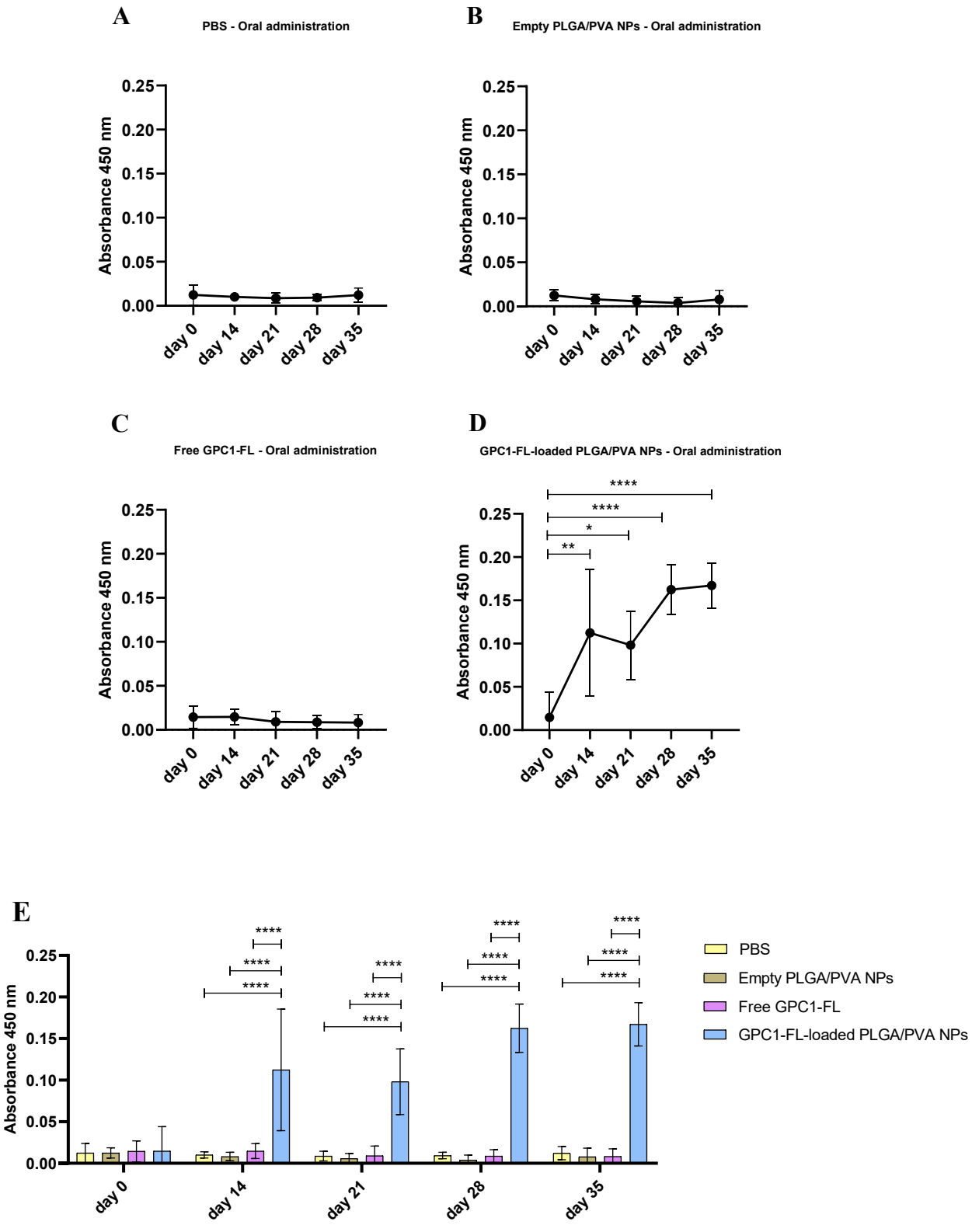

Figure 41. Anti-Glypican-1 (GPC1) IgG titer following oral (OS) immunization. ELISA results showing the detection over time of the anti-GPC1 IgG antibodies in mouse serum following OS administration of (A) PBS, (B) empty PLGA/PVA nanoparticles (NPs), (C) free GPC1-FL protein, and (D) GPC1-FL-loaded PLGA/PVA NPs. Graph (E) summarizes and compares the antibody responses elicited by the four different treatments. Statistical analysis was performed using one-way and two-way ANOVA: ns: ≥ 0.05; *: 0.05 < p ≤ 0.01; **: 0.01 < p ≤ 0.001; ***: 0.001 < p ≤ 0.0001; ****: p <0,0001.

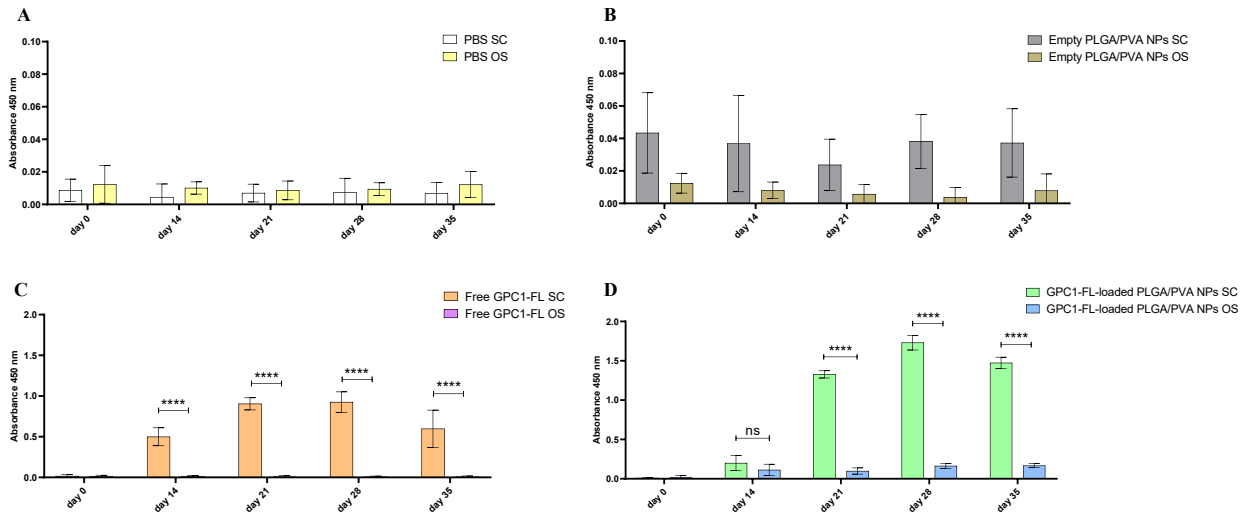

Figure 42. **Anti-Glypican-1 (GPC1) IgG titer following subcutaneous (SC) and oral (OS) immunization.** The graphs compare the anti-GPC1 IgG titers elicited by (A) PBS, (B) empty PLGA/PVA NPs, (C) free GPC1-FL, and (D) GPC1-FL-loaded PLGA/PVA NPs after SC and OS administration. Statistical analysis was performed using two-way ANOVA: ns: ≥ 0.05; ****: p <0,0001.

5.6.2 Mouse survival

5.6.2.1 SC administration

After the evaluation of the anti-GPC1 IgG response induced by mouse vaccination, the next step was to determine whether the immunization could also affect tumor prevention in a PDAC model that expresses the human GPC1. To this end, subcutaneously immunized mice were injected in the right flank with T-GPC1 PANC02 cells 25 days after the booster dose (day 39 of the schedule). Tumor growth was monitored over time, and animals were sacrificed upon reaching the humane endpoint (when the tumor dimension exceeded 12 mm in one axis, or it had an ulcer). Finally, the median survival time was studied by Kaplan-Meier estimator (Figure 43). At the experimental endpoint, median survival times were 43 days for PBS-treated mice, 29 days for mice receiving empty PLGA/PVA NPs, 27 days for those immunized with the free form of GPC1-FL, and 53 days for mice vaccinated with GPC1-FL-loaded PLGA/PVA NPs. The median survival of GPC1-FL-loaded PLGA/PVA NPs treated mice was significantly higher than that of PBS-treated mice ($p = 0.0134$). On the other hand, there was no significant difference between empty PLGA/PVA NPs and the PBS-treated group ($p = 0.1217$). Of note, the median survival of GPC1-FL-loaded PLGA/PVA NPs treated mice was significantly higher than that of empty PLGA/PVA NPs treated mice ($p = 0.0037$), whereas there was no significant difference between free GPC1-FL and empty PLGA/PVA NPs treated mouse groups ($p = 0.1750$). Finally, it is noteworthy that the median

survival of GPC1-FL-loaded PLGA/PVA NPs treated mice was significantly higher than that of free GPC1-FL-treated mice (p = 0.0037). However, mice immunized with free GPC1-FL protein displayed reduced survival compared with all other groups, suggesting possible toxicity due to rapid systemic exposure, excessive immune activation, or local inflammatory reactions at the injection site.

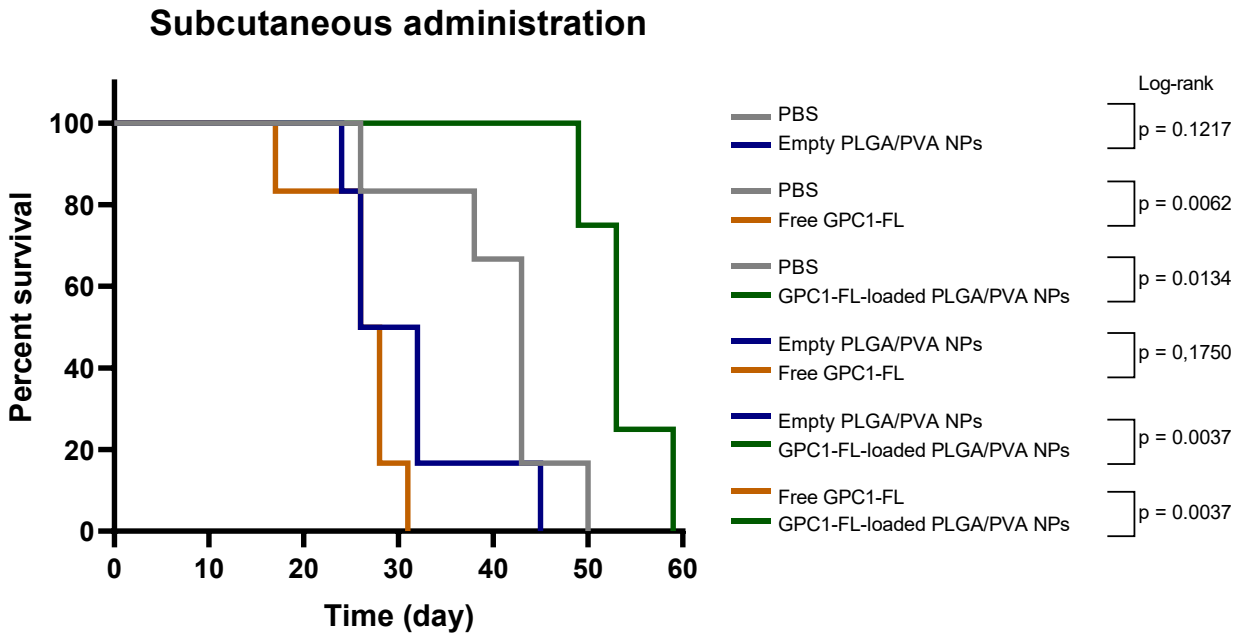

Figure 43. Mouse survival after subcutaneous (SC) GPC1-FL vaccination in a GPC1-expressing PDAC model. Mice were subcutaneously vaccinated with either free GPC1-FL or GPC1-FL-loaded PLGA/PVA NPs. Negative controls included PBS and empty PLGA/PVA NPs. Following inoculation with T-GPC1 PANC02 cells, tumor growth and survival were monitored. Survival curves were analyzed by the Kaplan-Meier estimator, and p-values were calculated using the log-rank test.

To confirm that the murine model was effective and that the improved survival observed in mice immunized subcutaneously was due to the immune system recognizing GPC1 expressed on tumor cells, immunofluorescence analyses were performed on tumor tissues. After mouse sacrifice, tumor masses derived from T-GPC1 PANC02 cells were collected, embedded, and sectioned for immunofluorescence staining to verify GPC1 expression *ex vivo* (Figure 44).

This analysis was carried out on tumors from all treatment groups immunized subcutaneously, thus mice that received PBS, empty PLGA/PVA NPs, free GPC1-FL, and GPC1-FL-loaded PLGA/PVA NPs. The results showed that the tumor samples from all treatment groups retained GPC1

expression. This finding confirms that the murine model was successfully established. Moreover, this result was in keeping with the reduced tumor growth observed in mice vaccinated subcutaneously with GPC1-FL-loaded NPs, thus suggesting a specific GPC1-targeted immune response, as defined by the production of anti-GPC1 antibodies.

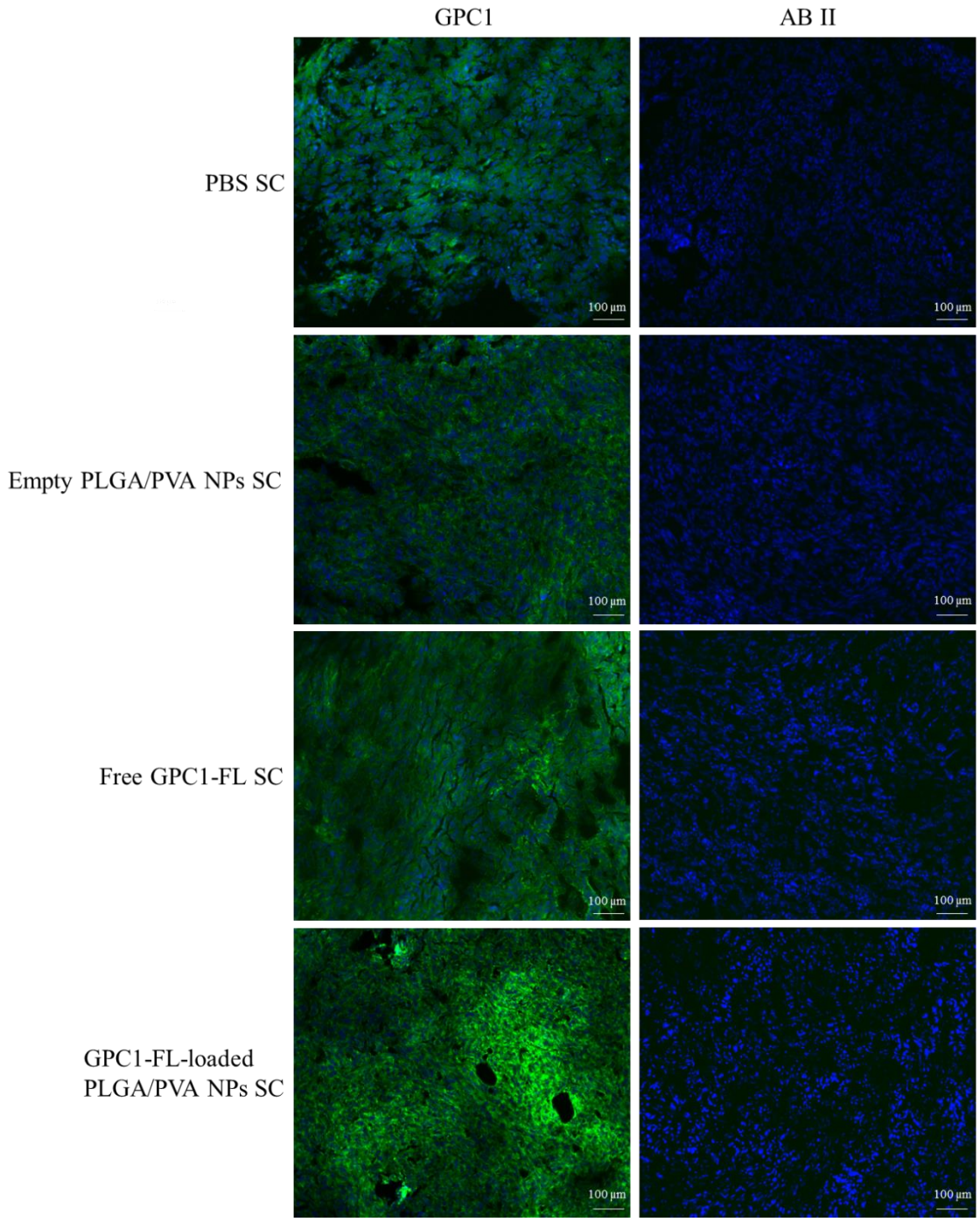

Figure 44. Representative *ex vivo* immunofluorescence analysis showing GPC1 expression in tumor masses derived from T-GPC1 PANC02 cells from mice immunized subcutaneously. Blue represents nuclei, and green indicates GPC1 expression. The anti-GPC1 antibody was used at a concentration of 6.8 µg/mL. Scale bar: 100 µm.

5.6.2.2 OS administration

Using the same scheduling and experimental conditions applied to mice receiving T-GPC1PANC02 after SC immunization, the orally immunized mice were also injected with T-GPC1 PANC02 cells 25 days after the booster dose (day 39 of the scheduling) and then subjected to survival analysis. The median survival times were 37 days for mice receiving PBS, 37 days for those treated with empty PLGA/PVA NPs, 40,5 days for mice administered with the free GPC1-FL, and 43 days for those vaccinated with GPC1-FL-loaded PLGA/PVA NPs (Figure 45). In contrast to what was observed for the SC administration, there was no significant difference in terms of survival among the different mouse treatment groups.

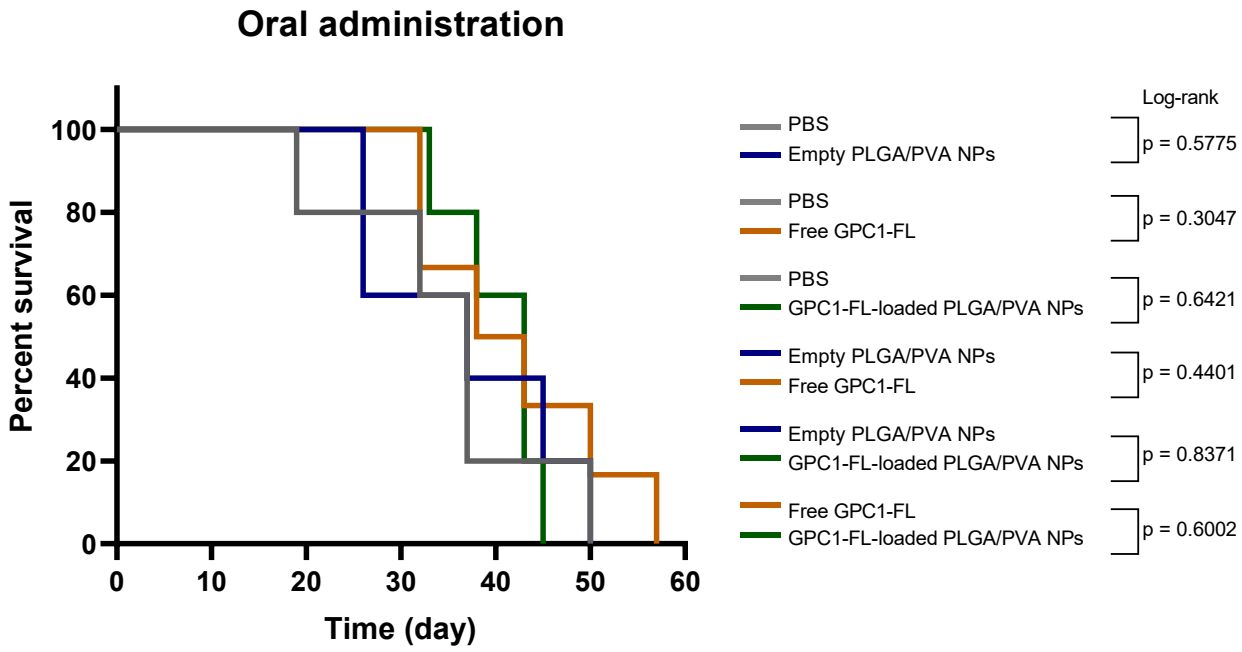

Figure 45. Mouse survival after oral (OS) GPC1-FL vaccination in a GPC1-expressing PDAC model. Mice were orally vaccinated with either free GPC1-FL or GPC1-FL-loaded PLGA/PVA NPs. Negative controls included PBS and empty PLGA/PVA NPs. Following inoculation with T-GPC1 PANC02 cells, tumor growth and survival were monitored. Survival curves were analyzed by the Kaplan-Meier estimator, and p-values were calculated using the log-rank test.

Again, the immunofluorescence analysis was performed on tumor tissues from mice immunized orally, confirming that GPC1 expression was also maintained in these tumor samples (Figure 46).

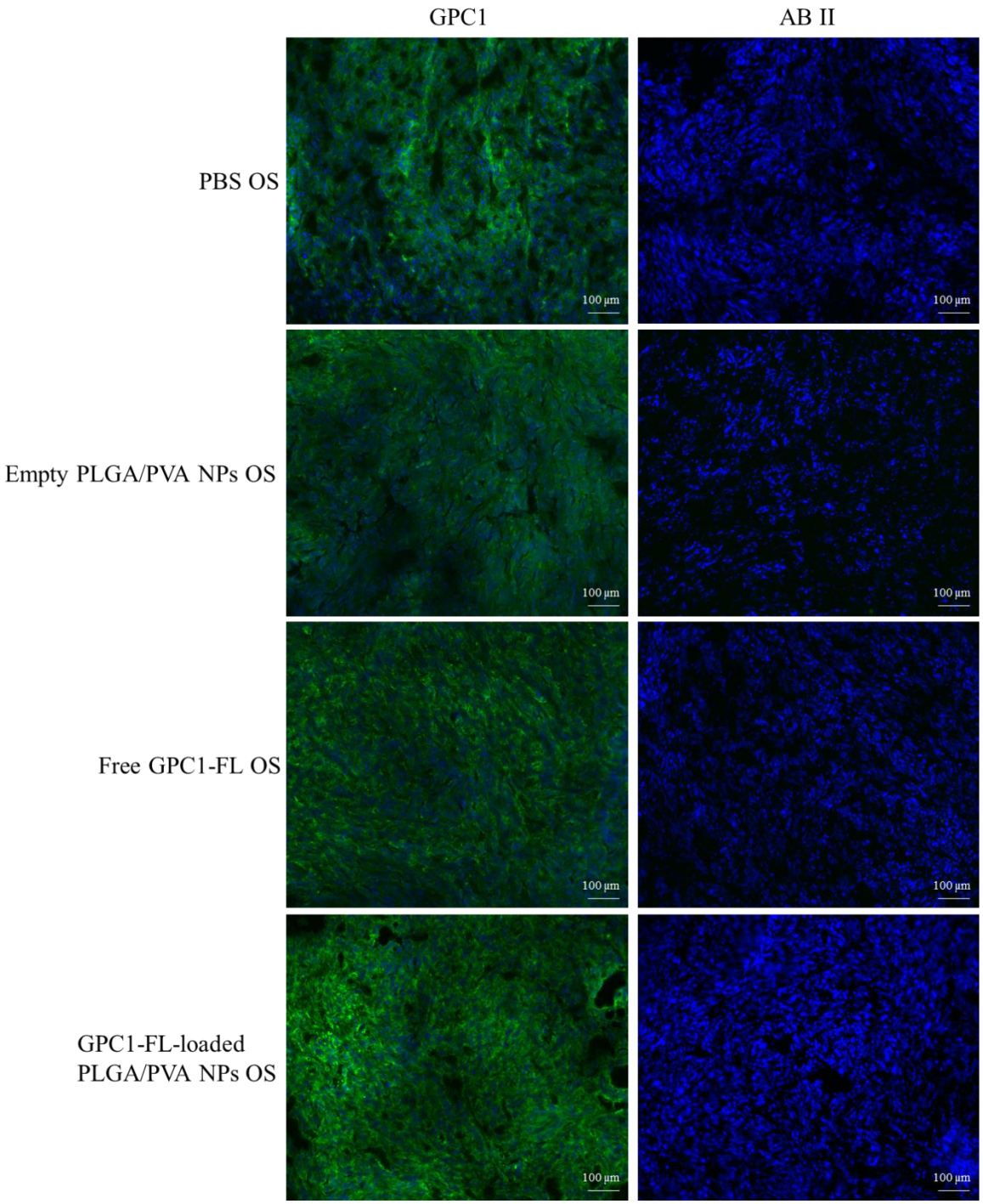

Figure 46. Representative *ex vivo* immunofluorescence analysis showing GPC1 expression in tumor masses derived from T-GPC1 PANC02 cells from mice immunized orally. Blue represents nuclei, and green indicates GPC1 expression. The anti-GPC1 antibody was used at a concentration of 6.8 µg/mL. Scale bar: 100 µm.

In addition, the survival curves of mouse groups treated with the same formulation or control were compared (Figure 47). The median survival of mouse groups that received the GPC1-FL-loaded PLGA/PVA NPs subcutaneously was significantly higher than the median survival of mouse groups

undergoing OS administration with GPC1-FL-loaded NPs (p = 0.0051). Moreover, the free GPC1-FL is safer after the OS administration compared to the SC (p = 0.0006). On the other hand, for both empty PLGA/PVA NPs and PBS treatments, there was no significant survival difference between mouse groups undergoing SC and OS administrations (p = 0.2415 and p = 0.3360, respectively).

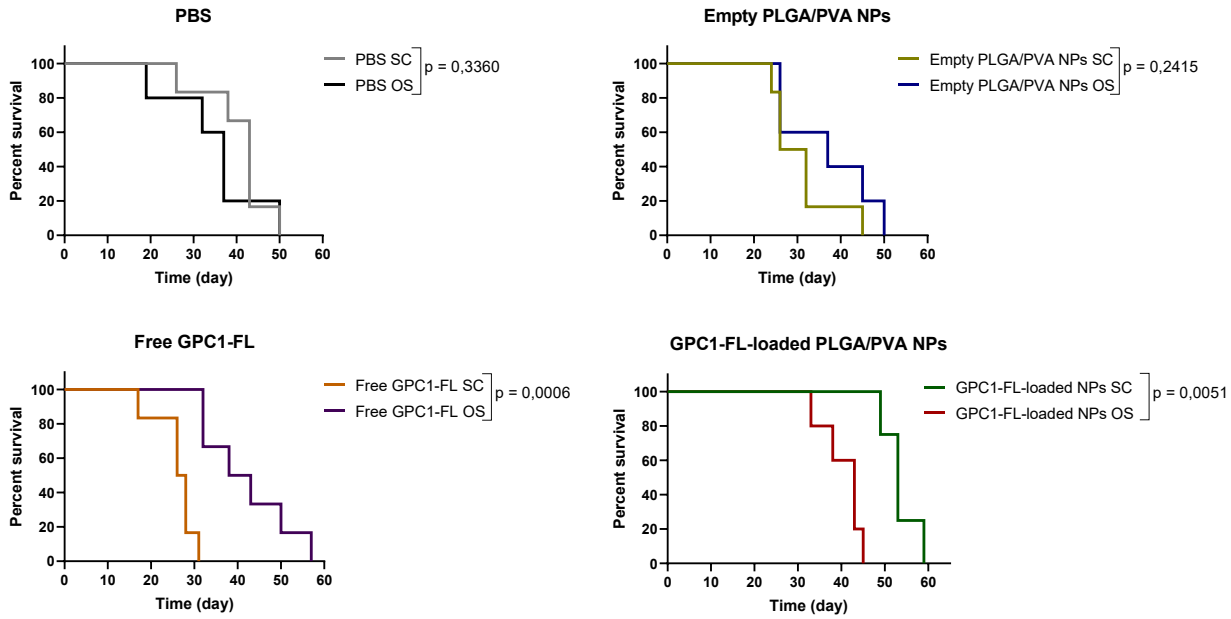

Figure 47. Survival curves of mice after oral (OS) or subcutaneous (SC) administration of the vaccine. Following inoculation with T-GPC1 PANC02, survival of mice vaccinated with free GPC1-FL or GPC1-FL-loaded PLGA/PVA NPs was compared following SC or OS administration. PBS and empty PLGA/PVA NPs were used as negative controls. Survival curves were analyzed by the Kaplan-Meier estimator, and p-values were calculated using the log-rank test.

5.6.3 *In vivo* Safety profile of free GPC1-FL and GPC1-FL-loaded PLGA/PVA NPs

All mice were weighed before vaccination, and their weight was monitored over time. Body weight remained stable throughout their lifespan. Moreover, no signs of stress, such as alopecia or abnormal behavior, were observed.

6 DISCUSSION

In the present thesis, we proposed the use of PLGA/PVA NPs as a carrier to protect and deliver a chimeric protein targeting GPC1 for PDAC treatment through either SC or OS administration [2,232]. Specifically, we engineered the chimeric protein GPC1-FL to be used as a protein-based cancer vaccine, and we produced PLGA/PVA NPs as an adjuvant component of the vaccine also useful for the delivery of the GPC1-FL protein and the preservation of its integrity in the gastrointestinal tract. In a syngeneic mouse model of human GPC1-expressing PDAC, we showed evidence of the immunogenicity of the GPC1-FL chimeric protein being capable of eliciting a specific anti-GPC1 IgG antibody response when subcutaneously administered. Moreover, we demonstrated that encapsulating GPC1-FL within PLGA/PVA NPs enhances the immunogenicity of the vaccine formulation, as evidenced by the higher anti-GPC1 IgG antibody titers observed after both SC and OS administration compared to the free GPC1-FL. This improved immune response was also associated with reduced tumor growth and increased mouse survival following SC administration. Therefore, we demonstrated both *in vitro* and *in vivo* that the PLGA/PVA NPs are able to protect the GPC1-FL during gastrointestinal transit and promote its delivery to the intestinal immune system after OS immunization. However, the observed immune response in the case of OS administration of the GPC1-FL-loaded PLGA/PVA NPs vaccine formulation was not sufficient to significantly delay tumor progression or improve survival in mice using the same administration scheduling that we employed for the SC route.

PDAC is the most common form of pancreatic cancer and one of the deadliest malignancies [2]. Its poor prognosis is mainly due to late diagnosis and to the limited effectiveness of available treatments. Indeed, current therapies are not sufficient to counteract this kind of cancer, and immunotherapy can be a strategy to support them [7–9,43]. In the context of immunotherapy, cancer vaccines represent a promising strategy to stimulate the immune system to recognize tumor cells and mount an effective response against them. An attractive target antigen for a PDAC vaccine is GPC1, a proteoglycan highly expressed on PDAC cells but absent or only weakly expressed in benign lesions and normal tissues [2,32,43].

However, TAAs such as GPC1 are generally less immunogenic than TSAs. For this reason, it is crucial to include adjuvants in the vaccine formulation to enhance the immune response. In the setting of both SC and OS vaccine administration, FL from *Salmonella typhi* may serve as a potent adjuvant, as it is recognized by TLR5, thereby activating innate immunity and promoting the induction of strong adaptive responses [178,180,181].

One of the aims of the project is to create an OS vaccine. However, as demonstrated by our results, after OS administration, GPC1-FL will be degraded in the stomach and intestine before it can be taken up by the intestinal epithelium. Under these conditions, the likelihood of its efficacy as an OS vaccine is very low. Therefore, it is necessary to encapsulate the GPC1-FL protein in a system capable of protecting it from the harsh conditions of the gastrointestinal tract [232]. Consequently, the goal is to obtain a NP platform able to protect the chimeric GPC1-FL in the gastrointestinal tract, promote its internalization by intestinal epithelium, and improve a specific immune response against GPC1. For the NP preparation, we have chosen PLGA because it is a biocompatible and biodegradable copolymer, and it is already approved by the FDA and EMA for biomedical applications [191]. The PLGA NPs need to have an average D(h) of approximately 200 nm, which promotes uptake by intestinal epithelium, a low PdI, and a strongly negative zeta potential to prevent NP aggregation. To this end, NPs were produced using the microfluidic nanoprecipitation method, which ensures highly controlled conditions [209]. Compared to conventional bulk methods, microfluidic offers higher reproducibility, precise control over particle size distribution, and scalability, making it particularly suitable for biomedical applications [207,208,213]. To obtain the desired NPs, it is essential to consider the microfluidic experimental conditions, in particular the FRR and the TFR. The FRR refers to the ratio between the flow rates (or volumetric flows) of two or more fluids introduced into a microchannel, while the TFR represents the total flow rate of all fluids entering the microfluidic device. Both FRR and TFR are critical parameters for controlling NP size. Specifically, increasing the FRR generally leads to smaller particles. Similarly, a higher TFR typically results in greater shear forces, which can reduce particle size and increase formation frequency. Moreover, the FRR can influence the amount of encapsulated material and the stability of the NPs [207].

In the first step of the project, we prepared empty PLGA and PLGA/PVA NPs to study the stability of the polymers. The results demonstrate the role of PVA as a stabilizing agent in maintaining NP integrity [198]. Indeed, PLGA NPs are not stable over time, and under simulated physiological conditions of the stomach and intestine. On the other hand, the stability data suggest that PLGA/PVA NPs, since they exhibit an acceptable degree of stability, represent a strategy for the OS delivery of the chimeric GPC1-FL protein. Indeed, the PLGA/PVA NPs demonstrated that they maintain their stability and therefore they can protect the GPC1-FL protein from the harsh pH and enzymatic conditions of the stomach and the intestine [198,232]. Consequently, thanks to this nanoplatform, GPC1-FL would reach the intestinal tract in its intact form, where it could be internalized by the intestinal epithelium and recognized by the intestinal immune system cells.

Furthermore, we prepared BSA-FITC-loaded PLGA/PVA NPs to investigate whether these NPs affect protein internalization in an *in vitro* model of intestinal epithelium [233]. Before that, we also evaluated the biocompatibility of the polymers with the *in vitro* model of intestinal epithelium and APCs [234].

The results demonstrated that PLGA/PVA NPs are biocompatible and improve the internalization of a protein compared to its free form, representing an advantage for enhancing its delivery across the intestinal barrier. This is particularly relevant given the physiological role of M cells, which are specialized epithelial cells located in the Peyer's patches of the GALT [99,102]. M cells are primarily involved in activating the intestinal immune system as they capture luminal particles, antigens, microbes, and macromolecules, and transcytose them intact to immune cells residing in their characteristic basolateral pocket. There, DCs are activated, leading to antigen presentation, T lymphocytes priming, and B lymphocytes stimulation for antibody production [99,102]. Therefore, increasing the amount of protein transported through M-cell-like models suggests a potential improvement in mucosal immune activation [99,102], highlighting the relevance of PLGA/PVA NP-based delivery systems in promoting efficient protein uptake.

To test the immunogenicity and efficacy of the vaccine GPC1-FL-loaded PLGA/PVA NPs, immunocompetent mice were required. For this purpose, C57BL/6 mice were used [235]. The aim was not only to observe whether the anti-tumor vaccine induces the production of specific anti-GPC1 IgG antibodies in the mouse serum [236,237], but also to determine whether these antibodies, and more in general the immune response induced by the vaccine, can prevent the development of PDAC in these mice. Therefore, we established a syngeneic mouse model of PDAC engineered to express the human GPC1.

First, mice were subcutaneously vaccinated with either free GPC1-FL protein or GPC1-FL encapsulated in PLGA/PVA NPs, and empty PLGA/PVA NPs or PBS as negative controls. This experimental design allowed us to assess the intrinsic immunogenicity of the GPC1-FL protein and to evaluate whether NP encapsulation provides an advantage in terms of enhancing the immune response compared to the free protein. We immunized mice at day 0 and day 14, and we checked the antibody response at days 14, 21, 28, and 35 of the schedule [236,237]. We observed a clear time-dependent effect: the antibody response increased following vaccination with both the free and the encapsulated protein over time but began to decline by day 35. Furthermore, the PLGA/PVA NP formulation consistently enhanced the antibody response compared to the free protein.

These data demonstrated that the GPC1-FL protein is immunogenic, as it elicits a strong anti-GPC1 IgG response, and that PLGA/PVA NPs can enhance the immunogenicity [236,237]. However, it is necessary to highlight that in both the free protein and the NP formulations, the antibody response

started to decline by day 35. This suggests that the current dose and booster regimen may not be sufficient to sustain the response over time [238]. Therefore, further studies will be conducted to optimize the vaccination schedule.

After validating the immunogenicity of the GPC1-FL protein and the role of PLGA/PVA NPs, we investigated whether GPC1-FL-loaded PLGA/PVA NPs were also able to immunize mice following OS administration. This aim was particularly relevant because previous *in vitro* studies performed using SDS-PAGE showed that GPC1-FL undergoes degradation after incubation for one hour at 37°C in SGF and SIF buffers [232], due to the pH and enzymatic activity present in these environments. Therefore, the goal of the NPs is to protect the GPC1-FL vaccine in the gastrointestinal tract and elicit a specific immune response, enabling OS administration, which offers advantages for both patients and healthcare providers in terms of compliance, convenience, and cost.

OS administration revealed that free GPC1-FL protein did not elicit any detectable anti-GPC1 IgG response. This confirms that, due to its extensive degradation once it reaches the stomach and intestine, the resulting fragments are unable to retain the conformational or linear epitopes necessary for activation of the immune system [232]. In contrast, an anti-GPC1 IgG signal was detected when the protein was administered encapsulated in PLGA/PVA NPs. These findings demonstrate that PLGA/PVA NPs significantly enhance the immunogenicity of the chimeric protein GPC1-FL after OS administration. The PLGA/PVA NPs protect the protein from enzymatic and acidic degradation, improving its stability and facilitating its uptake at the intestinal level, leading to the activation of APCs in the GALT, ultimately promoting a specific anti-GPC1 IgG antibody response. Notably, unlike the SC immunization, antibody levels did not decrease at day 35 following OS administration of the GPC1-FL-loaded PLGA/PVA NPs. This could be explained by a more gradual and prolonged release of the protein, ensuring a sustained antigen presentation to the intestinal immune system that led to the maintenance of the antibody response over time or the activation of memory B cells [239,240].

However, it must be observed that, although the anti-GPC1 IgG levels obtained with the OS NP-based vaccine were markedly higher than those induced by the free protein, they remained lower compared to the antibody titers achieved after SC vaccination with either free or encapsulated form of the protein GPC1-FL**.** Thus, although PLGA/PVA NPs effectively protect GPC1-FL in the gastrointestinal tract and enhance its immunogenicity, the antibody response they elicit remains significantly lower compared to parenteral delivery.

Finally, we investigated whether the anti-GPC1 IgG titers observed after SC and OS vaccination affected tumor growth and mouse survival [241]. To this end, mice were injected with T-GPC1

PANC02 cells to establish a PDAC tumor expressing the human GPC1. We observed that the survival in the group that received the GPC1-FL-loaded PLGA/PVA NPs subcutaneously is statistically higher compared to the other groups. Indeed, this group exhibited the highest survival rate among all tested conditions. This increased survival reflects the higher anti-GPC1 IgG titer measured by ELISA test. These findings indicate that SC delivery of GPC1-FL-loaded PLGA/PVA NPs not only enhances the induction of specific anti-GPC1 IgG, but also prolongs mouse survival [242]. Of note, mice immunized via SC injection with free GPC1-FL protein displayed significantly reduced survival compared with all other groups, suggesting possible toxicity due to rapid systemic exposure, excessive immune activation, or local inflammatory reactions at the injection site [243].
On the other hand, the anti-GPC1 IgG titer elicited following OS administration of GPC1-FL-loaded PLGA/PVA NPs was insufficient to delay tumor growth and extend survival significantly.
A cross-comparison was performed between the same treatments delivered subcutaneously or orally in terms of survival. Mice receiving PBS or empty PLGA/PVA NPs showed comparable median survival, regardless of the route of administration. Conversely, mice injected subcutaneously with the free protein exhibited a significantly shorter survival compared to those receiving it orally, possibly due to systemic effects associated with the SC administration [76,243]. Finally, mice treated with protein-loaded NPs subcutaneously displayed an increased survival compared to their orally immunized counterparts, whose survival remained like that of the PBS group. This finding also indicates that, although orally delivered NPs failed to delay tumor growth, they did not exhibit any detectable toxicity at the administered doses [244,245].

We have chosen to develop a protein-based cancer vaccine because this approach is relatively safe, easy to produce, and capable of inducing strong humoral responses, even if it often requires adjuvants to enhance immunogenicity and may be less effective in generating cytotoxic T-cell responses compared to other platforms, such as nucleic acid vaccines, particularly mRNA vaccines [246]. Indeed, the latter have recently gained attention due to their ability to induce both humoral and cellular immune responses, and mRNA vaccines in particular benefit from rapid manufacturing and flexibility in antigen design [247]. On the other hand, we have not considered viral vector-based vaccines because of safety concerns, and we excluded cell-based vaccines, such as dendritic cell vaccines, due to their high cost and labor-intensive production, making large-scale application unrealistic [248].
The validity of using peptides and proteins as a platform for cancer vaccines is further supported by clinical studies. Several peptide-based vaccines have been investigated for PDAC, showing promising immunogenicity and potential clinical benefit. GV1001, a 16-amino-acid peptide derived

from the catalytic subunit of human telomerase reverse transcriptase (hTERT), has been shown to elicit robust CD4+ and CD8+ T cell responses and to be effectively recognized by antigen-presenting cells. In early Phase I/II trials, 50–80% of PDAC patients developed GV1001-specific T cell responses, which correlated with improved median survival. Notably, in advanced PDAC patients with elevated eotaxin levels, combining GV1001 with chemotherapy led to better overall survival and delayed disease progression compared to chemotherapy alone [249].

Other peptide-based strategies include vaccines using HLA-A2402-restricted peptides, which have demonstrated promising activity in patients with advanced PDAC [249,250], and the ELI-002 2P vaccine, which combines Amphiphile-modified mutant KRAS peptides (G12D and G12R) with a CpG adjuvant designed to enhance lymph node delivery and immunogenicity. In the Phase I AMPLIFY-201 trial, 84% of pancreatic cancer patients developed T cell responses, with six patients showing declines in tumor biomarkers and a median relapse-free survival of 16.3 months [251].

These findings indicate that peptide-based vaccines can induce clinically relevant immune responses, though further studies are necessary to confirm their therapeutic efficacy.

Compared to other peptide- and protein-based cancer vaccines, such as GV1001, HLA-A2402-restricted peptides, and ELI-002, our GPC1-FL vaccine differs in two main aspects. First, it is delivered using PLGA/PVA NPs, which protect the antigen from degradation and allow controlled release of the vaccine [252]. Second, this platform enables oral administration, a route not feasible for conventional vaccines, which are typically administered subcutaneously or intradermally [246,249–251]. However, while our data demonstrate that NP encapsulation induces a specific anti-GPC1 IgG response after oral administration, the magnitude of this response remains lower compared to subcutaneous delivery. Nonetheless, PLGA/PVA NPs also enhance the immunogenicity of the protein following subcutaneous administration, in which case the anti-GPC1 antibody response is robust enough to slow tumor growth in the murine model. These observations indicate that the GPC1-FL anti-tumor vaccine has potential, but the oral delivery remains a limitation of our current approach and will require further optimization to achieve immune responses comparable to those elicited by subcutaneous vaccination.

7 CONCLUSIONS

In the present thesis, we aimed to obtain an OS nanotechnology-based vaccine platform as an adjuvant therapy for PDAC prevention.

Therefore, we engineered the chimeric protein GPC1-FL, combining the TAA GPC1 with *Salmonella typhi* FL, to enhance its immunogenicity. Concurrently, PLGA/PVA NPs were produced to protect the protein from the harsh gastrointestinal conditions and to facilitate its delivery and interaction with the intestinal immune system.

Our results demonstrated that GPC1-FL is intrinsically immunogenic and that PLGA/PVA NPs improve this immunogenicity: SC administration induced a specific anti-GPC1 IgG antibody response, which was further enhanced when the protein was encapsulated in the NPs. On the other hand, OS administration of the free protein failed to elicit a detectable immune response, confirming the need for a protective delivery system to prevent enzymatic and acidic degradation in the gastrointestinal tract. Encapsulation within PLGA/PVA NPs for the OS immunization preserved the protein, promoted its uptake by intestinal epithelial cells, and activated B cells within the GALT, resulting in an anti-GPC1 IgG response.

Despite these improvements, the immune response elicited by OS administration remained lower than that achieved with SC vaccination. According to the antibody response, only SC delivery of GPC1-FL-loaded PLGA/PVA NPs produced a significant effect on tumor progression, slowing tumor growth and prolonging survival. OS administration, while safe and non-toxic, did not improve survival, indicating that further optimization of dose, administration frequency, or formulation is necessary to achieve efficacy comparable to parenteral delivery.

In summary, the results of the present thesis showed evidence of: (i) the ability of the chimeric GPC1-FL protein to induce a specific immune response against GPC1; (ii) the critical role of PLGA/PVA NPs in enhancing protein stability and immunogenicity in both OS and SC administration; (iii) the superior efficacy of SC delivery in controlling tumor growth and extending survival; and (iv) the need for further studies to optimize OS vaccination. In detail, future studies are needed to further investigate the immune response elicited by GPC1-FL-loaded PLGA/PVA NPs, particularly T cell-mediated responses, and to optimize OS vaccination protocols, potentially by increasing the dose or number of administrations over time, while avoiding the induction of immune tolerance that could compromise vaccine efficacy.

These findings provide a foundation for the future development of NP-based cancer vaccines, with potential applications not only in PDAC prevention but also in other types of cancer, as well as in creating more effective and patient-friendly OS immunization strategies.

8 BIBLIOGRAPHY

1. Chen H, Yang G, Xiao J, Zheng L, You L, Zhang T. Neoantigen-based immunotherapy in pancreatic ductal adenocarcinoma (PDAC). Cancer Letters. 2020;490: 12–19. doi:10.1016/j.canlet.2020.06.011

2. Busato D, Mossenta M, Dal Bo M, Macor P, Toffoli G. The Proteoglycan Glypican-1 as a Possible Candidate for Innovative Targeted Therapeutic Strategies for Pancreatic Ductal Adenocarcinoma. IJMS. 2022;23: 10279. doi:10.3390/ijms231810279

3. Huang X, Zhang G, Tang T, Liang T. Identification of tumor antigens and immune subtypes of pancreatic adenocarcinoma for mRNA vaccine development. Mol Cancer. 2021;20: 44. doi:10.1186/s12943-021-01310-0

4. Kung H, Yu J. Targeted therapy for pancreatic ductal adenocarcinoma: Mechanisms and clinical study. MedComm. 2023;4: e216. doi:10.1002/mco2.216

5. Bannoura SF, Uddin MdH, Nagasaka M, Fazili F, Al-Hallak MN, Philip PA, et al. Targeting KRAS in pancreatic cancer: new drugs on the horizon. Cancer Metastasis Rev. 2021;40: 819–835. doi:10.1007/s10555-021-09990-2

6. Tanaka J, Nakagawa T, Ono Y, Kamura Y, Ishida T, Kawabata H, et al. Highly multiplexed digital PCR assay for simultaneous quantification of variant allele frequencies and copy number alterations of *KRAS* and *GNAS* in pancreatic cancer precursors. Molecular Oncology. 2025; 1878–0261.70011. doi:10.1002/1878-0261.70011

7. Hosein AN, Dougan SK, Aguirre AJ, Maitra A. Translational advances in pancreatic ductal adenocarcinoma therapy. Nat Cancer. 2022;3: 272–286. doi:10.1038/s43018-022-00349-2

8. Park W, Chawla A, O'Reilly EM. Pancreatic Cancer: A Review. JAMA. 2021;326: 851. doi:10.1001/jama.2021.13027

9. Gobbi PG, Bergonzi M, Comelli M, Villano L, Pozzoli D, Vanoli A, et al. The prognostic role of time to diagnosis and presenting symptoms in patients with pancreatic cancer. Cancer Epidemiology. 2013;37: 186–190. doi:10.1016/j.canep.2012.12.002

10. Conroy T, Desseigne F, Ychou M, Bouché O, Guimbaud R, Bécouarn Y, et al. FOLFIRINOX versus Gemcitabine for Metastatic Pancreatic Cancer. N Engl J Med. 2011;364: 1817–1825. doi:10.1056/NEJMoa1011923

11. Anderson EM, Thomassian S, Gong J, Hendifar A, Osipov A. Advances in Pancreatic Ductal Adenocarcinoma Treatment. Cancers. 2021;13: 5510. doi:10.3390/cancers13215510

12. Luo J. KRAS mutation in pancreatic cancer. Seminars in Oncology. 2021;48: 10–18. doi:10.1053/j.seminoncol.2021.02.003

13. Morton JP, Timpson P, Karim SA, Ridgway RA, Athineos D, Doyle B, et al. Mutant p53 drives metastasis and overcomes growth arrest/senescence in pancreatic cancer. Proc Natl Acad Sci USA. 2010;107: 246–251. doi:10.1073/pnas.0908428107

14. Dardare J, Witz A, Merlin J-L, Gilson P, Harlé A. SMAD4 and the TGFβ Pathway in Patients with Pancreatic Ductal Adenocarcinoma. IJMS. 2020;21: 3534. doi:10.3390/ijms21103534

15. Gkountakos A, Singhi AD, Westphalen CB, Scarpa A, Luchini C. Fusion genes in pancreatic tumors. Trends in Cancer. 2024;10: 430–443. doi:10.1016/j.trecan.2024.01.009

16. van Oosten AF, Groot VP, Dorland G, Burkhart RA, Wolfgang CL, van Santvoort HC, et al. Dynamics of Serum CA19-9 in Patients Undergoing Pancreatic Cancer Resection. Annals of Surgery. 2024;279: 493–500. doi:10.1097/SLA.0000000000005977

17. Lee T, Teng TZJ, Shelat VG. Carbohydrate antigen 19-9 — tumor marker: Past, present, and future. WJGS. 2020;12: 468–490. doi:10.4240/wjgs.v12.i12.468

18. Meng Q, Shi S, Liang C, Liang D, Xu W, Ji S, et al. Diagnostic and prognostic value of carcinoembryonic antigen in pancreatic cancer: a systematic review and meta-analysis. OTT. 2017;Volume 10: 4591–4598. doi:10.2147/OTT.S145708

19. Yokoyama S, Higashi M, Kitamoto S, Oeldorf M, Knippschild U, Kornmann M, et al. Aberrant methylation of *MUC1* and *MUC4* promoters are potential prognostic biomarkers for pancreatic ductal adenocarcinomas. Oncotarget. 2106;7: 42553–42565. doi:10.18632/oncotarget.9924

20. Tsujii S, Serada S, Fujimoto M, Uemura S, Namikawa T, Nomura T, et al. Glypican-1 Is a Novel Target for Stroma and Tumor Cell Dual-Targeting Antibody–Drug Conjugates in Pancreatic Cancer. Molecular Cancer Therapeutics. 2021;20: 2495–2505. doi:10.1158/1535-7163.MCT-21-0335

21. Bonneh-Barkay D, Shlissel M, Berman B, Shaoul E, Admon A, Vlodavsky I, et al. Identification of Glypican as a Dual Modulator of the Biological Activity of Fibroblast Growth Factors. Journal of Biological Chemistry. 1997;272: 12415–12421. doi:10.1074/jbc.272.19.12415

22. Iozzo RV, Schaefer L. Proteoglycan form and function: A comprehensive nomenclature of proteoglycans. Matrix Biol. 2015;42: 11–55. doi:10.1016/j.matbio.2015.02.003

23. Li N, Gao W, Zhang Y-F, Ho M. Glypicans as Cancer Therapeutic Targets. Trends in Cancer. 2018;4: 741–754. doi:10.1016/j.trecan.2018.09.004

24. Kolluri A, Ho M. The Role of Glypican-3 in Regulating Wnt, YAP, and Hedgehog in Liver Cancer. Front Oncol. 2019;9: 708. doi:10.3389/fonc.2019.00708

25. Filmus J, Capurro M. The role of glypicans in Hedgehog signaling. Matrix Biology. 2014;35: 248–252. doi:10.1016/j.matbio.2013.12.007

26. Liu YC, Wierbowski BM, Salic A. Hedgehog pathway modulation by glypican 3-conjugated heparan sulfate. Journal of Cell Science. 2022;135: jcs259297. doi:10.1242/jcs.259297

27. Sparn C, Dimou E, Meyer A, Saleppico R, Wegehingel S, Gerstner M, et al. Glypican-1 drives unconventional secretion of fibroblast growth factor 2. eLife. 2022;11: e75545. doi:10.7554/eLife.75545

28. Galli A, Roure A, Zeller R, Dono R. Glypican 4 modulates FGF signalling and regulates dorsoventral forebrain patterning in *Xenopus* embryos. Development. 2003;130: 4919–4929. doi:10.1242/dev.00706

29. Su G, Meyer K, Nandini CD, Qiao D, Salamat S, Friedl A. Glypican-1 Is Frequently Overexpressed in Human Gliomas and Enhances FGF-2 Signaling in Glioma Cells. The American Journal of Pathology. 2006;168: 2014–2026. doi:10.2353/ajpath.2006.050800

30. Pilia G, Hughes-Benzie RM, MacKenzie A, Baybayan P, Chen EY, Huber R, et al. Mutations in GPC3, a glypican gene, cause the Simpson-Golabi-Behmel overgrowth syndrome. Nat Genet. 1996;12: 241–247. doi:10.1038/ng0396-241

31. Tatenhorst L, Maass F, Paul H, Dambeck V, Bähr M, Dono R, et al. Glypican-4 serum levels are associated with cognitive dysfunction and vascular risk factors in Parkinson's disease. Sci Rep. 2024;14: 5005. doi:10.1038/s41598-024-54800-8

32. Pan J, Ho M. Role of glypican-1 in regulating multiple cellular signaling pathways. American Journal of Physiology-Cell Physiology. 2021;321: C846–C858. doi:10.1152/ajpcell.00290.2021

33. Awad W, Adamczyk B, Örnros J, Karlsson NG, Mani K, Logan DT. Structural Aspects of N-Glycosylations and the C-terminal Region in Human Glypican-1. Journal of Biological Chemistry. 2015;290: 22991–23008. doi:10.1074/jbc.M115.660878

34. Svensson G, Hyrenius Wittsten A, Linse S, Mani K. The Structural Role of N-Linked Glycans on Human Glypican-1. Biochemistry. 2011;50: 9377–9387. doi:10.1021/bi200218s

35. Svensson G, Awad W, Håkansson M, Mani K, Logan DT. Crystal Structure of N-Glycosylated Human Glypican-1 Core Protein. Journal of Biological Chemistry. 2012;287: 14040–14051. doi:10.1074/jbc.M111.322487

36. Lund ME, Campbell DH, Walsh BJ. The Role of Glypican-1 in the Tumour Microenvironment. In: Birbrair A, editor. Tumor Microenvironment. Cham: Springer International Publishing; 2020. pp. 163–176. doi:10.1007/978-3-030-40146-7_8

37. Kleeff J, Ishiwata T, Kumbasar A, Friess H, Büchler MW, Lander AD, et al. The cell-surface heparan sulfate proteoglycan glypican-1 regulates growth factor action in pancreatic carcinoma cells and is overexpressed in human pancreatic cancer. J Clin Invest. 1998;102: 1662–1673. doi:10.1172/JCI4105

38. Wang S, Wu Z, Zhou M, Liao W. Effect of GPC1 on epithelial-to-mesenchymal transition and stemness and interaction with ITGB1 in gastric cancer. JCO. 2017;35: e15580–e15580. doi:10.1200/JCO.2017.35.15_suppl.e15580

39. Wang S, Zheng Y, Yang F, Zhu L, Zhu X-Q, Wang Z-F, et al. The molecular biology of pancreatic adenocarcinoma: translational challenges and clinical perspectives. Sig Transduct Target Ther. 2021;6: 249. doi:10.1038/s41392-021-00659-4

40. Kaur SP, Verma A, Lee HeeK, Barnett LM, Somanath PR, Cummings BS. Inhibition of glypican-1 expression induces an activated fibroblast phenotype in a human bone marrow-derived stromal cell-line. Sci Rep. 2021;11: 9262. doi:10.1038/s41598-021-88519-7

41. Erdogan B, Webb DJ. Cancer-associated fibroblasts modulate growth factor signaling and extracellular matrix remodeling to regulate tumor metastasis. Biochemical Society Transactions. 2017;45: 229–236. doi:10.1042/BST20160387

42. Zhou C, Dong Y, Sun X, Sui X, Zhu H, Zhao Y, et al. High levels of serum glypican-1 indicate poor prognosis in pancreatic ductal adenocarcinoma. Cancer Medicine. 2018;7: 5525–5533. doi:10.1002/cam4.1833

43. Lu H, Niu F, Liu F, Gao J, Sun Y, Zhao X. Elevated glypican-1 expression is associated with an unfavorable prognosis in pancreatic ductal adenocarcinoma. Cancer Medicine. 2017;6: 1181–1191. doi:10.1002/cam4.1064

44. Fan T, Zhang M, Yang J, Zhu Z, Cao W, Dong C. Therapeutic cancer vaccines: advancements, challenges and prospects. Sig Transduct Target Ther. 2023;8: 450. doi:10.1038/s41392-023-01674-3

45. Pardoll D. Cancer and the Immune System: Basic Concepts and Targets for Intervention. Seminars in Oncology. 2015;42: 523–538. doi:10.1053/j.seminoncol.2015.05.003

46. Ruzzi F, Riccardo F, Conti L, Tarone L, Semprini MS, Bolli E, et al. Cancer vaccines: Target antigens, vaccine platforms and preclinical models. Molecular Aspects of Medicine. 2025;101: 101324. doi:10.1016/j.mam.2024.101324

47. Mellman I. Dendritic Cells: Master Regulators of the Immune Response. Cancer Immunology Research. 2013;1: 145–149. doi:10.1158/2326-6066.CIR-13-0102

48. Maurer DM, Butterfield LH, Vujanovic L. Melanoma vaccines: clinical status and immune endpoints. Melanoma Research. 2019;29: 109–118. doi:10.1097/CMR.0000000000000535

49. Sethna Z, Guasp P, Reiche C, Milighetti M, Ceglia N, Patterson E, et al. RNA neoantigen vaccines prime long-lived CD8+ T cells in pancreatic cancer. Nature. 2025;639: 1042–1051. doi:10.1038/s41586-024-08508-4

50. Sanaei M-J, Pourbagheri-Sigaroodi A, Rezvani A, Zaboli E, Salari S, Masjedi MR, et al. Lung cancer vaccination from concept to reality: A critical review of clinical trials and latest advances. Life Sciences. 2024;346: 122652. doi:10.1016/j.lfs.2024.122652

51. Kantoff PW, Higano CS, Shore ND, Berger ER, Small EJ, Penson DF, et al. Sipuleucel-T Immunotherapy for Castration-Resistant Prostate Cancer. N Engl J Med. 2010;363: 411–422. doi:10.1056/NEJMoa1001294

52. Kumar A, Dixit S, Srinivasan K, M D, Vincent PMDR. Personalized cancer vaccine design using AI-powered technologies. Front Immunol. 2024;15: 1357217. doi:10.3389/fimmu.2024.1357217

53. Liu D, Che X, Wang X, Ma C, Wu G. Tumor Vaccines: Unleashing the Power of the Immune System to Fight Cancer. Pharmaceuticals (Basel). 2023;16: 1384. doi:10.3390/ph16101384

54. Kaczmarek M, Poznańska J, Fechner F, Michalska N, Paszkowska S, Napierała A, et al. Cancer Vaccine Therapeutics: Limitations and Effectiveness-A Literature Review. Cells. 2023;12: 2159. doi:10.3390/cells12172159

55. Ye K, Zhong W, Wang P, Chen Y, Chi P. PD-1 blockage combined with vaccine therapy can facilitate immune infiltration in tumor microenvironment of Lynch syndrome colon cancer. Front Genet. 2022;13: 877833. doi:10.3389/fgene.2022.877833

56. Mundhara N, Sadhukhan P. Cracking the Codes behind Cancer Cells' Immune Evasion. IJMS. 2024;25: 8899. doi:10.3390/ijms25168899

57. van der Burg SH, Arens R, Ossendorp F, van Hall T, Melief CJM. Vaccines for established cancer: overcoming the challenges posed by immune evasion. Nat Rev Cancer. 2016;16: 219–233. doi:10.1038/nrc.2016.16

58. Lozano D, Larraga V, Vallet-Regí M, Manzano M. An Overview of the Use of Nanoparticles in Vaccine Development. Nanomaterials. 2023;13: 1828. doi:10.3390/nano13121828

59. Shetty S, Alvarado PC, Pettie D, Collier JH. Next-Generation Vaccine Development with Nanomaterials: Recent Advances, Possibilities, and Challenges. Annual Review of Biomedical Engineering. 2024;26: 273–306. doi:10.1146/annurev-bioeng-110122-124359

60. Curley SM, Putnam D. Biological Nanoparticles in Vaccine Development. Front Bioeng Biotechnol. 2022;10: 867119. doi:10.3389/fbioe.2022.867119

61. Sondak VK, Sabel MS, Mulé JJ. Allogeneic and Autologous Melanoma Vaccines: Where Have We Been and Where Are We Going? Clinical Cancer Research. 2006;12: 2337s–2341s. doi:10.1158/1078-0432.CCR-05-2555

62. Roy S, Sethi TK, Taylor D, Kim YJ, Johnson DB. Breakthrough concepts in immune-oncology: Cancer vaccines at the bedside. Journal of Leukocyte Biology. 2020;108: 1455–1489. doi:10.1002/JLB.5BT0420-585RR

63. Fritah H, Rovelli R, Chiang CL-L, Kandalaft LE. The current clinical landscape of personalized cancer vaccines. Cancer Treatment Reviews. 2022;106: 102383. doi:10.1016/j.ctrv.2022.102383

64. Li W, Joshi M, Singhania S, Ramsey K, Murthy A. Peptide Vaccine: Progress and Challenges. Vaccines. 2014;2: 515–536. doi:10.3390/vaccines2030515

65. Lee K-W, Yam JWP, Mao X. Dendritic Cell Vaccines: A Shift from Conventional Approach to New Generations. Cells. 2023;12: 2147. doi:10.3390/cells12172147

66. Pandya A, Shah Y, Kothari N, Postwala H, Shah A, Parekh P, et al. The future of cancer immunotherapy: DNA vaccines leading the way. Med Oncol. 2023;40: 200. doi:10.1007/s12032-023-02060-3

67. Sayour EJ, Boczkowski D, Mitchell DA, Nair SK. Cancer mRNA vaccines: clinical advances and future opportunities. Nat Rev Clin Oncol. 2024;21: 489–500. doi:10.1038/s41571-024-00902-1

68. Liao H-C, Liu S-J. Advances in nucleic acid-based cancer vaccines. J Biomed Sci. 2025;32: 10. doi:10.1186/s12929-024-01102-w

69. Liu J, Fu M, Wang M, Wan D, Wei Y, Wei X. Cancer vaccines as promising immuno-therapeutics: platforms and current progress. J Hematol Oncol. 2022;15: 28. doi:10.1186/s13045-022-01247-x

70. Zhou M, Tang Y, Xu W, Hao X, Li Y, Huang S, et al. Bacteria-based immunotherapy for cancer: a systematic review of preclinical studies. Front Immunol. 2023;14: 1140463. doi:10.3389/fimmu.2023.1140463

71. Nakagawa N, Hashii Y, Kayama H, Okumura R, Nakajima H, Minagawa H, et al. An oral WT1 protein vaccine composed of WT1-anchored, genetically engineered Bifidobacterium longum allows for intestinal immunity in mice with acute myeloid leukemia. Cancer Immunol Immunother. 2023;72: 39–53. doi:10.1007/s00262-022-03214-4

72. Munir M, Cheema AY, Ogedegbe OJ, Aslam MF, Kim S. William Coley: The Pioneer and the Father of Immunotherapy. Cureus. 2024;16: e69113. doi:10.7759/cureus.69113

73. Mu J, Lei L, Zheng Y, Li D, Li J, Fu Y, et al. Comparative study of subcutaneous, intramuscular, and oral administration of bovine pathogenic Escherichia coli bacterial ghost vaccine in mice. Front Immunol. 2022;13: 1008131. doi:10.3389/fimmu.2022.1008131

74. Van der Wielen M, Van Damme P. Intramuscular vaccines: good administration practice. Vacunas. 2001;2: 149–152. doi:10.1016/S1576-9887(01)70256-7

75. Childress B-C, Montney JD, Albro EA. Making evidence-based selections of influenza vaccines. Hum Vaccin Immunother. 2014;10: 2729–2732. doi:10.4161/hv.29340

76. Lago-Deibe FI, Valladares-Cabaleiro M, Fernández-Domínguez MJ, Fernández-Fernández I, Clavería A, Rodríguez-Pastoriza S, et al. Effectiveness and safety of tetanus vaccine administration by intramuscular vs. subcutaneous route in anticoagulated patients: Randomized clinical trial in primary care. Front Med. 2022;9: 1054988. doi:10.3389/fmed.2022.1054988

77. Hong T, Chung Y-J, Kim T-Y, Kim I-H, Choe Y-K, Lee J, et al. Safety and immunogenicity of a single intramuscular dose of a tetanus-diphtheria toxoid (Td) vaccine (BR-TD-1001) in healthy Korean adult subjects. Human Vaccines & Immunotherapeutics. 2015;11: 2440–2445. doi:10.1080/21645515.2015.1054582

78. González ML, Usandizaga M, Alomar P, Salvá F, Martín F, Erroz MJ, et al. Intradermal and intramuscular route for vaccination against hepatitis B. Vaccine. 1990;8: 402–405. doi:10.1016/0264-410X(90)90102-R

79. Cook IF. Subcutaneous vaccine administration – an outmoded practice. Human Vaccines & Immunotherapeutics. 2021;17: 1329–1341. doi:10.1080/21645515.2020.1814094

80. Zuckerman JN. The importance of injecting vaccines into muscle. BMJ. 2000;321: 1237–1238. doi:10.1136/bmj.321.7271.1237

81. Reef S, Plotkin SA. Chapter 4 Rubella Vaccine. Perspectives in Medical Virology. Elsevier; 2006. pp. 79–93. doi:10.1016/S0168-7069(06)15004-1

82. Riedel S. Edward Jenner and the History of Smallpox and Vaccination. Baylor University Medical Center Proceedings. 2005;18: 21–25. doi:10.1080/08998280.2005.11928028

83. Yin W, Xu Z, Ma F, Deng B, Zhao Y, Zuo X, et al. Nano-adjuvant based on lipo-imiquimod self-assembly for enhanced foot-and-mouth disease virus vaccine immune responses via intradermal immunization. Materials Today Bio. 2025;31: 101567. doi:10.1016/j.mtbio.2025.101567

84. Lee S, Kim T, Seong K-Y, Yim S-G, Lee W-K, Kim S, et al. Microneedle-mediated intradermal delivery of Bacille Calmette-Guérin (BCG) vaccines for single-dose tuberculosis vaccination. Tuberculosis. 2025;151: 102608. doi:10.1016/j.tube.2025.102608

85. Rezapour E, Kariminezhad H, Mostafazadeh A, Ghasemi R, Pourbagher R, Neyshaburi EZ. Enhancement of transdermal vaccination using electrothermal active interfaces. Journal of Drug Delivery Science and Technology. 2024;96: 105639. doi:10.1016/j.jddst.2024.105639

86. Zhu W, Wei T, Xu Y, Jin Q, Chao Y, Lu J, et al. Non-invasive transdermal delivery of biomacromolecules with fluorocarbon-modified chitosan for melanoma immunotherapy and viral vaccines. Nat Commun. 2024;15: 820. doi:10.1038/s41467-024-45158-6

87. Jin G, Wang R, Jin Y, Song Y, Wang T. From intramuscular to nasal: unleashing the potential of nasal spray vaccines against coronavirus disease 2019. Clin & Trans Imm. 2024;13: e1514. doi:10.1002/cti2.1514

88. Liu Y, Lam DM-K, Luan M, Zheng W, Ai H. Recent development of oral vaccines (Review). Exp Ther Med. 2024;27: 223. doi:10.3892/etm.2024.12511

89. Cao Y, Rewatkar P, Wang R, Hasnain SZ, Popat A, Kumeria T. Nanocarriers for oral delivery of biologics: small carriers for big payloads. Trends in Pharmacological Sciences. 2021;42: 957–972. doi:10.1016/j.tips.2021.08.005

90. Sabin AB. Oral Poliovirus Vaccine: History of Its Development and Use and Current Challenge to Eliminate Poliomyelitis from the World. Journal of Infectious Diseases. 1985;151: 420–436. doi:10.1093/infdis/151.3.420

91. Tahrat H, Munir A, Marchetti F. Rotavirus vaccine coverage, completion, and compliance: A systematic literature review. Human Vaccines & Immunotherapeutics. 2025;21: 2442780. doi:10.1080/21645515.2024.2442780

92. Smith J, Lipsitch M, Almond JW. Vaccine production, distribution, access, and uptake. Lancet. 2011;378: 428–438. doi:10.1016/S0140-6736(11)60478-9

93. Waheed MT, Sameeullah M, Khan FA, Syed T, Ilahi M, Gottschamel J, et al. Need of cost-effective vaccines in developing countries: What plant biotechnology can offer? Springerplus. 2016;5: 65. doi:10.1186/s40064-016-1713-8

94. Takiishi T, Fenero CIM, Câmara NOS. Intestinal barrier and gut microbiota: Shaping our immune responses throughout life. Tissue Barriers. 2017;5: e1373208. doi:10.1080/21688370.2017.1373208

95. Sender R, Weiss Y, Navon Y, Milo I, Azulay N, Keren L, et al. The total mass, number, and distribution of immune cells in the human body. Proc Natl Acad Sci USA. 2023;120: e2308511120. doi:10.1073/pnas.2308511120

96. Lavelle EC, Ward RW. Mucosal vaccines — fortifying the frontiers. Nat Rev Immunol. 2022;22: 236–250. doi:10.1038/s41577-021-00583-2

97. Shao T, Hsu R, Rafizadeh DL, Wang L, Bowlus CL, Kumar N, et al. The gut ecosystem and immune tolerance. Journal of Autoimmunity. 2023;141: 103114. doi:10.1016/j.jaut.2023.103114

98. Brown H, Esterházy D. Intestinal immune compartmentalization: implications of tissue specific determinants in health and disease. Mucosal Immunology. 2021;14: 1259–1270. doi:10.1038/s41385-021-00420-8

99. Mabbott NA, Donaldson DS, Ohno H, Williams IR, Mahajan A. Microfold (M) cells: important immunosurveillance posts in the intestinal epithelium. Mucosal Immunology. 2013;6: 666–677. doi:10.1038/mi.2013.30

100. Luciani C, Hager FT, Cerovic V, Lelouard H. Dendritic cell functions in the inductive and effector sites of intestinal immunity. Mucosal Immunology. 2022;15: 40–50. doi:10.1038/s41385-021-00448-w

101. Dillon A, Lo DD. M Cells: Intelligent Engineering of Mucosal Immune Surveillance. Front Immunol. 2019;10: 1499. doi:10.3389/fimmu.2019.01499

102. Kobayashi N, Takahashi D, Takano S, Kimura S, Hase K. The Roles of Peyer's Patches and Microfold Cells in the Gut Immune System: Relevance to Autoimmune Diseases. Front Immunol. 2019;10: 2345. doi:10.3389/fimmu.2019.02345

103. Gambirasi M, Safa A, Vruzhaj I, Giacomin A, Sartor F, Toffoli G. Oral Administration of Cancer Vaccines: Challenges and Future Perspectives. Vaccines. 2023;12: 26. doi:10.3390/vaccines12010026

104. Coombes JL, Siddiqui KRR, Arancibia-Cárcamo CV, Hall J, Sun C-M, Belkaid Y, et al. A functionally specialized population of mucosal CD103+ DCs induces Foxp3+ regulatory T cells via a TGF-β– and retinoic acid–dependent mechanism. The Journal of Experimental Medicine. 2007;204: 1757–1764. doi:10.1084/jem.20070590

105. Sun C-M, Hall JA, Blank RB, Bouladoux N, Oukka M, Mora JR, et al. Small intestine lamina propria dendritic cells promote de novo generation of Foxp3 T reg cells via retinoic acid. The Journal of Experimental Medicine. 2007;204: 1775–1785. doi:10.1084/jem.20070602

106. Tsuji M, Komatsu N, Kawamoto S, Suzuki K, Kanagawa O, Honjo T, et al. Preferential Generation of Follicular B Helper T Cells from $Foxp3^+$ T Cells in Gut Peyer's Patches. Science. 2009;323: 1488–1492. doi:10.1126/science.1169152

107. Cerutti A. The regulation of IgA class switching. Nat Rev Immunol. 2008;8: 421–434. doi:10.1038/nri2322

108. Fagarasan S, Kawamoto S, Kanagawa O, Suzuki K. Adaptive Immune Regulation in the Gut: T Cell–Dependent and T Cell–Independent IgA Synthesis. Annu Rev Immunol. 2010;28: 243–273. doi:10.1146/annurev-immunol-030409-101314

109. Berkowska MA, Driessen GJA, Bikos V, Grosserichter-Wagener C, Stamatopoulos K, Cerutti A, et al. Human memory B cells originate from three distinct germinal center-dependent and -independent maturation pathways. Blood. 2011;118: 2150–2158. doi:10.1182/blood-2011-04-345579

110. Brandtzaeg P. Secretory IgA: Designed for Anti-Microbial Defense. Front Immunol. 2013;4. doi:10.3389/fimmu.2013.00222

111. Brandtzaeg P. Induction of secretory immunity and memory at mucosal surfaces. Vaccine. 2007;25: 5467–5484. doi:10.1016/j.vaccine.2006.12.001

112. Dickinson BL, Badizadegan K, Wu Z, Ahouse JC, Zhu X, Simister NE, et al. Bidirectional FcRn-dependent IgG transport in a polarized human intestinal epithelial cell line. J Clin Invest. 1999;104: 903–911. doi:10.1172/JCI6968

113. Yoshida M, Claypool SM, Wagner JS, Mizoguchi E, Mizoguchi A, Roopenian DC, et al. Human Neonatal Fc Receptor Mediates Transport of IgG into Luminal Secretions for Delivery of Antigens to Mucosal Dendritic Cells. Immunity. 2004;20: 769–783. doi:10.1016/j.immuni.2004.05.007

114. van Wijk F, Cheroutre H. Mucosal T cells in gut homeostasis and inflammation. Expert Review of Clinical Immunology. 2010;6: 559–566. doi:10.1586/eci.10.34

115. Cheroutre H, Madakamutil L. Acquired and natural memory T cells join forces at the mucosal front line. Nat Rev Immunol. 2004;4: 290–300. doi:10.1038/nri1333

116. Müller S, Bühler-Jungo M, Mueller C. Intestinal Intraepithelial Lymphocytes Exert Potent Protective Cytotoxic Activity During an Acute Virus Infection. The Journal of Immunology. 2000;164: 1986–1994. doi:10.4049/jimmunol.164.4.1986

117. Hoekstra ME, Vijver SV, Schumacher TN. Modulation of the tumor micro-environment by CD8+ T cell-derived cytokines. Curr Opin Immunol. 2021;69: 65–71. doi:10.1016/j.coi.2021.03.016

118. Koh C-H, Lee S, Kwak M, Kim B-S, Chung Y. CD8 T-cell subsets: heterogeneity, functions, and therapeutic potential. Exp Mol Med. 2023;55: 2287–2299. doi:10.1038/s12276-023-01105-x

119. Rodrigues LS, Barreto AS, Bomfim LGS, Gomes MC, Ferreira NLC, da Cruz GS, et al. Multifunctional, TNF-α and IFN-γ-Secreting CD4 and CD8 T Cells and CD8High T Cells Are Associated With the Cure of Human Visceral Leishmaniasis. Front Immunol. 2021;12: 773983. doi:10.3389/fimmu.2021.773983

120. Agace W. Generation of gut-homing T cells and their localization to the small intestinal mucosa. Immunology Letters. 2010;128: 21–23. doi:10.1016/j.imlet.2009.09.012

121. Mora JR, Iwata M, Eksteen B, Song S-Y, Junt T, Senman B, et al. Generation of Gut-Homing IgA-Secreting B Cells by Intestinal Dendritic Cells. Science. 2006;314: 1157–1160. doi:10.1126/science.1132742

122. Mowat AMcI. Anatomical basis of tolerance and immunity to intestinal antigens. Nat Rev Immunol. 2003;3: 331–341. doi:10.1038/nri1057

123. Hieshima K, Kawasaki Y, Hanamoto H, Nakayama T, Nagakubo D, Kanamaru A, et al. CC Chemokine Ligands 25 and 28 Play Essential Roles in Intestinal Extravasation of IgA Antibody-Secreting Cells. The Journal of Immunology. 2004;173: 3668–3675. doi:10.4049/jimmunol.173.6.3668

124. DeNucci CC, Mitchell JS, Shimizu Y. Integrin Function in T-Cell Homing to Lymphoid and Nonlymphoid Sites: Getting There and Staying There. Crit Rev Immunol. 2009;29: 87–109. doi:10.1615/CritRevImmunol.v29.i2.10

125. Jou J, Harrington KJ, Zocca M-B, Ehrnrooth E, Cohen EEW. The Changing Landscape of Therapeutic Cancer Vaccines—Novel Platforms and Neoantigen Identification. Clinical Cancer Research. 2021;27: 689–703. doi:10.1158/1078-0432.CCR-20-0245

126. Maurer JM, Schellekens RCA, van Rieke HM, Wanke C, Iordanov V, Stellaard F, et al. Gastrointestinal pH and Transit Time Profiling in Healthy Volunteers Using the IntelliCap System Confirms Ileo-Colonic Release of ColoPulse Tablets. Padmanabhan P, editor. PLoS ONE. 2015;10: e0129076. doi:10.1371/journal.pone.0129076

127. Homayun B, Lin X, Choi H-J. Challenges and Recent Progress in Oral Drug Delivery Systems for Biopharmaceuticals. Pharmaceutics. 2019;11: 129. doi:10.3390/pharmaceutics11030129

128. Mooij MG, de Koning BA, Huijsman ML, de Wildt SN. Ontogeny of oral drug absorption processes in children. Expert Opinion on Drug Metabolism & Toxicology. 2012;8: 1293–1303. doi:10.1517/17425255.2012.698261

129. Zhu Q, Chen Z, Paul PK, Lu Y, Wu W, Qi J. Oral delivery of proteins and peptides: Challenges, status quo and future perspectives. Acta Pharmaceutica Sinica B. 2021;11: 2416–2448. doi:10.1016/j.apsb.2021.04.001

130. Fallingborg J, Christensen LA, Jacobsen BA, Rasmussen SN. Very low intraluminal colonic pH in patients with active ulcerative colitis. Digest Dis Sci. 1993;38: 1989–1993. doi:10.1007/BF01297074

131. Sasaki Y, Hada R, Nakajima H, Fukuda S, Munakata A. Improved localizing method of radiopill in measurement of entire gastrointestinal pH profiles: colonic luminal pH in normal subjects and patients with Crohn's disease. Am J Gastroenterol. 1997;92: 114–118.

132. Pridgen EM, Alexis F, Farokhzad OC. Polymeric Nanoparticle Technologies for Oral Drug Delivery. Clinical Gastroenterology and Hepatology. 2014;12: 1605–1610. doi:10.1016/j.cgh.2014.06.018

133. Janiak MC. Digestive enzymes of human and nonhuman primates. Evolutionary Anthropology. 2016;25: 253–266. doi:10.1002/evan.21498

134. Haddadzadegan S, Dorkoosh F, Bernkop-Schnürch A. Oral delivery of therapeutic peptides and proteins: Technology landscape of lipid-based nanocarriers. Advanced Drug Delivery Reviews. 2022;182: 114097. doi:10.1016/j.addr.2021.114097

135. Miner-Williams WM, Stevens BR, Moughan PJ. Are intact peptides absorbed from the healthy gut in the adult human? Nutr Res Rev. 2014;27: 308–329. doi:10.1017/S0954422414000225

136. Paone P, Cani PD. Mucus barrier, mucins and gut microbiota: the expected slimy partners? Gut. 2020;69: 2232–2243. doi:10.1136/gutjnl-2020-322260

137. Javitt G, Khmelnitsky L, Albert L, Bigman LS, Elad N, Morgenstern D, et al. Assembly Mechanism of Mucin and von Willebrand Factor Polymers. Cell. 2020;183: 717-729.e16. doi:10.1016/j.cell.2020.09.021

138. Parrish A, Boudaud M, Kuehn A, Ollert M, Desai MS. Intestinal mucus barrier: a missing piece of the puzzle in food allergy. Trends in Molecular Medicine. 2022;28: 36–50. doi:10.1016/j.molmed.2021.10.004

139. Johansson MEV, Hansson GC. Immunological aspects of intestinal mucus and mucins. Nat Rev Immunol. 2016;16: 639–649. doi:10.1038/nri.2016.88

140. Birchenough GMH, Johansson ME, Gustafsson JK, Bergström JH, Hansson GC. New developments in goblet cell mucus secretion and function. Mucosal Immunology. 2015;8: 712–719. doi:10.1038/mi.2015.32

141. McShane A, Bath J, Jaramillo AM, Ridley C, Walsh AA, Evans CM, et al. Mucus. Current Biology. 2021;31: R938–R945. doi:10.1016/j.cub.2021.06.093

142. Shan M, Gentile M, Yeiser JR, Walland AC, Bornstein VU, Chen K, et al. Mucus Enhances Gut Homeostasis and Oral Tolerance by Delivering Immunoregulatory Signals. Science. 2013;342: 447–453. doi:10.1126/science.1237910

143. Mowat AM, Agace WW. Regional specialization within the intestinal immune system. Nat Rev Immunol. 2014;14: 667–685. doi:10.1038/nri3738

144. Chelakkot C, Ghim J, Ryu SH. Mechanisms regulating intestinal barrier integrity and its pathological implications. Exp Mol Med. 2018;50: 1–9. doi:10.1038/s12276-018-0126-x

145. Suzuki T. Regulation of the intestinal barrier by nutrients: The role of tight junctions. Animal Science Journal. 2020;91: e13357. doi:10.1111/asj.13357

146. Kulkarni DH, Newberry RD. Intestinal Macromolecular Transport Supporting Adaptive Immunity. Cellular and Molecular Gastroenterology and Hepatology. 2019;7: 729–737. doi:10.1016/j.jcmgh.2019.01.003

147. Wang M, Gao Z, Zhang Z, Pan L, Zhang Y. Roles of M cells in infection and mucosal vaccines. Human Vaccines & Immunotherapeutics. 2014;10: 3544–3551. doi:10.4161/hv.36174

148. Ohno H, Hase K. Glycoprotein 2 (GP2): grabbing the $FimH^+$ bacteria into M cells for mucosal immunity. Gut Microbes. 2010;1: 407–410. doi:10.4161/gmic.1.6.14078

149. Dhurjad P, Dhavaliker C, Gupta K, Sonti R. Exploring Drug Metabolism by the Gut Microbiota: Modes of Metabolism and Experimental Approaches. Drug Metabolism and Disposition. 2022;50: 224–234. doi:10.1124/dmd.121.000669

150. The Human Microbiome Project Consortium. Structure, function and diversity of the healthy human microbiome. Nature. 2012;486: 207–214. doi:10.1038/nature11234

151. Zhao Q, Chen Y, Huang W, Zhou H, Zhang W. Drug-microbiota interactions: an emerging priority for precision medicine. Sig Transduct Target Ther. 2023;8: 386. doi:10.1038/s41392-023-01619-w

152. Morrison DJ, Preston T. Formation of short chain fatty acids by the gut microbiota and their impact on human metabolism. Gut Microbes. 2016;7: 189–200. doi:10.1080/19490976.2015.1134082

153. den Besten G, van Eunen K, Groen AK, Venema K, Reijngoud D-J, Bakker BM. The role of short-chain fatty acids in the interplay between diet, gut microbiota, and host energy metabolism. Journal of Lipid Research. 2013;54: 2325–2340. doi:10.1194/jlr.R036012

154. Pilla L, Ferrone S, Maccalli C. Methods for improving the immunogenicity and efficacy of cancer vaccines. Expert Opinion on Biological Therapy. 2018;18: 765–784. doi:10.1080/14712598.2018.1485649

155. Slingluff CL. The Present and Future of Peptide Vaccines for Cancer: Single or Multiple, Long or Short, Alone or in Combination? The Cancer Journal. 2011;17: 343–350. doi:10.1097/PPO.0b013e318233e5b2

156. Kumar H, Kawai T, Akira S. Pathogen Recognition by the Innate Immune System. International Reviews of Immunology. 2011;30: 16–34. doi:10.3109/08830185.2010.529976

157. Bandyopadhyay AS, Garon J, Seib K, Orenstein WA. Polio Vaccination: Past, Present and Future. Future Microbiol. 2015;10: 791–808. doi:10.2217/fmb.15.19

158. Van der Weken H, Cox E, Devriendt B. Advances in Oral Subunit Vaccine Design. Vaccines. 2020;9: 1. doi:10.3390/vaccines9010001

159. Wang J, Gusti V, Saraswati A, Lo DD. Convergent and Divergent Development among M Cell Lineages in Mouse Mucosal Epithelium. The Journal of Immunology. 2011;187: 5277–5285. doi:10.4049/jimmunol.1102077

160. Sadiq A, Bostan N, Jadoon Khan, Aziz A. Effect of rotavirus genetic diversity on vaccine impact. Reviews in Medical Virology. 2022;32: e2259. doi:10.1002/rmv.2259

161. Snäkä T, Fasel N. Behind the Scenes: Nod-Like Receptor X1 Controls Inflammation and Metabolism. Front Cell Infect Microbiol. 2020;10: 609812. doi:10.3389/fcimb.2020.609812

162. Rehwinkel J, Gack MU. RIG-I-like receptors: their regulation and roles in RNA sensing. Nat Rev Immunol. 2020;20: 537–551. doi:10.1038/s41577-020-0288-3

163. Brown GD, Willment JA, Whitehead L. C-type lectins in immunity and homeostasis. Nat Rev Immunol. 2018;18: 374–389. doi:10.1038/s41577-018-0004-8

164. Jhunjhunwala S, Hammer C, Delamarre L. Antigen presentation in cancer: insights into tumour immunogenicity and immune evasion. Nat Rev Cancer. 2021;21: 298–312. doi:10.1038/s41568-021-00339-z

165. Giannasca PJ, Giannasca KT, Leichtner AM, Neutra MR. Human Intestinal M Cells Display the Sialyl Lewis A Antigen. Sansonetti PJ, editor. Infect Immun. 1999;67: 946–953. doi:10.1128/IAI.67.2.946-953.1999

166. Kim S, Jung D, Yang I, Kim J, Lee K, Nochi T, et al. M cells expressing the complement C5a receptor are efficient targets for mucosal vaccine delivery. Eur J Immunol. 2011;41: 3219–3229. doi:10.1002/eji.201141592

167. Pridgen EM, Alexis F, Kuo TT, Levy-Nissenbaum E, Karnik R, Blumberg RS, et al. Transepithelial Transport of Fc-Targeted Nanoparticles by the Neonatal Fc Receptor for Oral Delivery. Sci Transl Med. 2013;5. doi:10.1126/scitranslmed.3007049

168. Fox BE, Vilander AC, Gilfillan D, Dean GA, Abdo Z. Oral Vaccination Using a Probiotic Vaccine Platform Combined with Prebiotics Impacts Immune Response and the Microbiome. Vaccines. 2022;10: 1465. doi:10.3390/vaccines10091465

169. Tawde SA, Chablani L, Akalkotkar A, D'Souza C, Chiriva-Internati M, Selvaraj P, et al. Formulation and evaluation of oral microparticulate ovarian cancer vaccines. Vaccine. 2012;30: 5675–5681. doi:10.1016/j.vaccine.2012.05.073

170. Liu E, Zhao S, Li X, Meng X, Liu B. Preparation, characterization of PLGA/chitosan nanoparticles as a delivery system for controlled release of DHA. International Journal of Biological Macromolecules. 2021;185: 782–791. doi:10.1016/j.ijbiomac.2021.06.190

171. Trovato M. Novel antigen delivery systems. WJV. 2015;4: 156. doi:10.5501/wjv.v4.i3.156

172. Xie J, Xu R. Trends in orally viral vector gene delivery and therapy. Nanostructures for Oral Medicine. Elsevier; 2017. pp. 123–146. doi:10.1016/B978-0-323-47720-8.00006-7

173. Mohsen MO, Bachmann MF. Virus-like particle vaccinology, from bench to bedside. Cell Mol Immunol. 2022;19: 993–1011. doi:10.1038/s41423-022-00897-8

174. Serradell MC, Rupil LL, Martino RA, Prucca CG, Carranza PG, Saura A, et al. Efficient oral vaccination by bioengineering virus-like particles with protozoan surface proteins. Nat Commun. 2019;10: 361. doi:10.1038/s41467-018-08265-9

175. Choukaife H, Seyam S, Alallam B, Doolaanea AA, Alfatama M. Current Advances in Chitosan Nanoparticles Based Oral Drug Delivery for Colorectal Cancer Treatment. IJN. 2022;Volume 17: 3933–3966. doi:10.2147/IJN.S375229

176. Kaneko K, McDowell A, Ishii Y, Hook S. Liposomal α-galactosylceramide is taken up by gut-associated lymphoid tissue and stimulates local and systemic immune responses. Journal of Pharmacy and Pharmacology. 2017;69: 1724–1735. doi:10.1111/jphp.12814

177. Harnack U, Eckert K, Fichtner I, Pecher G. Oral administration of a soluble 1–3, 1–6 β-glucan during prophylactic survivin peptide vaccination diminishes growth of a B cell lymphoma in mice. International Immunopharmacology. 2009;9: 1298–1303. doi:10.1016/j.intimp.2009.07.013

178. Yoon S, Kurnasov O, Natarajan V, Hong M, Gudkov AV, Osterman AL, et al. Structural Basis of TLR5-Flagellin Recognition and Signaling. Science. 2012;335: 859–864. doi:10.1126/science.1215584

179. Hajam IA, Dar PA, Shahnawaz I, Jaume JC, Lee JH. Bacterial flagellin—a potent immunomodulatory agent. Exp Mol Med. 2017;49: e373–e373. doi:10.1038/emm.2017.172

180. Vijay-Kumar M, Gewirtz AT. Flagellin: key target of mucosal innate immunity. Mucosal Immunology. 2009;2: 197–205. doi:10.1038/mi.2009.9

181. Sierro F, Dubois B, Coste A, Kaiserlian D, Kraehenbuhl J-P, Sirard J-C. Flagellin stimulation of intestinal epithelial cells triggers CCL20-mediated migration of dendritic cells. Proc Natl Acad Sci USA. 2001;98: 13722–13727. doi:10.1073/pnas.241308598

182. Panchapakesan B, Wickstrom E. Nanotechnology for Sensing, Imaging, and Treating Cancer. Surgical Oncology Clinics of North America. 2007;16: 293–305. doi:10.1016/j.soc.2007.03.002

183. Díez-Pascual AM. Nanoparticle Reinforced Polymers. Polymers. 2019;11: 625. doi:10.3390/polym11040625

184. Malik S, Muhammad K, Waheed Y. Nanotechnology: A Revolution in Modern Industry. Molecules. 2023;28: 661. doi:10.3390/molecules28020661

185. Fan D, Cao Y, Cao M, Wang Y, Cao Y, Gong T. Nanomedicine in cancer therapy. Sig Transduct Target Ther. 2023;8: 293. doi:10.1038/s41392-023-01536-y

186. Hou S, Hasnat M, Chen Z, Liu Y, Faran Ashraf Baig MM, Liu F, et al. Application Perspectives of Nanomedicine in Cancer Treatment. Front Pharmacol. 2022;13: 909526. doi:10.3389/fphar.2022.909526

187. Romero G, Moya SE. Synthesis of Organic Nanoparticles. Frontiers of Nanoscience. Elsevier; 2012. pp. 115–141. doi:10.1016/B978-0-12-415769-9.00004-2

188. Unnikrishnan G, Joy A, Megha M, Kolanthai E, Senthilkumar M. Exploration of inorganic nanoparticles for revolutionary drug delivery applications: a critical review. Discover Nano. 2023;18: 157. doi:10.1186/s11671-023-03943-0

189. Joudeh N, Linke D. Nanoparticle classification, physicochemical properties, characterization, and applications: a comprehensive review for biologists. J Nanobiotechnol. 2022;20: 262. doi:10.1186/s12951-022-01477-8

190. Mitchell MJ, Billingsley MM, Haley RM, Wechsler ME, Peppas NA, Langer R. Engineering precision nanoparticles for drug delivery. Nat Rev Drug Discov. 2021;20: 101–124. doi:10.1038/s41573-020-0090-8

191. Makadia HK, Siegel SJ. Poly Lactic-co-Glycolic Acid (PLGA) as Biodegradable Controlled Drug Delivery Carrier. Polymers. 2011;3: 1377–1397. doi:10.3390/polym3031377

192. Kim K-T, Lee J-Y, Kim D-D, Yoon I-S, Cho H-J. Recent Progress in the Development of Poly(lactic-co-glycolic acid)-Based Nanostructures for Cancer Imaging and Therapy. Pharmaceutics. 2019;11: 280. doi:10.3390/pharmaceutics11060280

193. Zhang B, Sai Lung P, Zhao S, Chu Z, Chrzanowski W, Li Q. Shape dependent cytotoxicity of PLGA-PEG nanoparticles on human cells. Sci Rep. 2017;7: 7315. doi:10.1038/s41598-017-07588-9

194. Hoyos-Ceballos GP, Ruozi B, Ottonelli I, Da Ros F, Vandelli MA, Forni F, et al. PLGA-PEG-ANG-2 Nanoparticles for Blood–Brain Barrier Crossing: Proof-of-Concept Study. Pharmaceutics. 2020;12: 72. doi:10.3390/pharmaceutics12010072

195. Aranaz I, Alcántara AR, Civera MC, Arias C, Elorza B, Heras Caballero A, et al. Chitosan: An Overview of Its Properties and Applications. Polymers. 2021;13: 3256. doi:10.3390/polym13193256

196. Shi Y, xue J, Jia L, Du Q, Niu J, Zhang D. Surface-modified PLGA nanoparticles with chitosan for oral delivery of tolbutamide. Colloids and Surfaces B: Biointerfaces. 2018;161: 67–72. doi:10.1016/j.colsurfb.2017.10.037

197. Suk JS, Xu Q, Kim N, Hanes J, Ensign LM. PEGylation as a strategy for improving nanoparticle-based drug and gene delivery. Advanced Drug Delivery Reviews. 2016;99: 28–51. doi:10.1016/j.addr.2015.09.012

198. Vandervoort J, Ludwig A. Biocompatible stabilizers in the preparation of PLGA nanoparticles: a factorial design study. International Journal of Pharmaceutics. 2002;238: 77–92. doi:10.1016/S0378-5173(02)00058-3

199. Kumbhar PS, Nadaf S, Manjappa AS, Jha NK, Shinde SS, Chopade SS, et al. D-α-tocopheryl polyethylene glycol succinate: A review of multifarious applications in nanomedicines. OpenNano. 2022;6: 100036. doi:10.1016/j.onano.2022.100036

200. Rocha CV, Gonçalves V, da Silva MC, Bañobre-López M, Gallo J. PLGA-Based Composites for Various Biomedical Applications. IJMS. 2022;23: 2034. doi:10.3390/ijms23042034

201. Alvi M, Yaqoob A, Rehman K, Shoaib SM, Akash MSH. PLGA-based nanoparticles for the treatment of cancer: current strategies and perspectives. AAPS Open. 2022;8: 12. doi:10.1186/s41120-022-00060-7

202. Iqbal M, Zafar N, Fessi H, Elaissari A. Double emulsion solvent evaporation techniques used for drug encapsulation. International Journal of Pharmaceutics. 2015;496: 173–190. doi:10.1016/j.ijpharm.2015.10.057

203. Zielińska A, Carreiró F, Oliveira AM, Neves A, Pires B, Venkatesh DN, et al. Polymeric Nanoparticles: Production, Characterization, Toxicology and Ecotoxicology. Molecules. 2020;25: 3731. doi:10.3390/molecules25163731

204. Crucho CIC, Barros MT. Polymeric nanoparticles: A study on the preparation variables and characterization methods. Materials Science and Engineering: C. 2017;80: 771–784. doi:10.1016/j.msec.2017.06.004

205. Wang Y, Li P, Truong-Dinh Tran T, Zhang J, Kong L. Manufacturing Techniques and Surface Engineering of Polymer Based Nanoparticles for Targeted Drug Delivery to Cancer. Nanomaterials. 2016;6: 26. doi:10.3390/nano6020026

206. Salatin S, Barar J, Barzegar-Jalali M, Adibkia K, Kiafar F, Jelvehgari M. Development of a nanoprecipitation method for the entrapment of a very water soluble drug into Eudragit RL nanoparticles. Res Pharma Sci. 2017;12: 1. doi:10.4103/1735-5362.199041

207. Xu J, Zhang S, Machado A, Lecommandoux S, Sandre O, Gu F, et al. Controllable Microfluidic Production of Drug-Loaded PLGA Nanoparticles Using Partially Water-Miscible Mixed Solvent Microdroplets as a Precursor. Sci Rep. 2017;7: 4794. doi:10.1038/s41598-017-05184-5

208. Gimondi S, Ferreira H, Reis RL, Neves NM. Microfluidic Devices: A Tool for Nanoparticle Synthesis and Performance Evaluation. ACS Nano. 2023;17: 14205–14228. doi:10.1021/acsnano.3c01117

209. Shrimal P, Jadeja G, Patel S. A review on novel methodologies for drug nanoparticle preparation: Microfluidic approach. Chemical Engineering Research and Design. 2020;153: 728–756. doi:10.1016/j.cherd.2019.11.031

210. Niculescu A-G, Chircov C, Bîrcă AC, Grumezescu AM. Nanomaterials Synthesis through Microfluidic Methods: An Updated Overview. Nanomaterials. 2021;11: 864. doi:10.3390/nano11040864

211. Surdo S, Diaspro A, Duocastella M. Micromixing with spark-generated cavitation bubbles. Microfluid Nanofluid. 2017;21: 82. doi:10.1007/s10404-017-1917-4

212. Volk AA, Epps RW, Abolhasani M. Accelerated Development of Colloidal Nanomaterials Enabled by Modular Microfluidic Reactors: Toward Autonomous Robotic Experimentation. Advanced Materials. 2021;33: 2004495. doi:10.1002/adma.202004495

213. Ma J, Lee SM-Y, Yi C, Li C-W. Controllable synthesis of functional nanoparticles by microfluidic platforms for biomedical applications – a review. Lab Chip. 2017;17: 209–226. doi:10.1039/C6LC01049K

214. Wong V-L, Isaac Ng C-A, Irene Teo L-R, Lee C-W. Microfluidic Synthesis of Functional Materials as Potential Sorbents for Water Remediation and Resource Recovery. In: Ren Y, editor. Advances in Microfluidic Technologies for Energy and Environmental Applications. IntechOpen; 2020. doi:10.5772/intechopen.89302

215. Cabeza VS. High and Efficient Production of Nanomaterials by Microfluidic Reactor Approaches. In: Yu X-Y, editor. Advances in Microfluidics - New Applications in Biology, Energy, and Materials Sciences. InTech; 2016. doi:10.5772/64347

216. Rezvantalab S, Drude NI, Moraveji MK, Güvener N, Koons EK, Shi Y, et al. PLGA-Based Nanoparticles in Cancer Treatment. Front Pharmacol. 2018;9: 1260. doi:10.3389/fphar.2018.01260

217. Pérez-Herrero E, Fernández-Medarde A. Advanced targeted therapies in cancer: Drug nanocarriers, the future of chemotherapy. European Journal of Pharmaceutics and Biopharmaceutics. 2015;93: 52–79. doi:10.1016/j.ejpb.2015.03.018

218. Sivakumar B, Aswathy RG, Romero-Aburto R, Mitcham T, Mitchel KA, Nagaoka Y, et al. Highly versatile SPION encapsulated PLGA nanoparticles as photothermal ablators of cancer cells and as multimodal imaging agents. Biomater Sci. 2017;5: 432–443. doi:10.1039/C6BM00621C

219. Wu J, Wang X, Wang Y, Xun Z, Li S. Application of PLGA in Tumor Immunotherapy. Polymers. 2024;16: 1253. doi:10.3390/polym16091253

220. Koerner J, Horvath D, Groettrup M. Harnessing Dendritic Cells for Poly (D,L-lactide-co-glycolide) Microspheres (PLGA MS)—Mediated Anti-tumor Therapy. Front Immunol. 2019;10: 707. doi:10.3389/fimmu.2019.00707

221. Contreras-Magallanes YG, Durán-Aguilar M, Sosa-Gallegos SL, Álvarez ÁH, Andrade-Santillán FA, Bárcenas-Reyes I, et al. Prime Vaccination with Chitosan-Coated Phipps BCG and Boosting with CFP-PLGA against Tuberculosis in a Goat Model. Animals. 2021;11: 1046. doi:10.3390/ani11041046

222. Tondeur EGM, Voerman JSA, Geleijnse MAA, van Hofwegen LS, van Krimpen A, Koerner J, et al. Sec22b and Stx4 Depletion Has No Major Effect on Cross-Presentation of PLGA Microsphere–Encapsulated Antigen and a Synthetic Long Peptide In Vitro. The Journal of Immunology. 2023;211: 1203–1215. doi:10.4049/jimmunol.2200473

223. Kalashnikova I, Cambell H, Kolpek D, Park J. Optimization and characterization of miRNA-129-5p-encapsulated poly (lactic- *co* -glycolic acid) nanoparticles to reprogram activated microglia. Nanoscale Adv. 2023;5: 3439–3452. doi:10.1039/D3NA00149K

224. Liu J, Liu X, Han Y, Zhang J, Liu D, Ma G, et al. Nanovaccine Incorporated with Hydroxychloroquine Enhances Antigen Cross-Presentation and Promotes Antitumor Immune Responses. ACS Appl Mater Interfaces. 2018;10: 30983–30993. doi:10.1021/acsami.8b09348

225. Cao S, Xu S, Wang H, Ling Y, Dong J, Xia R, et al. Nanoparticles: Oral Delivery for Protein and Peptide Drugs. AAPS PharmSciTech. 2019;20: 190. doi:10.1208/s12249-019-1325-z

226. Islam MA, Firdous J, Badruddoza AZM, Reesor E, Azad M, Hasan A, et al. M cell targeting engineered biomaterials for effective vaccination. Biomaterials. 2019;192: 75–94. doi:10.1016/j.biomaterials.2018.10.041

227. Wang Y, Li H, Rasool A, Wang H, Manzoor R, Zhang G. Polymeric nanoparticles (PNPs) for oral delivery of insulin. J Nanobiotechnol. 2024;22: 1. doi:10.1186/s12951-023-02253-y

228. Fang G, Tang B. Advanced delivery strategies facilitating oral absorption of heparins. Asian Journal of Pharmaceutical Sciences. 2020;15: 449–460. doi:10.1016/j.ajps.2019.11.006

229. Hedrington MS, Davis SN. Oral semaglutide for the treatment of type 2 diabetes. Expert Opinion on Pharmacotherapy. 2019;20: 133–141. doi:10.1080/14656566.2018.1552258

230. Amini Y, Amel Jamehdar S, Sadri K, Zare S, Musavi D, Tafaghodi M. Different methods to determine the encapsulation efficiency of protein in PLGA nanoparticles. BME. 2017;28: 613–620. doi:10.3233/BME-171705

231. Busato D, Capolla S, Durigutto P, Mossenta M, Bozzer S, Sblattero D, et al. A novel complement-fixing IgM antibody targeting GPC1 as a useful immunotherapeutic strategy for the treatment of pancreatic ductal adenocarcinoma. J Transl Med. 2023;21: 864. doi:10.1186/s12967-023-04745-9

232. Morelli L, Gimondi S, Sevieri M, Salvioni L, Guizzetti M, Colzani B, et al. Monitoring the Fate of Orally Administered PLGA Nanoformulation for Local Delivery of Therapeutic Drugs. Pharmaceutics. 2019;11: 658. doi:10.3390/pharmaceutics11120658

233. Magogotya M, Vetten M, Roux-van der Merwe M, Badenhorst J, Gulumian M. In vitro toxicity and internalization of gold nanoparticles (AuNPs) in human epithelial colorectal adenocarcinoma (Caco-2) cells and the human skin keratinocyte (HaCaT) cells. Mutation Research/Genetic Toxicology and Environmental Mutagenesis. 2022;883–884: 503556. doi:10.1016/j.mrgentox.2022.503556

234. Nkabinde LA, Shoba-Zikhali LNN, Semete-Makokotlela B, Kalombo L, Swai H, Grobler A, et al. Poly (D,L-lactide-co-glycolide) nanoparticles: Uptake by epithelial cells and cytotoxicity. Express Polym Lett. 2014;8: 197–206. doi:10.3144/expresspolymlett.2014.23

235. Agadjanian H, Karlan BY, Walsh CS, Orsulic S. Immunocompetent C57BL/6 syngeneic mouse ovarian cancer models with defined genetic alterations. Sci Rep. 2025;15: 34969. doi:10.1038/s41598-025-18960-5

236. Mishra N, Tiwari S, Vaidya B, Agrawal GP, Vyas SP. Lectin anchored PLGA nanoparticles for oral mucosal immunization against hepatitis B. Journal of Drug Targeting. 2011;19: 67–78. doi:10.3109/10611861003733946

237. Sarti F, Perera G, Hintzen F, Kotti K, Karageorgiou V, Kammona O, et al. In vivo evidence of oral vaccination with PLGA nanoparticles containing the immunostimulant monophosphoryl lipid A. Biomaterials. 2011;32: 4052–4057. doi:10.1016/j.biomaterials.2011.02.011

238. Park HJ, Gonsalves GS, Tan ST, Kelly JD, Rutherford GW, Wachter RM, et al. Comparing frequency of booster vaccination to prevent severe COVID-19 by risk group in the United States. Nat Commun. 2024;15: 1883. doi:10.1038/s41467-024-45549-9

239. Syeda MZ, Hong T, Huang C, Huang W, Mu Q. B cell memory: from generation to reactivation: a multipronged defense wall against pathogens. Cell Death Discov. 2024;10: 117. doi:10.1038/s41420-024-01889-5

240. Hines DJ, Kaplan DL. Poly(lactic-co-glycolic) Acid-Controlled-Release Systems: Experimental and Modeling Insights. Crit Rev Ther Drug Carrier Syst. 2013;30: 257–276. doi:10.1615/CritRevTherDrugCarrierSyst.2013006475

241. Xia L, Schrump DS, Gildersleeve JC. Whole-Cell Cancer Vaccines Induce Large Antibody Responses to Carbohydrates and Glycoproteins. Cell Chemical Biology. 2016;23: 1515–1525. doi:10.1016/j.chembiol.2016.10.012

242. Zheng B, Lou D, Ding J, Zhuo X, Ding H, Kong Q, et al. GRA24-Based DNA Vaccine Prolongs Survival in Mice Challenged With a Virulent Toxoplasma gondii Strain. Front Immunol. 2019;10: 418. doi:10.3389/fimmu.2019.00418

243. Zhi L, Liu D, Shameem M. Injection site reactions of biologics and mitigation strategies. AAPS Open. 2025;11: 5. doi:10.1186/s41120-025-00108-4

244. Semete B, Booysen L, Lemmer Y, Kalombo L, Katata L, Verschoor J, et al. In vivo evaluation of the biodistribution and safety of PLGA nanoparticles as drug delivery systems. Nanomedicine: Nanotechnology, Biology and Medicine. 2010;6: 662–671. doi:10.1016/j.nano.2010.02.002

245. Navarro SM, Swetledge S, Morgan T, Astete CE, Stout R, Coulon D, et al. Biodistribution of orally administered poly(lactic-co-glycolic) acid nanoparticles for 7 days followed by 21 day recovery in F344 rats. NanoImpact. 2017;5: 1–5. doi:10.1016/j.impact.2016.12.002

246. Esmaeili A. Investigating the Impact of Peptide-Based Vaccines on Various Types of Cancer: A Systematic Review. Cancer Investigation. 2025;43: 657–680. doi:10.1080/07357907.2025.2568964

247. Yaremenko AV, Khan MM, Zhen X, Tang Y, Tao W. Clinical advances of mRNA vaccines for cancer immunotherapy. Med. 2025;6: 100562. doi:10.1016/j.medj.2024.11.015

248. Ruzzi F, Riccardo F, Conti L, Tarone L, Semprini MS, Bolli E, et al. Cancer vaccines: Target antigens, vaccine platforms and preclinical models. Molecular Aspects of Medicine. 2025;101: 101324. doi:10.1016/j.mam.2024.101324

249. Wang Y, Huang P, Li C, Tu S, Yang H. Therapeutic cancer vaccines in pancreatic cancer. Front Immunol. 2025;16: 1674743. doi:10.3389/fimmu.2025.1674743

250. Cai Z, Li Z, Zhong W, Lin F, Dong X, Ye H, et al. Targeting Mesothelin Enhances Personalized Neoantigen Vaccine Induced Antitumor Immune Response in Orthotopic Pancreatic Cancer Mouse Models. Advanced Science. 2025;12: 2407976. doi:10.1002/advs.202407976

251. Pant S, Wainberg ZA, Weekes CD, Furqan M, Kasi PM, Devoe CE, et al. Lymph-node-targeted, mKRAS-specific amphiphile vaccine in pancreatic and colorectal cancer: the phase 1 AMPLIFY-201 trial. Nat Med. 2024;30: 531–542. doi:10.1038/s41591-023-02760-3

252. Omidian H, Wilson RL. PLGA Implants for Controlled Drug Delivery and Regenerative Medicine: Advances, Challenges, and Clinical Potential. Pharmaceuticals. 2025;18: 631. doi:10.3390/ph18050631

Acknowledgments

I want to thank all my colleagues from the Experimental and Clinical Pharmacology Unit at the National Cancer Institute (IRCCS CRO Aviano).

I am grateful to my supervisor, Dr. Giuseppe Toffoli, for allowing me to be part of his research group. I also thank my tutor, Dr. Michele Dal Bo, for his guidance and help throughout these years, and Prof. Paolo Macor for his advice regarding the project.

I also wish to thank all the members of the Vaccine Group: Idris, Franca, Amin, and Aurora, especially Idris Vruzhaj, for his guidance, patience, and continuous support during these three years. A special thank you also to Davide, a member of the Nanomedicine group, for his presence, continuous advice, and help.

I am sincerely grateful to all my family, especially my mother, my brother, and my father, who, unfortunately, could not see this work completed.

Finally, I would like to thank all my friends and everyone who stood by my side.